NACA·TN 2189

NATIONAL ADVISORY COMMITTEE FOR AERONAUTICS

TECHNICAL NOTE 2189

THE DEVELOPMENT AND PERFORMANCE OF TWO SMALL TUNNELS

CAPABLE OF INTERMITTENT OPERATION AT MACH

NUMBERS BETWEEN 0.4 AND 4.0

By Walter F. Lindsey and William L. Chew

Langley Aeronautical Laboratory
Langley Air Force Base, Va.

NACA

Washington

September 1950

TABLE OF CONTENTS

NATIONAL ADVISORY COMMITTEE FOR AERONAUTICS

TECHNICAL NOTE 2189

THE DEVELOPMENT AND PERFORMANCE OF TWO SMALL TUNNELS

CAPABLE OF INTERMITTENT OPERATION AT MACH

NUMBERS BETWEEN 0.4 AND 4.0

By Walter F. Lindsey and William L. Chew

SUMMARY

The design, development, and performance of equipment suitable
for use by educational institutions for student training and basic
compressible-flow research are described. The equipment consists of
an induction tunnel having a 4- by 16-inch test section and capable of
operating at Mach numbers ranging from about 0.4 to 1.4 and a blowdown
tunnel having a 4- by 4-inch test section for supersonic Mach numbers
up to about 4.0. The tunnels are actuated by dry compressed air stored
at a pressure of 300 pounds per square inch in a 2,000-cubic-foot tank
by a 150-horsepower reciprocating air compressor. The air supply per-
mits intermittent operation of the tunnels for test periods ranging up
to 400 seconds (depending on the stagnation pressures maintained) at
approximately $\frac{1}{2}$- hour intervals.

Nozzle pressure-distribution tests made in the induction tunnel
showed satisfactory performance at subsonic speeds. At low-supersonic
speeds (Mach numbers of 1.2 and 1.4), however, adverse condensation
effects were encountered when tests were made under high-humidity con-
ditions. The results presented indicate that the installation of the
induction tunnel in a small room which acts as a return passage would
permit the attainment of stagnation relative humidities sufficiently
low to permit satisfactory operation at Mach numbers around 1.2. An
alternate arrangement for operating the 4- by 16-inch tunnel at super-
sonic speeds is to equip the induction tunnel with an alternate entrance
cone designed for direct blowdown.

The supersonic nozzles of the blowdown tunnel produced average Mach
numbers close to the design values and sufficiently uniform velocity
distributions for most of the intended uses of this equipment.

INTRODUCTION

During the past 5 years great progress has been made toward the understanding and solution of many of the aerodynamic problems associated with transonic and supersonic flight. The operation of military and research aircraft and missiles in these speed ranges is now a reality. Flight in these relatively new speed regions has increased the demand for transonic and supersonic aerodynamic research to such an extent that existing experimental facilities and the number of technically trained personnel are inadequate.

One part of the Unitary Plan for procurement of high-speed research facilities recently formulated by the National Advisory Committee for Aeronautics, the Air Force, and the Navy called for the erection of high-speed aerodynamic research equipment in educational institutions in the belief that such equipment will serve both as a means of training research personnel and as a source of transonic and supersonic research information. In anticipation of the problems that will be faced by many educational institutions in the procurement of suitable high-speed research equipment, the NACA, in cooperation with the Office of Naval Research, has designed, constructed, and tested a unit which, on the basis of NACA experience, is a suitable facility both for student training and for fundamental transonic and supersonic research. The purpose of this paper is to describe the design, development, and performance of this unit.

Briefly described, the unit consists of a source of dried high-pressure air used with an induction tunnel and with a direct-blowdown supersonic tunnel. The induction tunnel is capable of operating at Mach numbers ranging from 0.3 to 1.4 and the blowdown tunnel is capable of operating at Mach numbers up to 4.0. The compressed-air supply consists of a 2,000-cubic-foot tank in which dry air is stored at a pressure of 300 pounds per square inch by a 150-horsepower compressor. A primary feature of the unit is its inherent adaptability to a wide variety of compressible-flow problems.

Upon completion of the preliminary performance tests discussed herein, the unit, by prior agreement, was turned over to the United States Naval Academy, Annapolis, Md., for use in student instruction and in high-speed research.

SYMBOLS

A area, square inches

c model chord, inches

d free aperture of optical system

f	focal length of lens
g	acceleration due to gravity
h	tunnel height, inches
i	image distance from lens
k	numerical constant
M	Mach number
n	polytropic exponent, as in $p = k\rho^n$
o	object distance from lens
P	diameter of flow field in schlieren photograph, inches
p	absolute pressure, pounds per square inch
Q	compressor flow rate, cubic feet of free air per minute
R	Reynolds number
R	gas constant (53.33 ft/°R)
S	maximum cross-sectional area of model, square inches
T	temperature, degrees Rankine (°Fahrenheit + 460°)
t	time, seconds
v	volume of air-storage tank, cubic feet
w	weight, pounds
x	horizontal distance along nozzle region
y	maximum model thickness (usually t), inches
α	angle of attack, degrees
β	angle of shock, degrees
δ	flow deviation through compression shock, degrees
μ	coefficient of viscosity, pound-seconds per square foot

ϕ off-axis angle of a reflecting schlieren system, degrees

ρ mass density

Subscripts:

a   atmospheric $(p_a = 14.7 \text{ lb/sq in.})$

c   compressor

ch   choked condition in stream

e   tunnel exit

j   induction-jet chamber

m   minimum cross section where $M = 1.0$, as in supersonic nozzle
           or in induction jet

min   minimum

max   maximum

o   stagnation conditions

1   before or at start

2   after or at end

SPECIFICATIONS

Because low initial and operating costs were primary considerations in the design of this equipment, it was essential to keep the size and performance requirements at the minimum values considered adequate to accomplish significant fundamental flow research at subsonic and supersonic speeds. NACA experience in the design and use of high-speed research equipment was utilized in the selection of minimum size and performance specifications as follows:

Mach number range . . . . 0.3 to 4.0
Choked Mach number range . . . . 0.85 to 1.15
Minimum Reynolds number for two-dimensional tests
   (for $M = 0.8$ or above) . . . . 1×10^6
Minimum size of two-dimensional pressure-distribution model:
   Chord, inches 2
   Span, inches 4
Duration of test:
   Subsonic (range of speeds), seconds 60
   Supersonic (single test speed), seconds 30
Maximum average time between tests, minutes 30
Dryness of stored air; that is, dew point at
   atmospheric pressure, °F . . . . -40

DESIGN

Systems of Tunnel Operation

The various types of high-speed tunnels can be classified as continuous or intermittent according to the method of operation. Tunnels of the continuous type, as the name implies, are capable of operating continuously, whereas those of the intermittent type are capable of operating for a short time, followed by a relatively long period of inactivity. The inactive period is utilized to store up energy at a slow rate so that a large amount will be available to produce the desired air flow through the tunnel for a short duration. As a consequence of the differences in the methods of operation, the horsepower requirements of tunnels of the continuous type are considerably in excess of the power required for tunnels of the intermittent type. For equipment complying with the minimum specifications previously outlined, the power required by tunnels of the intermittent type would be around 10 percent of the installed horsepower of tunnels of the continuous type. For some investigations, such as heat-transfer studies in which steady flows are required to be maintained for a relatively long duration of test, the continuously operating tunnel has obvious advantages.

Because the initial cost and the horsepower requirements of the tunnels and auxiliaries were to be held at low values, it was mandatory that the equipment be intermittent in operation. For such operation, two modes of power supply were available - the first designated as "compression system" and the second, "evacuation system." In the evacuation system, air would flow from the atmosphere through the tunnel into an evacuated tank. In the compression system, air would flow from a compressed-air-storage tank through tunnel passages and exhaust into the atmosphere. The two systems were studied with respect to aerodynamic performance, flexibility of operation, and initial cost.

The study showed that the advantages of the compression system over an evacuation system of comparable cost are as follows:

Supersonic speeds:

(1) A higher test Reynolds number can be obtained.

(2) The stagnation pressure can be regulated to vary the test Reynolds number independently of the model size.

(3) The size of the drying-equipment installation is minimized, inasmuch as the air can be dried during the long compression period and at high density.

(4) Air discharge to the atmosphere simplifies modifications of the basic unit to permit a wide variety of investigations, such as studies of cascades, ducts, burners, and so forth.

Subsonic and transonic speeds:

Pressure-ratio requirements in this speed range permit use of an induction type of tunnel which can be actuated conveniently by high-pressure air from the storage tank of the compression system. The induction type has the advantage of a twofold to fourfold increase in air flow and tunnel size as compared with a direct-blowdown system. The increase in tunnel size is of prime importance at transonic speeds.

The main disadvantage of the compression system is that the stagnation temperature in the supersonic stream of the direct-blowdown tunnel decreases during a test run because of the expansion of the air in the compressed-air-storage tank. The rate of decrease, however, is generally sufficiently low to permit recording by commercial instruments. A second disadvantage is that the induction tunnel is essentially an evacuation type, with its inherent drying difficulties. The humidity problem can be alleviated, however, by enclosing the tunnel in a small room to permit recirculation of the mixed dry air from the induction nozzle with the air induced through the tunnel. This arrangement, in effect, simulates a return passage for the tunnel.

Experience with the compression system in the laboratories of the NACA (references 1, 2, and 3) has demonstrated its adaptability and economy of operation, and this system was chosen for the unit shown in figure 1.

Tunnel Sizes

Subsonic speeds.- From figure 2 or appendix A it can be determined that in the induction tunnel, in which the stagnation pressure p_o is 1 atmosphere and the stagnation temperature is approximately 60° F, a 2.7-inch-chord test model is required at a Mach number of 0.8 for the specified Reynolds number of 1×10^6. This value is somewhat greater than the specified minimum chord of 2 inches.

In order to obtain the specified choke Mach number of 0.85, figure 3(a) and appendix B show that the ratio of model area to tunnel area is 0.02. For two-dimensional models (models spanning the tunnel) the ratio of maximum thickness to tunnel height will also be 0.02. If a thickness ratio of 10 percent is assumed as a representative value, the thickness of a 2.6-inch-chord model would be 0.26 inch and the minimum tunnel height would have to be 13 inches. A height of 16 inches and a width of 4 inches were chosen. Approximately these proportions had been found to be satisfactory from the standpoints of model installation, tunnel-diffuser design, and schlieren photography in the Langley rectangular high-speed tunnel (references 3 and 4). There are other types of test sections, such as the open throat, that permit an extension

of the speed range (reference 5). These other types, still in the development stage for transonic speeds, can be expected to require more power and higher pressure.

Supersonic speeds.- Supersonic speeds up to a Mach number of about 1.4 can be obtained in either the induction type or in the blowdown type of tunnel. The blowdown type is used for the higher supersonic speeds. The Mach numbers considered in the subsequent design studies are 1.2, 1.4, 2.0, 3.0, and 4.0.

For the induction tunnel in which the stagnation pressure is constant and equal to the atmospheric pressure (stagnation temperature approximately 60° F), figure 2 provides the means of evaluating the chord required to obtain a Reynolds number of at least 1×10^6. For Mach numbers of 1.2 and 1.4, a chord of 2.4 inches is required to obtain the specified minimum Reynolds number.

The determination of the model size for the blowdown tunnel wherein the stagnation pressure can vary is somewhat more difficult than for the induction tunnel. The minimum stagnation pressure at which the tunnel will operate for different Mach numbers can be obtained from figure 4, discussed in appendix C (see also references 6 and 7). With the use of the curve of moderate efficiency $\left(\dfrac{p_2}{p_e} = 1.25 \quad \text{for} \quad M = 1.0 \right)$ the lowest stagnation pressure at which the tunnel will start can be obtained as p_2, which is equal to p_0 for this example. Because, in practice, the operating pressure of the tunnel will generally be somewhat higher than the calculated starting pressure, a pressure increment of from 4 to 10 pounds per square inch was added to the pressures obtained from figure 4 to assure a downstream location of the tunnel shock. The resulting pressures were used with figure 2 to determine the model chord required to obtain a Reynolds number of 1×10^6. The summarized results are:

M	$p_2 = p_0$ calculated (fig. 4)	$p_2 = p_0$ to operate	c for $R = 1 \times 10^6$
1.4	19	23	1.7
2.0	25	30	1.6
3.0	56	65	1.2
4.0	132	140	.9

The computed model chords are smaller than the minimum chord of 2 inches given in the specifications. Thus, the minimum Reynolds number requirement will be exceeded in all the blowdown tunnels if 2-inch-chord or larger models are used.

The first step in determining minimum size required for the test section of a supersonic tunnel is to evaluate the height-chord ratios that would permit the tunnel to start (appendix B). For two-dimensional tests on a model of a given thickness-chord ratio, the ratio of maximum model cross-sectional area to tunnel test-section area S/A can be converted into a ratio of tunnel height to model chord h/c. The second step is to evaluate the minimum height-chord ratios that would prevent shocks originating on the forward part of the model from being reflected by the tunnel walls onto the model (see appendix D). The minimum values of the height-chord ratios are tabulated as a function of Mach number in appendix D.

For a 2-inch-chord model the tunnel heights based on the minimum practical values of h/c for the avoidance of interference from reflected shocks (appendix D) are as follows:

M	$\left(\dfrac{h}{c}\right)_{min}$	h (in.)
1.2	9.0	18.0
1.4	4.0	8.0
2.0	1.3	2.6
3.0	1.0	2.0
4.0	1.0	2.0

A 4-inch height is thus more than adequate for two-dimensional tests at Mach numbers of 2.0 or above. From considerations of the requirements of tests of axially symmetric bodies it appeared that these tunnels should have square cross sections and, consequently, the dimensions 4 by 4 inches were selected.

For the lowest supersonic speed considered ($M = 1.2$) an 18-inch depth is desirable. The 16-inch depth of the induction tunnel, however, is adequate for all but the extreme detached-shock conditions. This size was therefore selected for $M = 1.2$ and $M = 1.4$.

Tank Pressure and Volume

Induction-tunnel requirements.- Experience with the operation of
induction tunnels such as the Langley 11-inch high-speed tunnel (refer-
ence 1), the Langley 24-inch high-speed tunnel (reference 2), and the
Langley 4- by 18-inch high-speed tunnel (references 3 and 4) indicated
that a jet pressure of 180 pounds per square inch was needed in a jet
having a ratio of test-section area to minimum jet area A/A_m of 35 in
order to obtain sonic velocity in the tunnel. From a value of 180 pounds
per square inch for p_2, and 300 pounds per square inch and 560° R
(100° F) as suitable initial values for p_1 and T_1, the value of the
test-duration parameter $t\dfrac{A_m\sqrt{T_1}}{v}$ is 1.95 for an adiabatic process
(fig. 5 and appendix E). In the test parameter, A_m is the minimum
area of the induction nozzle (square inches) through which the inducing
air flows at sonic velocity and v is the volume of the air-storage
tank (cubic feet). With A_m equal to $A/35$ or 1.83 square inches for
the induction tunnel and t equal to 60 seconds, the volume of the tank
is found from the test-duration parameter to be 1,300 cubic feet. This
estimate is somewhat conservative, inasmuch as an adiabatic process was
assumed (see fig. 5) and the high-pressure air was not throttled (compare
figs. 5 and 6).

For the operation of an induction tunnel at supersonic speeds, the
jet-chamber pressure required will necessarily increase above that for
subsonic speeds. An analytical determination of the pressure requires
many uncertain assumptions, particularly as to losses and method of
mixing, and is an involved process (see references 8 to 10). Limited
test results in the Langley 4- by 18-inch high-speed tunnel indicated
that a jet-chamber pressure of approximately 225 pounds per square inch
would be required to obtain a Mach number of about 1.3. If the value
225 pounds per square inch is used, a test duration of 30 seconds
requires a tank of about the same size as that needed for subsonic
operation (1,300 cu ft).

Blowdown-tunnel requirements.- In order to realize the inherent
capability of the blowdown tunnel to operate at various Reynolds numbers,
the tank must be large enough for the required running time at stagna-
tion pressures well in excess of the minimum operating values. If only
30-second runs at the minimum operating pressures previously given in
the section entitled "Tunnel Sizes" were required, the tank requirements
would be much smaller than those for the induction tunnel. Inasmuch as
the 1,300-cubic-foot tank needed for the induction tunnel appeared to
be a practicable size, this value was used in calculations of the stag-
nation pressures that could be maintained constant in the blowdown

tunnel during a 30-second run. The results, which are easily computed with the aid of figure 6, are as follows:

M	p_2 (lb/sq in.)	$\dfrac{p_2}{p_{2_{min}}}$
2.0	125	4.2
3.0	190	2.9
4.0	250	1.7

It is evident that the Reynolds number can be varied by a factor of 4.2 at M = 2.0 and of 1.7 at M = 4.0.

In order to extend the permissible operating range and to facilitate performance studies, a tank of 2,000-cubic-foot capacity was chosen. In this case the Reynolds number can be varied by a factor of about 5.0 at M = 2.0 and of 2.0 at M = 4.0.

Compressed-Air Supply

Compressor.- With atmospheric air intake and a maximum working pressure of 300 pounds per square inch, the compressor must operate at a maximum compression ratio of 20. As a consequence of the high compression ratio and relatively low flow rates, a reciprocating type was chosen.

The size of the compressor can be specified by its rated pumping capacity in cubic feet of free air per minute Q. The quantity Q is shown in appendix F and figure 7 to depend on tank volume v, pump-up time t_c, and the pressure at the beginning of pump-up p_2 (the pressure at the end of the preceding test). From previously specified values, v is 2,000 cubic feet and an average value of t_c is 30 minutes. The pressure at the beginning of the pump-up was estimated to be 160 pounds per square inch, based on the previous design computations and on experience derived from operation of similar equipment at the Langley Laboratory. From the aforementioned quantities and figure 7 (n = 1.0 since the compression cycle should approach an isothermal process), the pumping capacity of the compressor was found to be about 600 cubic feet per minute and would require a 150-horsepower drive motor. The compressor is shown in figure 8.

Tank.- In the general design of the tank it was specified that the length-diameter ratio be between 2 and 4 and that the construction conform to the ASME code for unfired pressure vessels (paragraph U-68). The tank obtained was 9 feet in diameter, 34 feet $9\frac{3}{4}$ inches long (excluding fittings), had a storage capacity of 2,000 cubic feet, and weighed 34 tons. The tank was built for a working pressure of 300 pounds per square inch and was hydrostatically tested to 600 pounds per square inch.

Air dryer.- The specified -40° F dew point at atmospheric pressure is generally accepted to be sufficiently low to avoid condensation shock, although that degree of dryness does not preclude the possibility of supersaturation of the flow, particularly at some of the higher Mach numbers. The specified -40° F dew point at atmospheric pressure for supersonic operation is readily obtained with standard commercial air-drying equipment. The other operational requirements which determine the selection of the dryer are working pressure, compressor flow quantity, adsorption period, and reactivation period. The adsorption period is the length of time the dryer is capable of drying the required air-flow quantity to the specified dew point. For the usual 8-hour work day it was estimated that the compressor would probably be operated for a period of 6 hours on alternate days; as a consequence, a 6-hour adsorption period was specified for a dryer having one drying tank. During the reactivation period the dryer is out of operation and the adsorbed water is removed from the drying agent by heating. A reactivation period of 8 hours was specified to permit operation on alternate days. The air dryer is shown in figure 8.

A means of avoiding interruption of research is to use a dryer having two tanks containing desiccants. While one tank is being used to dry the air, the other tank is in the process of reactivation. For intermittent operation a single tank is sufficient, as in the present design, provided that automatic reactivation controls are used to permit the reactivation cycle to be conducted overnight.

Oil filter.- It is well-known that the air in high-speed tunnels must be dry and free of oil or other impurities. These requirements are necessary to avoid condensation shock (previously discussed) and to avoid fouling of the model and schlieren windows. In blowdown tunnels in which the compressed air from the compressor is used as a working fluid, provision must be made to dry the air and remove the oil. The drying agents, however, generally consisting of aluminum or silicon oxides, have a great affinity for oil. It is necessary, therefore, that the oil be removed before the air is dried in order to protect the desiccant in the air dryer.

In the present design an adsorbing type of oil filter was used, capable of handling 600 cubic feet of free air per minute at a working pressure of 300 pounds per square inch. A schematic drawing of the oil filter is presented in figure 9. In future designs it is recommended that a simple mechanical oil filter be installed ahead of the adsorption filter.

Induction Tunnel

The induction tunnel is shown pictorially in figure 1 and by line drawings in figure 10(a). Figure 10(a) also names the various parts of the tunnel. A general view of the tunnel is shown in the background of figure 10(b), while a close-up view of the nozzle region, transition cone, induction nozzle, and a part of the diffuser can be seen in figure 10(c).

The air flowing through the induction tunnel enters the entrance cone, where it passes through a $5\frac{1}{2}$- by 9-foot 30-mesh screen used to smooth out the flow. The air is accelerated in the three-dimensional entrance cone to a 4- by 26-inch area at the juncture of the entrance cone and the nozzle region. The nozzle region consists of a rectangular-shaped passage of variable height and constant 4-inch width. The constant width is maintained by two vertical, parallel, steel plates. Solid duralumin nozzle blocks are used to form the desired two-dimensional profile of the nozzle inlet, test section, and diffuser (fig. 11). The inlet portion of the nozzle fairs into the entrance cone, whereas the rear part of the nozzle blocks forms the beginning of the diffuser (see fig. 11). Ordinates of the nozzle blocks are given in table I.

The transition cone provides a uniform increase in area of the air passage from a 4- by $21\frac{1}{2}$-inch shape at the end of the nozzle blocks to a 13.4-inch-diameter passage at the induction nozzle in a 33-inch length. The induction nozzle is torus-shaped and encircles the tunnel air passage (figs. 10(a) and 11). High-pressure dry air from the tank flows through the jet chamber and thence to the outer periphery of the tunnel air passage through an annular nozzle (fig. 10(a)). The interchange of momentum between this flow and the air in the tunnel induces the flow through the tunnel. Downstream of the induction nozzle the diffuser has a conical shape, with a $4\frac{1}{2}^{\circ}$ total included angle.

Although no tests were made on the induction tunnel to determine the effect of diffuser length on tunnel performance, some data have been obtained from the Langley 24-inch high-speed tunnel. The results showed that the performance is not adversely affected if the diffuser length is

reduced so that the ratio of exit diameter to diameter just downstream of induction nozzle is approximately 2.0. On the basis of those limited results, it appears that the length of diffuser on the induction tunnel could be reduced from its initial length of 21 feet 5 inches to 14 feet 6 inches.

The design of the induction tunnel was based on that of the Langley 4- by 18-inch high-speed tunnel (references 3 and 4). In designing the tunnel to cover both the subsonic and low-supersonic speed ranges, however, one major compromise was necessary. In order to obtain a Mach number of 1.4 without changing the entrance cone, the length of the nozzle ahead of the test section had to be increased appreciably beyond that needed for subsonic or near-sonic operation. A fixed slope of the upstream end of the nozzle block was required in the design so that the nozzle block would fair in with the entrance cone (see fig. 11). The length of the subsonic-flow region in the forward part of the nozzle, as well as the height at the minimum area, had to decrease with increasing Mach number because of the fixed length of the nozzle region ahead of the test section and the fixed height of the test section for all Mach numbers. These requirements led to nozzle blocks in which the shape of the contracting subsonic portion of the nozzle varies in the low-supersonic range (figs. 12 and 13). It was necessary also to locate the test section closer to the transition-cone inlet than was done in the Langley 4- by 18-inch high-speed tunnel. The effect of these compromises on the performance of the tunnel could not be predicted. It was believed, however, that any adverse effects could be reduced or eliminated through slight modifications that could be made during initial performance tests of the unit.

The design of the induction jet was based on that of the Langley 11-inch high-speed tunnel (reference 1) and later used for the 4- by 18-inch high-speed tunnel. The jet was designed so that variations in minimum area could be made.

The shape of the nozzle block used for subsonic speeds (M = 1.0 in fig. 12 and table I) was adapted from the shape of the passage in the Langley 4- by 18-inch high-speed tunnel. In all nozzle blocks the design of the entrance portion ahead of the first minimum section was based on one-dimensional flow to maintain an approximately uniform increase in Mach number along the axis to a value of Mach number of 0.95. The rate of area change was then reduced to provide a more gradual increase in Mach number to a value of 1.0 (fig. 13).

The shapes of the supersonic nozzle blocks (downstream of the first minimum) for Mach numbers of 1.2 and 1.4 were designed by the Prandtl-Busemann characteristics method (reference 11, also described in reference 12), which neglected viscous effects. Approximate formulas for the computation of turbulent boundary-layer momentum thicknesses in compressible flows available in reference 13 can be used to evaluate a correction

for the boundary-layer growth on the nozzle blocks where two-dimensional flow can be assumed to occur (see also reference 14). Along the side walls the radial flow, combined with a gradient in velocity normal to the flow, presents a more complicated problem. At the intersection of the side walls and the nozzle blocks a complex flow in a corner is produced that has not been treated theoretically. Although, in practice, the summation of these effects might tend to reduce the over-all effect by interaction, the uncertainty of the boundary-layer growth and the usual necessity of applying the entire correction to the two nozzle blocks lead to large uncertainties as to the adequacy of the method. The problem was especially critical when the widths of the two nozzle blocks constituted only a small part of the total tunnel perimeter, as well as cases in which small area changes can produce relatively large effects on the flow as at low-supersonic Mach numbers. As a consequence, the usual method employed was to design the nozzle shape, apply an approximate correction, and then determine from test results the amount of the additional correction and the variation along the nozzle. The additional corrections so determined would constitute only a slight alteration insofar as machine work was concerned.

A first-order correction for boundary-layer growth in the test section was made by diverging the 10-inch length of test-section walls (nozzle block only from the 38-inch to 48-inch stations, table I) by an angle of 0.8°. The angle was based on an analysis of data on the divergence required for zero pressure gradients in the Langley 4- by 18-inch high-speed tunnel near sonic speeds. The ordinates for the supersonic nozzle blocks are presented in table I and the profiles are shown in figure 12. Because of the low values of the supersonic Mach numbers, a second minimum area was not included in the design of the nozzle blocks.

A straight-sided, continuously divergent nozzle was also investigated to determine the feasibility of this shape for low-supersonic Mach numbers. The design utilized the forward subsonic part of the $M = 1.4$ nozzle block (table I). At the minimum area the new design incorporated a sharp bend, followed by a straight-line divergence. An angle of divergence was chosen so that a Mach number of 1.2 could be expected at the test section on the basis of area ratio. An additional divergence was incorporated into each of the nozzle blocks to account for increases in boundary-layer thickness along the tunnel walls. The assumed growth in boundary-layer thickness was the same as that for the previously described nozzle blocks. The resulting total divergence in each nozzle block was $1\frac{1}{4}^{\circ}$ (table I).

Blowdown Tunnel

The supersonic blowdown tunnel is shown pictorially in the general layout in figure 1 and by line drawings in figure 14(a). A general view is shown in figures 10(b) and 14(b).

The tunnel is of the direct-blowdown type; that is, dry air from the storage tank passes directly through the 4- by 4-inch test section of the tunnel. Two valves were installed in the supply line, a manually controlled gate valve and an automatic pressure-regulating valve which can be used to maintain constant stagnation pressure. Downstream of the valves is a 19-inch-diameter settling chamber approximately 3 feet long. Installed in the central part of the chamber to improve the uniformity of the flow are two 30- by 30-mesh bronze screens (0.009-inch-diameter wire), spaced 3/4 inch apart. In the downstream 14-inch length of the chamber two metal fairings are installed which serve as a part of the entrance cone of the tunnel (see fig. 14(a)). The fairings have circular-arc cross sections $\left(16\frac{3}{4}\text{- inch radius}\right)$ and reduce the air passage from the original 19-inch diameter to a section 4 inches wide by approximately 19 inches high. Between the settling chamber and the nozzle-block region there is an adapter that serves as a continuation of the entrance cone and reduces the area to a 4- by 10-inch section. In this region the Mach number of the flow is always less than 0.2. The nozzle region is formed in a manner similar to that of the induction tunnel; that is, two flat steel plates, which are the side walls, form vertical boundaries for the 4-inch-width passage through the nozzle region. Nozzle blocks installed at the top and bottom form the upper and lower boundaries of the flow (compare figs. 14(a) and 15). Downstream of the nozzle blocks is a short transition section transforming the air passage from a 4- by 4-inch square shape to a $5\frac{1}{2}$- inch-diameter circular shape at the beginning of the conical diffuser having a $3\frac{1}{2}^{\circ}$ total included angle.

The shapes of the nozzle blocks were determined by the Prandtl-Busemann characteristics method to provide specific supersonic Mach numbers of 2.0, 2.8, and 4.1 at the test section. A first-order correction for boundary-layer growth in the test section of the blowdown tunnel was made by diverging the 6-inch length of each nozzle block at the test section (from the 21.5-inch to 27.5-inch stations (table II)) by an angle of 0.25°. The divergence in terms of area increment per unit length per unit perimeter was less in the blowdown tunnel than in the induction tunnel. A decreased divergence was used in the blowdown tunnel because it was desirable that the initial nozzles have insufficient rather than excessive divergence. The insufficient divergence was required to facilitate the remachining of the nozzle contour as determined by preliminary tests to provide uniform flow in the test section without velocity gradients. This procedure was in accord with standard practice for equipment of this size.

The nozzle blocks for the blowdown tunnel were designed with a region of reduced area downstream from the test section - a second-minimum area. The purpose of the second minimum is to permit the tunnel to operate at a lower pressure ratio than the ratio required to start the tunnel (reference 15). The minimum area theoretically allowable is given by figure 3(b) (also appendix B). The predicted reduction, however, is based on inviscid fluid and, consequently, the reduction in area of the second minimum of a tunnel must be less than the theoretical value. In the design the decrease in area was about 65 percent of the theoretical value. The profiles of the nozzle blocks are shown in figure 16 and the ordinates are given in table II.

An additional factor which affects the design of a supersonic nozzle is the location of the second minimum. Theoretically, the start of the second minimum could be located immediately adjacent to the downstream end of the test section. Yet the probability of shock-boundary-layer interaction neglected by the inviscid theory requires a more rearward location. Although these generalities were known, no information was available on the required downstream displacement or on the effects of Mach number and Reynolds number on the required displacement. In the design of these nozzles a minimum downstream displacement of the second minimum of one-half the tunnel height was incorporated.

The wide range of Mach numbers, together with the fixed over-all length of nozzle, again necessitated compromises in the design of the nozzle blocks for the various Mach numbers. The supersonic portion of the nozzle tended to increase in length with increase in test Mach number, and, although the length of the nozzle for Mach number of 4.1 approached the minimum possible value, nozzles for the lower-supersonic speeds were longer than those generally used. In both the induction and blowdown tunnels the extent of the compromise regarding the nozzle shape would have been reduced had the test-section position been allowed to vary along the axis, but difficulties in connection with the size or location of the windows that were required at the test section would have been introduced.

Auxiliary Equipment

The auxiliary equipment normally needed with a unit of this kind consists of optical apparatus for flow visualization and manometers for measuring pressures. Forces and moments can be determined in many cases by integration of pressure-distribution diagrams. If a large amount of routine force determinations are required, a balance is also desirable but has not been included in the present design. Multiple-tube manometers, such as those shown near the entrance cone of the transonic tunnel in figures 10(b) and 10(c), are generally satisfactory for use with research equipment of this kind.

Flow visualization is accomplished through the use of either the shadowgraph, schlieren, or interferometer techniques. For the compressible-flow unit a schlieren system (references 16 to 18) was designed and used. A schlieren system can easily be converted into a shadowgraph system (reference 17) if desired.

The schlieren system is shown in figures 1, 17, and 18 and the principle upon which it operates is described in appendix G. Components of the system used can be seen in the region of the test section of the tunnels in figures 10(b) and 14(b). Because mirrors of high optical quality are more readily available and more economical than lenses of comparable quality, mirrors were used in the system. Two factors were considered in specifying the focal lengths and diameters of the mirrors for the schlieren system. The first factor concerned was the ratio of focal length to diameter F of the mirrors. It was known that a ratio of focal length to diameter of 8 could be used very easily in an off-axis symmetrical system as shown in figure 18. Also, a system using mirrors having an F number of 5 has been found to function satisfactorily in the same arrangement, although the system was much more difficult to aline and adjust.

The second factor considered was the size of the photograph of the flow field that could be obtained. At the Langley Laboratory a variety of schlieren systems employing various types of light sources having durations from 1 to 4 microseconds have been used. One of the types of light sources is the point-source spark gap and spark generator schematically shown in figure 19 (duration, 2 microseconds). Experience has demonstrated that the largest actual size of schlieren photograph obtained of the flow field P_{max} is limited by the ratio of the focal length of the optics f to the free aperture of the system d (diameter of the flow field (figs. 17 and 18)). The empirical relation obtained is $P \leq 45 \times \dfrac{d}{f}$ inches.

For a 5-inch-diameter field measured along the flow direction of the supersonic blowdown tunnel, a system having a ratio of focal length to free aperture of 8 would permit full-size photographs (magnification of 1) to be obtained. In the induction tunnel in which the models would have chords less than 4 inches, the 5-inch field might be considered the minimum size of flow field acceptable. The mirrors were therefore specified to have 5-inch diameters and approximately 40-inch focal lengths.

The mirrors were made from glass having a low coefficient of thermal expansion. The paraboloidal surface of the mirror was required to have a smooth curve sufficiently accurate so that the mirror could pass a Foucault knife-edge test for uniform graying of the light field without light or dark zones under a condition of parallel light impinging upon

the surface of the mirror with the knife edge being gradually inserted at the focal point.

A mount was designed to hold the mirrors (fig. 10(c)) which provided five degrees of freedom, three in translation and two in rotation. The light source and the knife-edge holders were designed to provide four degrees of freedom, three in translation and one in rotation. The axis of rotation was vertical in the system shown in figure 10(c).

PERFORMANCE OF TUNNELS

Induction Tunnel

Method of operation.- Because an induction tunnel can be actuated with undried air, it was important to determine whether the use of the air dryer could be reduced by alternate operation of the induction tunnel with undried air and the blowdown tunnel with dry air. Tests showed that this technique was impractical because the water adhered to the walls of the air-storage tank and in the pipe lines for approximately three tank blowdowns of dry air following one blowdown of undried air. As a consequence, the compressed-air bypass for the air dryer that had been designed for use during pumping up the tank for operating the induction tunnel with wet air was eliminated. The use of dried air for actuating the induction tunnel has the advantage of greater effectiveness in drying the air in the test room, which is shown subsequently to be an important factor in satisfactory use of the induction tunnel at transonic speeds.

Speed control.- The velocity of air through the test section of the induction tunnel in the subsonic range was regulated by manually throttling the flow of compressed air into the induction jet. The pressure of the air in the jet chamber was thereby varied with corresponding changes in the momentum of the flow from the induction jet. For supersonic operation at $M = 1.2$ and $M = 1.4$, nozzle blocks designed to produce the desired Mach numbers were installed and the pressure in the jet chamber was increased until the supersonic flow was established. Further increase in the jet-chamber pressure would only decrease the duration of the test (compare figs. 5 and 6) because the increased pressure increases the mass flow through the jet and causes the tank pressure to decrease more rapidly.

<u>Initial performance tests.</u>- Initial tests in the induction tunnel
at subsonic speeds indicated reasonably good velocity distributions
along the center line of the test section, but the flow was subject to
velocity pulsations and the pressure required to obtain a Mach number
of 1.0 at the test section was excessive, approximately 260 pounds per
square inch, as compared with 180 pounds per square inch in design.
The combination of pulsing flow and the large power requirement in the
induction tunnel could have resulted from flow separation in the air
passages or could have resulted from some of the compromise changes in
the design from that of the Langley 4- by 18-inch high-speed tunnel.
Since some of the troubles might be arising from differences between
the induction tunnel and the 4- by 18-inch tunnel and from some small
irregularities in the fairing of the entrance cone at its juncture with
the nozzle region, the entrance cone was redesigned to conform more
nearly with the short entrance cone of the Langley 4- by 18-inch high-
speed tunnel. The short length of the entrance cone permitted access
to the juncture between the entrance cone and the nozzle region, and
care was taken to provide an accurate fit at the juncture. The rede-
signed entrance cone attached to a 6- by 5- by 3-foot box, five sides
of which were formed by screens, was then installed (see figs. 11 and 20).
Changes which consisted of an improved fairing at the beginning of the
transition cone were also made.

While these two parts were being constructed, the flow through the
tunnel was investigated for flow separation. Flow studies consisting
of pressure measurements revealed no trouble in the diffuser. At a
station approximately halfway along the length of the transition cone,
however, some separation occurred. Screens and grids of parallel wire
were installed separately ahead of the separation point. The screens
reduced the flow pulsations in the test section but the tunnel operation
remained unsatisfactory because of the high power requirement. Similar
effects were obtained with the parallel wire grids.

The new entrance cone resulted in a marked reduction in the flow
pulsations in the tunnel and produced a reduction of 30 pounds per
square inch in the pressure required to obtain a Mach number of 1.0.
The improved fairing in the entrance of the transition cone caused an
additional reduction of 5 pounds per square inch in power requirement
and eliminated the formerly observed separation in the transition cone
and thus made unnecessary the use of screens or grids.

Induction-jet studies.- With the foregoing changes in the tunnel, the pressure required to operate (225 lb/sq in.) remained appreciably greater than the design estimate of 180 pounds per square inch for attainment of a Mach number of 1.0. Attempts to attain supersonic Mach numbers were unsuccessful because of the high power requirement. The source of this difficulty was finally traced to the induction jet. Examination of the induction jet showed that, although the design called for a minimum throat of 0.045 inch, the jet was assembled with a throat of 0.031 inch. The 0.031-inch throat corresponded to a ratio of tunnel area to minimum jet area of 52, as compared with the design ratio of approximately 35. Since the design permitted the two parts of the jet to be displaced relative to each other to change the minimum jet area, the effect on tunnel performance of changing the jet area was studied. The variation of jet-chamber pressure p_j with time is shown in figure 21 for various minimum jet areas A_m. The data have been adjusted to represent the pressure variation for an instantaneous opening of the throttle valve and for an initial pressure of 300 pounds per square inch in the air-storage tank. The differences in the jet-chamber pressure shown in figure 21 at zero time are representative of the pressure drops in the flow through the pipe line connecting the tank and the jet chamber. The data of figure 21 cannot be extrapolated directly with the area of the minimum section, as would be indicated by figure 5, because the rate of change of pressure with time has an effect on the heat transfer and, consequently, on the numerical value of the polytropic exponent n (appendix E).

The results of simultaneous measurements of pressures along the nozzle region (see fig. 10(a)) and in the jet chamber are presented in figure 22 to show the variation with jet pressure of the maximum measured Mach number for various induction-nozzle and entrance-cone conditions. The increases in maximum Mach number and the reductions in the jet-chamber pressure required to obtain a given test Mach number resulting from the new entrance cone, from the modified transition cone, and from progressive increases in the minimum area of the induction jet are apparent in this figure.

Data from figures 21 and 22 were used in figure 23 to show how the performance was affected by the ratio of test-section area to minimum jet area. As the ratio of test-section area to minimum jet area decreased from the value of 52 to 21, the duration of the test and the maximum attainable Mach number increased and the jet-chamber pressure required to obtain a Mach number of 1.0 decreased. Further decrease in the area ratio resulted in a reversal of the trends. For the optimum condition (area ratio of 21), the test duration for a Mach number of 1.0 was somewhat in excess of 100 seconds and the jet pressure required was approximately 130 pounds per square inch. The optimum area ratio of about 21 (fig. 23) probably applies only to the particular test-section shape used.

In general, in induction-tunnel designs the jet nozzle should be adjustable to allow the optimum setting for each configuration.

Analysis of performance data.- Further analysis of the performance data indicated that the ratio of the mass flow through the tunnel to the mass flow from the induction nozzle decreased from about 5.3 at a Mach number of 0.6 to 3.5 at a Mach number of 1.0 for the tunnel with A/A_m equal to 52. When A/A_m was decreased from 52 to 21, the test duration at Mach number 1.0 was increased, but the mass-flow-rate ratios were reduced to approximately 3.5 at Mach number 0.6 and to 2.2 at a Mach number of 1.0. This large reduction in the mass-flow advantage of the induction tunnel at high Mach numbers made it desirable to compare the performance of the induction and direct-blowdown systems for the low-supersonic speeds $(M = 1.2$ and $M = 1.4)$. With the use of figures 6, 7, and 22 and a final tank pressure of 25 pounds per square inch for the blowdown tunnel, the following performance estimates were obtained:

M	Induction				Blowdown		
	p_j	p_0	$t\dfrac{A\sqrt{T_1}}{v}$	$\dfrac{t_cQ}{60v}$	p_0	$t\dfrac{A\sqrt{T_1}}{v}$	$\dfrac{t_cQ}{60v}$
1.0	133	14.7	113	11	18.4	61	19
1.2	165	14.7	65	9	18.5	62	19
1.4	230	14.7	23	5	19.2	65	19

where

p_j induction-jet-chamber pressure in pounds per square inch absolute

p_0 test-section stagnation pressure in pounds per square inch absolute

$t\dfrac{A\sqrt{T_1}}{v}$ test-duration parameter

$\dfrac{t_cQ}{60v}$ pump-up-time parameter

For Mach number 1.0 the table shows that a blowdown tunnel would have approximately one-half the test duration and one-half the test frequency,

so that the over-all performance would be approximately one-fourth as good as that for an induction tunnel. At $M = 1.2$ the running time becomes about equal to that of the induction type and at 1.4 the blow-down running time is nearly three times that of the induction tunnel. The pump-up times are longer for the blowdown case, however, so that in terms of total running time per day the induction type would appear to have a 2-to-1 advantage at $M = 1.2$ and a 4-to-3 advantage at $M = 1.4$. Beyond a Mach number of 1.4, the blowdown type is superior in all respects. This so-called advantage of the induction type in daily operating time at these speeds is largely illusory, because of the necessity of devoting a large part of the operating time to lowering the humidity by mixing and recirculation to the point at which test data can be taken. The blowdown system, of course, completely avoids the humidity problem and this consideration far outweighs the questionable advantage of the induction system from the viewpoint of total daily running time. Inasmuch as equal or longer test runs free from humidity effects are attainable by use of direct blowdown, it is concluded that this system should be used at all supersonic speeds.

Suggested design modification.- The 4- by 16-inch test section needed at $M = 1.2$ and $M = 1.4$ could not be incorporated in the present blowdown tunnel without major changes in the design. A larger settling chamber and larger height (wider parallel walls) would be required. The entrance cone on the induction tunnel, however, is easy to remove. The present cone could be replaced by a settling chamber incorporating the entrance-cone shape at one end and an attachment for the compressed-air supply line at the opposite end. The new settling chamber, designed for a working pressure of 20 pounds per square inch, would have screens installed to smooth out the flow and baffles near the compressed-air entrance to distribute properly the inlet air. This chamber could be installed when changing subsonic nozzle blocks for supersonic blocks and would permit the induction tunnel to operate at supersonic speeds as a direct-blowdown type.

Blowdown Tunnel

The only major difficulty encountered in the initial operation of the blowdown tunnel was air leakage due to inadequate seals between the nozzle blocks and the side walls. For simplicity of construction the seals had been designed to be installed at a common location on all the nozzle blocks (see the straight-line groove near the bolt holes in the outer portion of the nozzle blocks in fig. 15). Two methods of sealing the nozzles were used satisfactorily. The first consisted of using a soft plastic gasket material, such as Permatex. The material was spread along the sides of the nozzle but slightly below the contoured surface (see nozzle block in fig. 11). The second consisted of installing a strip of rubber (0.02 by 0.1 inch) in a similar location. Either of

these methods could cause flow distortions if the gasket material were accidentally squeezed out into the flow passage.

In operating the tunnel the manually controlled valve was gradually opened, and the pressure in the settling chamber was thereby increased until the value required to establish supersonic flow in the tunnel was reached. Throttling was also accomplished through the use of the automatic pressure-regulating valve adjusted to maintain a preselected pressure in the settling chamber. The performance of this standard commercial pressure-regulating valve was adversely affected by large changes in the rate of flow and pressure. The valve had V-shaped ports actuated by a diaphragm. It was found desirable to estimate the valve opening required to maintain the desired settling-chamber pressure and to set the valve at that position before opening the manually operated valve, since the automatic valve normally required approximately 30 seconds to move from fully open to fully closed. The aforementioned procedure permitted the settling-chamber pressure to be maintained constant within ±1 pound per square inch; this range was within the accuracy of the test pressure gauge used.

The variation in the settling-chamber pressure with time (without throttling) is shown in figure 24 for each of the three nozzles tested. The rapid increase in the rate of change of pressure with decrease in Mach number is due to the increase in minimum area in the nozzles with decrease in Mach number for a constant test-section area. In figure 24 the pressure was adjusted so that zero time corresponds to a tank pressure of 300 pounds per square inch. The differences in pressure at zero time for the different nozzles are representative of the change in line losses resulting from the change in mass-flow requirements.

The pressure required to establish supersonic flow at the test section (without a model installed) was measured for each set of nozzle blocks. In addition, the total duration of the test was determined for the throttled and unthrottled conditions. The results are as follows:

M	p_0 to start (lb/sq in.)	Pressure at cut-off without throttling	Test duration (sec)		Test pressure (lb/sq in.)
			Without throttling	With throttling	With throttling
2.0	23	28	110	395	28
2.8	48	58	147	368	58
4.1	157	167	165	330	167

NOZZLE PRESSURE DISTRIBUTIONS

Induction Tunnel

Measurements of the static-pressure distribution were made on one
of the side walls along a line midway between the nozzle blocks (see
fig. 10(c)). Simultaneously, measurements of the induction-jet pressure
were made to obtain an indication of the power required. The rate of
change of all the pressures was small and the response of the measuring
and recording equipment was sufficiently rapid that a time history of
the changes could be obtained. Data were obtained at approximately
10-second intervals without throttling the high-pressure air flowing
into the induction jet. The total elapsed time since the start of the
test t is given in seconds in the data figures for each distribution.

Subsonic.- The Mach numbers computed from the measured static
pressures, assuming no loss in total pressure through the tunnel, are
shown as they vary along the tunnel axis for different jet pressures in
figure 25. These pressure measurements constitute an adequate method
of calibrating this tunnel for subsonic speeds, since in this two-
dimensional tunnel the pressures at the side wall are essentially equal
to those in the free stream. A Mach number of 0.58 was obtained with
the lowest jet pressure investigated (67 lb/sq in.) and the variation
in Mach number along the axis of the tunnel in the test section (cen-
tered at the 43-in. station) was insignificant over a 6-inch length.
The tunnel was designed to have a 10-inch-length test section extending
from the 38-inch to the 48-inch stations. The Mach number at the 48-inch
station is about $1\frac{1}{2}$ percent less than that at the 38-inch station. At
Mach numbers above 0.9 the velocity gradients in the test section became
larger. Further increase in jet pressure produced velocities somewhat
in excess of Mach number 1.0 in the test section and thus provided an
indication of slightly excessive nozzle-block divergence at the test
section. Since the maximum design Mach number for this tunnel was 0.9,
no change was made in the nozzle. The longitudinal gradients at and
below Mach number 0.9 are considered to be sufficiently small. Examin-
ation of the static-pressure measurements made at orifices installed at
stations from 7 inches above to 7 inches below the center line (at the
43-inch station) showed that the vertical velocity gradient was essen-
tially zero throughout the speed range.

An analysis of calibration tests in the Langley 24-inch and 4-
by 18-inch high-speed tunnels has shown that the effects of humidity of
the entering air on the calibration of the empty tunnel were less than
1 percent for Mach numbers below 0.9 and relative humidities at stag-
nation of 60 percent or less. The required minimum humidity for model
tests will necessarily decrease because of possible local condensation.

For the test results presented, the humidity of the air at zero time was 60 percent and decreased during the test. The effects of humidity on the data presented in figure 25 at jet-chamber pressures of 152 pounds per square inch or less are believed, therefore, to be insignificant.

Supersonic.- Available information on condensation at supersonic Mach numbers (for example, references 19 to 21), although showing that the problem is serious, does not permit the limiting humidity conditions to be accurately predicted. The information, however, indicates that the degree of supersaturation in the nozzle and the length of time the supersaturated condition exists (a function of flow velocity and nozzle length) are important factors (reference 20). Time limitations on the completion of the test schedule brought about by the necessity of dismantling the equipment required that the tests of the induction tunnel at supersonic speeds be conducted during the summer months. In the test locality the prevailing high relative humidities of the atmosphere, combined with the necessity of conducting the tests in a large room, limited the minimum obtainable humidities to between 50 and 60 percent at the start of a test. Even though condensation effects were inevitable, the tests were conducted and the results are presented to determine the magnitude of the effects of excessive moisture content.

The measured distributions along the side walls obtained with the straight divergent nozzle blocks are presented in figures 26(a) and 26(b) for different humidity conditions.

The data in figure 26(a) were obtained when the relative humidity for the entrance air (stagnation pressure and temperature) at the beginning of the test was 66 percent. During the course of the test the humidity decreased through recirculation to 52 percent. Figure 26(b) is the distribution obtained on the following day, for which the initial humidity was approximately 50 percent and the final relative humidity was 38 percent.

The $M = 1.2$ nozzle blocks designed by the characteristics method produced the velocity distributions shown in figure 26(c). The data were obtained for an initial relative humidity of the entering air of 68 percent and a final value of 52 percent.

The distributions obtained along the side-wall center line with the $M = 1.4$ nozzle blocks installed are shown in figure 26(d). In these tests the initial humidity was about 55 percent and the final value was 41 percent.

The results presented showed that serious humidity effects were encountered. The most apparent condensation shocks occurred at these low-supersonic Mach numbers when the relative humidity was in excess of 50 percent (stagnation temperature about 84° F). The corresponding

moisture content of the air was in excess of approximately 0.012 pound per pound of dry air. The relatively high values of humidity that persisted during the tests did not permit an evaluation of the minimum value required to obtain valid data.

Unpublished results of recent tests in the Langley 4- by 4-foot supersonic tunnel show the effect on Mach number and the Mach number distribution through the nozzle of increasing humidity or dew point. The results presented in figure 27 show that the Mach number in the test section decreased and the distribution along the test section became more erratic as the moisture content was increased from 0.4 to 20 parts in 1,000 parts of dry air. From an analysis of the points of divergence ($M = 1.2$ for 42° F dew point to $M = 1.6$ for -10° F dew point), it is estimated that condensation will not occur at Mach numbers of 1.2 and 1.4 if the moisture content of the air is less than 2 parts in 1,000. For atmospheric stagnation pressure and a temperature of 60° F, a relative humidity of 20 percent corresponds to a moisture content of 2 parts in 1,000. From these limited results it appears that the flow through the induction tunnel would have been essentially free of condensation if the relative humidity of the entering air could have been reduced to 20 percent or less.

Effect of enclosure.- Data obtained during the tests of the induction tunnel (figs. 21, 25, and 26) generally showed that the relative humidity of the air entering the tunnel decreased between 12 and 20 percent during a test run having a duration of approximately 200 seconds. This decrease occurred in the 54,000-cubic-foot room enclosing the tunnel (see fig. 10(b)). The large room acted as a crude return passage for the tunnel. It permitted mixing of the continuous flow of dry air from the induction nozzle with the air in the room and resulted in a continuous decrease in the relative humidity of the air in the room during a test. Inasmuch as the method is essentially a mixing process between dry induction air and initially moist room air, the effectiveness of the process in reducing the humidity of the air in the room (the air that flows through the test section) obviously increases as the volume of the room decreases. Although, in the present setup (figs. 1 and 10(b)), it was not expedient to reduce the volume of the room enclosing the tunnel, some data obtained in the Langley 24-inch high-speed tunnel after it had been enclosed in a tank, as illustrated by figure 28, show the beneficial effect of a small enclosure. The results of several tests in the Langley 24-inch high-speed tunnel while the atmospheric humidity was approximately 70 percent are as follows:

Time	Relative humidity (percent)
Before test	70
At end of 1-minute test	30
At end of 4-minute test	10 to 20
30 minutes after end of test	10 to 20
24 hours after end of test	50 to 60

An enclosure for the induction tunnel of a size comparable to that of the 24-inch high-speed tunnel (fig. 28), based on volume per unit flow rate through the tunnel, is 5,700 cubic feet. From the values of humidity obtainable and required it appears that the small enclosure would permit the induction tunnel to be operated at low-supersonic Mach numbers.

Blowdown Tunnel

As previously discussed, the available boundary-layer theories are inadequate to account completely for boundary-layer growth in supersonic nozzles. Experience has shown that in the initial design a nozzle shape adequately compensated for boundary layer can be obtained only as a result of tests on the nozzle and subsequent alterations to that shape based on the test results. The tests constitute an initial evaluation only, and time did not permit the shape of the nozzles to be altered.

The Mach number distribution along the center line of the supersonic blowdown tunnel, measured at orifices installed in one of the side walls, is shown in figure 29(a) for the nozzle blocks designed for a Mach number of 2.0. The lowest settling-chamber pressure of 22 pounds per square inch is obviously too small to establish the flow, although supersonic expansion has started and the tunnel shock is located about 4 inches downstream from the throat. The small increase in pressure to a value of 23 pounds per square inch was sufficient to establish the flow through the tunnel. The distribution at higher pressures shows that the Mach number as measured at the tunnel side wall was constant at a value of about 1.96 in the region of the test section centered at the 24-inch station. Although the cause of the deceleration near the 16-inch station is not known, the distribution along the test section appears from this initial evaluation to be satisfactory.

The distribution in the nozzle designed for a Mach number of 2.8 (fig. 29(b)) shows a Mach number gradient having a total decrement along the 5-inch test section of 3 percent of the stream value. For an increase in stagnation pressure from 48 to 58 pounds per square inch, there was a slight decrease in the gradient. This increase in stagnation pressure corresponded to an increase in Reynolds number, and a decrease in the positive pressure gradient with increase in Reynolds number is generally to be expected. Although for some studies at supersonic speeds a Mach number gradient of approximately this magnitude is acceptable (reference 22), for other work, such as precise pressure measurements and shock-boundary-layer-interaction studies, a high degree of refinement is needed and a uniform velocity distribution is required. Further analysis of the data (fig. 29(b)) indicates that the small gradients were probably the result of either insufficient divergence in the test section or the close proximity of the second minimum to the test section or both.

The results for the Mach number 4.1 nozzle (fig. 29(c)) indicate a Mach number decrement along the 5-inch length of the test section of 3 percent of the stream value, as in the case of the $M = 2.8$ nozzle blocks. The average rate of decrease of Mach number is 0.02 per inch, or a total of 0.08 in 1 tunnel height for a stagnation pressure of 167 pounds per square inch or greater. Unpublished results obtained from a 9- by 9-inch tunnel having the same supersonic-nozzle shape but no divergence in the test section showed a decrease in Mach number of 0.01 per inch or 0.09 in 1 tunnel height. There is, however, one additional geometric difference between the two nozzles. In the 4-inch nozzle the second minimum started at a location less than 1 tunnel height downstream from the center line of the test section, whereas in the 9-inch nozzle the second minimum began approximately 3 tunnel heights downstream of the center line of the test section. The close proximity of the second minimum to the test section for the data in figure 29(c) could, through propagation of pressures in the subsonic part of the boundary layer, have influenced the Mach number gradient in the test section.

In regard to pressure-propagation considerations, the second minimum on the nozzle block can be represented as a line of sources placed across the nozzle block, whereas a model support strut used to form a second minimum would represent only a point source at each tunnel-wall-strut juncture. It appears, therefore, that the model support strut would have appreciably less influence on the measured side-wall pressures through pressure propagation in the boundary layer than would the conventional second minimum. Because time limitation precluded tests of these deductions in the 4- by 4-inch blowdown tunnel, brief tests were made in the 9- by 9-inch tunnel previously mentioned. The results are presented in figure 30 and show that the conventional second minimum formed on the nozzle blocks influenced the side-wall pressure measurements for a distance of approximately 0.7 tunnel height ahead of the

start of the second minimum. A model support strut installed with its span parallel to the side walls, having a cross-sectional area approximately equal to the area blocked by the second minimum, had its influence on the side-wall pressures limited to the region beginning 0.3 tunnel height downstream from the plane of the leading edge.

It is therefore recommended that a model support strut be used to form the second minimum. The strut could probably be located in the same position as the present second minimum without any appreciable adverse effects.

SCHLIEREN PHOTOGRAPHS

Photographs of the flow during the starting of the blowdown tunnel with the Mach number 2.0 nozzle blocks installed are presented as figure 31. The first photograph is the zero-flow condition and is presented to show faults in the glass windows. The second photograph at a stagnation pressure of 21 pounds per square inch corresponds to near-sonic velocities. An increase in pressure of 1 pound per square inch caused the shock to move down into the test region. Another 1-pound-per-square-inch increase in pressure caused the shock to move farther downstream. At a pressure of 24 pounds per square inch the flow was established. The photographs at stagnation pressures of 24 and 27 pounds per square inch indicate weak but not serious disturbances in the test region. The disturbed flow along the straight-line edges at the top and bottom of the photographs (figs. 31(e) and 31(f)) are indicative of boundary-layer flow.

Photographs of the starting process with Mach number 4.1 nozzle blocks installed in the tunnel are shown in figure 32. The first photograph was for the zero-flow condition and is presented to show the faults in the glass windows. The second photograph shows that an increase in stagnation pressure to 128 pounds per square inch produced supersonic velocities in the lower part of the flow in the test section, but in the upper part the flow appears to have completely separated from the nozzle block. An increase in pressure to 138 pounds per square inch produced an increase in velocity over a wider region in the test section. At 140 pounds per square inch the flow became symmetrical about the center line and contained strong oblique shocks (fig. 32(d)). A 2-pound-per-square-inch increase in pressure completely established the flow and no apparent changes occurred with further increases in pressure. The photograph of the established flow shows that the flow is practically free of any disturbances (compare figs. 32(e) and 32(f) with fig. 32(a)).

Repeat tests showed that the flow during the starting cycle was consistently unsymmetrical and separated from either the top or bottom

nozzle block. The unsymmetrical starting, although not affecting the final flow, can produce extremely high loads on a test model during the starting phase.

The photographs were obtained before the flow area through the second minimum had been enlarged 18 percent to the value as given by table II. The 15-pound-per-square-inch increase in starting pressure (see the section entitled "Performance of Tunnels") is believed to be a direct result of the unsymmetrical starting, with supersonic compression occurring on one side of the second minimum before starting had been effected.

Photographs of the flow past a 2.5-inch-chord NACA 0012 airfoil in the induction tunnel at subsonic speeds are presented as figure 33 for a 9-inch-diameter field of flow. The photographs illustrate the effect of increasing speed on the flow past the airfoil at an angle of attack of about 4°. The photographs cover a speed range from a value near the critical speed at which sonic velocity is first reached locally to the choking Mach number. The general nature of the flow is in accord with reported results of compressible-flow investigations (see references 3, 4, and 23).

CONCLUDING REMARKS

The design, development, and performance of equipment suitable for use by educational institutions in student training and basic compressible-flow research have been described. The main elements of the equipment are an induction tunnel having a 4- by 16-inch test section for high-subsonic and low-supersonic testing and a blowdown tunnel having a 4- by 4-inch test section for supersonic testing up to a Mach number of about 4.0, actuated by dry compressed air stored at a pressure of 300 pounds per square inch in a 2,000-cubic-foot tank by a 150-horsepower reciprocating air compressor. The air supply is sufficient for test runs of the order of 100 seconds at a Mach number of 1.0 in the induction tunnel and up to 400 seconds in the blowdown tunnel, depending on the stagnation pressure maintained. A $\frac{1}{2}$-hour pump-up period is generally required to reach design tank pressure after a test.

Pressure-distribution studies in the induction-tunnel nozzles revealed that the flow in the subsonic test section was satisfactorily uniform and not critically affected by the humidity of the air induced from the test room. At low-supersonic speeds (Mach numbers of 1.2 and 1.4), however, adverse condensation effects were encountered when tests were made under high humidity conditions. The results presented indicate that the installation of the induction tunnel in a small

room which acts as a return passage would permit the attainment of stagnation relative humidities of 20 percent or less. This value is estimated to be sufficiently low to permit operation at Mach numbers around 1.2. An alternate arrangement for operating the 4- by 16-inch tunnel at supersonic speeds is to equip the induction tunnel with an alternate entrance cone designed for direct blowdown. Calculations based on performance data obtained during the present tests indicate that runs of duration equal to that of the induction system at a Mach number of 1.2 and greater than that of the induction system at a Mach number of 1.4 can be obtained with direct blowdown, with the use of a fixed stagnation pressure of about 20 pounds per square inch.

Supersonic nozzles designed for Mach numbers of 2.0, 2.8, and 4.1 were tested in the blowdown tunnel and produced average Mach numbers close to the design values. The velocity distributions were sufficiently uniform for most of the intended uses of this equipment. For experimentation in which the streamwise pressure gradient is a critical factor, it would be desirable to eliminate small gradients found in the Mach number 2.8 and 4.1 nozzles. The tests indicate that this can be accomplished by locating the second minimum farther downstream.

Langley Aeronautical Laboratory
    National Advisory Committee for Aeronautics
        Langley Air Force Base, Va., June 5, 1950

APPENDIX A

REYNOLDS NUMBER

The Reynolds number can be expressed in terms of the Mach number, temperature, pressure, viscosity, and model chord as follows:

$$R = 0.3428 \frac{M p_o c}{\left(1 + 0.2 M^2\right)^3 \sqrt{T_o}\, \mu}$$

The coefficient of viscosity μ as given by Sutherland's formula for air (reference 24) is a function only of the static temperature, as follows:

$$\mu = \frac{258.3}{T + 216}\left(\frac{T}{500}\right)^{3/2} 10^{-6}$$

where

$$T = \frac{T_o}{1 + 0.2 M^2}$$

Figure 2 shows the Reynolds number per inch per pound-per-square-inch stagnation pressure plotted against Mach number for various stagnation temperatures.

APPENDIX B

CHOKING MACH NUMBERS

Subsonic.- The choke Mach number for the subsonic tunnel can be estimated by assuming one-dimensional flow and computing the Mach number of the flow in the tunnel ahead of the model which corresponds to the attainment of sonic velocity in the flow region between the model and the tunnel walls. In this region a reduction in area is produced by the model frontal area S. With the use of equations for conservation of mass and energy, the relation between the ratio of model area to tunnel test-sectional area S/A and the choke Mach number is

$$\frac{S}{A} = 1 - \frac{1.728 M_{ch}}{\left(1 + 0.2 M_{ch}^2\right)^3} \tag{B1}$$

The equation is graphically presented in figure 3(a).

The values of choke Mach number from equation (B1) represent maximum theoretical values. The tunnel-wall boundary layers, however, can be affected by the flow field of the model and thereby affect the flow area in the region of the model by changing it from the assumed value. As a result of the change in the boundary layer, experimental values of the choke Mach number can be obtained that are in excess of those computed, but, generally, equation (B1) gives a good approximation (reference 25).

Supersonic.- A similar choking condition exists in the supersonic Mach number range. In general, however, it is not possible to start the flow in a supersonic tunnel for choking-model proportions as computed from equation (B1). The additional factor is the tunnel normal shock which generally occurs during the starting process. The normal shock, with its attendant decrease in total pressure, produces a reduction in mass flow per unit area. If equation (B1) is applied downstream of the normal shock corresponding to the design Mach number, the relation between the ratio of the model area to the test-section area and the minimum supersonic Mach number at which the tunnel will start is

$$\frac{S}{A} = 1 - \frac{\left(M^2 + 5\right)^{1/2}\left(7M^2 - 1\right)^{5/2}}{216 M^6} \tag{B2}$$

Equation (B2) is shown graphically in figure 3(b).

APPENDIX C

REQUIRED PRESSURE RATIOS FOR SUPERSONIC TUNNELS

The pressure ratio required to establish supersonic flow in the test section of a blowdown tunnel such as that shown in figure 14 can be divided into ratios required to counteract two separate types of losses - viscous and compression shock. The pressure ratio needed for the viscous losses depends on the general tunnel design, particularly on the diffuser efficiency (references 6, 7, 22, and 26). Since the viscous losses change only slightly beyond $M = 1.0$ (reference 6), it is assumed for estimation purposes that the ratio is constant for Mach numbers between 1.0 and 4.0. The pressure ratio required to counteract the shock losses can be readily estimated from the theoretical loss in total pressure across a normal shock at the desired test Mach number. The estimated pressure ratio required to start the blowdown tunnel is thus the product of the pressure ratio required to operate at a Mach number of 1.0, $\left(\dfrac{p_2}{p_e}\right)_{M=1}$, and the total-pressure loss across a normal shock. That is,

$$\frac{p_2}{p_e} = \left(\frac{p_2}{p_e}\right)_{M=1}\left(\frac{7M^2 - 1}{6}\right)^{5/2}\left(\frac{M^2 + 5}{6M^2}\right)^{7/2} \tag{C1}$$

Equation (C1) is shown graphically in figure 4 for typical sonic-pressure ratios of 1.15 and 1.25 (references 6, 7, 22, and 26).

APPENDIX D

SUPERSONIC-TUNNEL SIZE REQUIREMENTS

The minimum tunnel height for a given model chord $\left(\dfrac{h}{c}\right)_{min}$ is determined primarily by considerations of shock reflection rather than choking. A shock reflected from the tunnel walls which strikes the model affects the pressures and forces acting on the model. It is necessary, therefore, that the ratio of tunnel height to model chord be sufficiently large to prevent reflected shocks from striking the model. A first approximation to the required h/c values can be determined by assuming a weak shock or Mach line originating from the leading edge of a flat plate of insignificant thickness or an extremely slender body, either body being at zero angle of attack in the center of the tunnel. For the weak shock,

$$\frac{h}{c} = \tan \text{ arc } \sin \frac{1}{M}$$

or

$$\left(\frac{h}{c}\right)_{min} = \frac{1}{\sqrt{M^2 - 1}} \tag{D1}$$

Values of $\left(\dfrac{h}{c}\right)_{min}$ from equation (D1) are tabulated at the end of this appendix.

A second and more practical approximation to the minimum height-chord ratio can be obtained by determining the value of h/c required to avoid interference from a reflected strong shock generated by a flat plate at an angle of attack. The angle of attack chosen was the maximum value for each stream Mach number that would permit supersonic flow to be retained throughout the flow field. The shock was inclined at an angle β to the flow direction ahead of the shock and produced a flow deviation δ equal and opposite to the flow deviation at the reflected shock. The Mach number of the flow behind the reflected shock was 1.0. Values of the initial shock angle β_1, the reflected shock angle β_2, and δ were obtained from reference 24. For the strong shock,

$$\left(\frac{h}{c}\right)_{min} = \frac{2 \tan \beta_1 \tan (\beta_2 - \delta)}{\tan \beta_1 + \tan (\beta_2 - \delta)} \tag{D2}$$

The ratios of tunnel height to model chord for detached shocks cannot be readily determined theoretically. A rough approximation can be obtained, however, by using an empirical method (reference 27). The following table presents the values of $\left(\frac{h}{c}\right)_{min}$ computed for the starting condition and the various shock-reflection conditions for several Mach numbers:

Test Mach number	Values of $\left(\frac{h}{c}\right)_{min}$				
	To start $\frac{y}{c} = 0.09$	Weak shock	Strong shock	Detached shock	Suggested practical value
1.2	3.9	1.5	2.1	7	9
1.4	1.4	1.0	1.5	3	4
2.0	.5	.6	1.0	-	1.3
3.0	.3	.4	.8	-	1.0
4.0	.3	.3	.8	-	1.0

The detached-shock cases are of interest primarily at the lower Mach numbers and were computed only for $M = 1.2$ and $M = 1.4$. The table shows that the strong-shock or detached-shock conditions require tunnel heights considerably in excess of those for which starting can be effected. In practice it is necessary to use values of h/c somewhat larger than the largest values in the table to allow for the presence of tunnel-wall boundary layer and to permit the reflected shocks to pass appreciably downstream of the trailing edge. If the shocks lie closer than about $0.1c$ to the trailing edge, they can appreciably affect the airfoil characteristics through interaction with the wake and boundary layer. Suggested values of $\left(\frac{h}{c}\right)_{min}$ for use as a guide in tunnel-design applications were obtained by multiplying the largest values for the strong-shock or detached-shock cases by the factor 1.3, based on experience (last column of preceding table).

A secondary consideration which affects the width of supersonic tunnels is the disturbance which occurs at the intersection of the leading edge of airfoil models and the side-wall boundary layers of the tunnel. This disturbance affects the flow in roughly conical regions originating near the leading-edge - wall juncture. The effect can be

eliminated in center-line pressure-distribution tests by employing a sufficiently large ratio of tunnel width to model chord, so that the intersection of the conical-disturbance zone takes place downstream of the trailing edge at the tunnel center line. In small equipment at the lower-supersonic Mach numbers, however, it is generally impossible to avoid the effect because to do so would require prohibitively large ratios of model span to model chord. The best that can be done in this case is to measure the magnitudes of the disturbances and to apply approximate corrections if they are significantly large.

DURATION OF TEST RUN

Without throttling.- The duration of a test run is the time required for the pressure in the tank to drop from its initial design pressure p_1 to the minimum pressure of the test run p_2. The air is assumed to flow out through an area A_m at sonic velocity and the decrease in pressure in the tank is accomplished through a polytropic expansion. The tank-pressure variation with time can be determined from thermodynamic relations as follows:

The polytropic gas law in derivative form is

$$\frac{dp}{dt} = n\frac{p}{\rho}\frac{d\rho}{dt}$$

From the gas relations

$$\rho = \frac{w}{vg}$$

and

$$\frac{p}{\rho} = \frac{RgT}{144}$$

there is obtained

$$\frac{dp}{dt} = \frac{nRT}{144v}\frac{dw}{dt} \tag{E1}$$

For flow out of the tank at sonic velocity through an area A_m, the change in weight of air in the tank per unit of time is

$$\frac{dw}{dt} = -\frac{A_m p}{1.46}\sqrt{\frac{g}{RT}} \tag{E2}$$

The instantaneous values of pressure p and temperature T in equations (E1) and (E2) are the same in the absence of throttling or line losses. Combining equations (E1) and (E2) yields

$$\frac{dp}{dt} = -\frac{nA_m\sqrt{RgT_1}}{1.46v}p\left(\frac{p}{p_1}\right)^{\frac{n-1}{2n}} \tag{E3}$$

Integrating equation (E3) to determine the time t required for the pressure to decrease from p_1 to p_2 leads to

$$t = \frac{0.0706}{n - 1} \frac{v}{A_m} \frac{144}{\sqrt{T_1}} \left[\left(\frac{p_1}{p_2} \right)^{\frac{n-1}{2n}} - 1 \right] \qquad (E4)$$

For an isothermal expansion of the air in the tank,

$$t = 0.0353 \frac{v}{A_m} \frac{144}{\sqrt{T_1}} \log_e \frac{p_1}{p_2} \qquad (E5)$$

Equations (E4) and (E5) are shown graphically in figure 5 for different values of n. The values of n are chosen to cover various gas processes from an isothermal, wherein the temperature in the tank remains constant, to an adiabatic $(n = 1.4)$, in which no heat is taken from or added to the air during the expansion process.

   With throttling.- In many tests it is highly desirable that the stagnation pressure of the air entering the nozzle be maintained at a constant value, in which case the high-pressure air supply must be throttled either through manual or automatic pressure-regulating equipment. For the throttled condition, the value of pressure in equation (E2 is the constant stagnation pressure p_2 at A_m. The test duration for the throttled condition can then be determined in the same manner as in the preceding section (equations (E1) to (E5)) by using a modified form of equation (E2). For a polytropic expansion in the tank,

$$t = \frac{0.0706}{n + 1} \frac{v}{A_m} \frac{144}{\sqrt{T_1}} \left[1 - \left(\frac{p_2}{p_1} \right)^{\frac{n+1}{2n}} \right] \frac{p_1}{p_2} \qquad (E6)$$

For isothermal expansions,

$$t = 0.0353 \frac{v}{A_m} \frac{144}{\sqrt{T_1}} \left(\frac{p_1}{p_2} - 1 \right) \qquad (E7)$$

Plots of equations (E6) and (E7) are presented in figure 6.

   Heat-transfer effects.- Some of the heat from the walls of the compressed-air-storage tank and connecting pipe lines is transferred to the compressed air during a blowdown. As a result, the gas process tends to approach an isothermal condition $(n = 1.0)$. This effect

results in an increase in test duration, as indicated by figures 5 and 6. The beneficial effect of heating is, of course, dependent on the rate of evacuation of the tank. In cases in which the tank is evacuated in only a few seconds, the heating effect can be neglected and an adiabatic process can be assumed. In computations to estimate the test duration or tank volume required, an adiabatic process is generally assumed in order to provide conservative values.

APPENDIX F

FREQUENCY OF TESTS

The frequency of the tests so far as the equipment is concerned is determined by the minimum time required to recharge the air-storage tank to its designed pressure p_1 following a test in which the pressure has dropped to p_2. Since the compressor will handle a fixed quantity of air expressed in cubic feet of free air per minute Q, the time required can be determined from thermodynamic relations and is

$$t_c = \frac{60vT_a}{Qp_a}\left(\frac{p_1}{T_1} - \frac{p_2}{T_2}\right)$$

With the use of a polytropic process in the air-storage tank, as in appendix E, the time for recharging becomes

$$t_c = \frac{60v}{Q}\frac{T_a}{p_aT_1}\left[p_1 - p_2\left(\frac{p_1}{p_2}\right)^{\frac{n-1}{n}}\right] \tag{F1}$$

This relation can be simplified, if isothermal changes in the tank are assumed, to the expression usually given by compressor manufacturers as

$$t_c = \frac{60v}{14.7Q}(p_1 - p_2) \tag{F2}$$

Equations (F1) and (F2) are presented graphically in figure 7 with the following assumed values:

$$T_a = 520^{\circ}\ R$$

$$T_1 = 560^{\circ}\ R$$

$$p_a = 14.7\ \text{pounds per square inch}$$

and

$$p_1 = 300\ \text{pounds per square inch}$$

APPENDIX G

PRINCIPLES OF SCHLIEREN SYSTEM

The principle upon which the schlieren system operates is illus-
trated by figure 17, in which a perfect optical system is assumed. A
light source is placed at the principal focus of a collecting lens and
produces a column of essentially parallel light. The parallel beam of
light passes through a test region to a condensing lens at a distance o
from the test region. An image of the light source is then formed by
the condensing lens at its principal focus, a distance f_2 from the
lens. Beyond the principal focus the light diverges and falls upon a
screen at a distance i from the collecting lens. The distance i is
adjusted so that the test region is focused on the screen by the con-
densing lens. The distances are related in accordance with the simple
lens formula as follows:

$$\frac{1}{o} + \frac{1}{i} = \frac{1}{f_2}$$

If a knife edge is inserted at the principal focus of the condensing
lens and is moved into the image of the light source so that part of the
light-source image is masked by the knife edge, the illumination on the
screen will be uniformly decreased by the amount of light cut off. If,
now, a glass wedge is placed in the upper part of the test region so
that light is deviated upward, that light ray will pass over the knife
edge and will increase the illumination on the screen in the region of
the image of the glass wedge. Conversely, the light deviated downward
by a similar wedge will fall upon the knife edge and be blocked, so that
a region of lesser illumination occurs on the screen. If the knife edge
is removed from the system, then the deviation of the light at the test
region by the glass wedges will not be apparent on the screen because
the wedges are focused by the condensing lens on the screen. Thus, the
effect at the screen of moderate angular deviations of light in the
plane of observation would be nullified by the lens. The deviated light
rays, however, undergo a displacement at the principal focus of the
condensing lens. It is the blocking or passing of the refracted light
rays by a knife edge that is utilized by a schlieren system in flow
visualization. The glass wedges assumed in figure 17 produce the same
effect as density gradients that occur in the air flowing around a test
model. (Additional information on schlieren systems is given in the
section entitled "Auxiliary Equipment.")

REFERENCES

1. Stack, John: The N.A.C.A. High-Speed Wind Tunnel and Tests of Six Propeller Sections. NACA Rep. 463, 1933.

2. Stack, John, Lindsey, W. F., and Littell, Robert E.: The Compressibility Burble and the Effect of Compressibility on Pressures and Forces Acting on an Airfoil. NACA Rep. 646, 1938.

3. Stack, John: Compressible Flow in Aeronautics. Jour. Aero. Sci., vol. 12, no. 2, April 1945, pp. 127-148.

4. Daley, Bernard N., and Humphreys, Milton D.: Effects of Compressibility on the Flow past Thick Airfoil Sections. NACA TN 1657, 1948.

5. Ferri, Antonio: Completed Tabulation in the United States of Tests of 24 Airfoils at High Mach Numbers (Derived from Interrupted Work at Guidonia, Italy, in the 1.31- by 1.74-Foot High-Speed Tunnel). NACA ACR L5E21, 1945.

6. Crocco, Luigi: High-Speed Wind Tunnels. Translation No. 366, Materiel Command, U. S. Army Air Corps, July 30, 1943.

7. Lilley, G. M.: Some Notes on the Performance of Small High Speed Wind Tunnels. Rep. No. 23, College of Aero. (Cranfield), Dec. 1948.

8. Keenan, J. H., and Neumann, E. P.: A Simple Air Ejector. Jour. Appl. Mech., vol. 9, no. 2, June 1942, pp. A-75 - A-81.

9. Winter, H.: On the Use of Jet Drives for Wind Tunnels of High Velocity. Translation 219, David Taylor Model Basin, Navy. Dept., April 1947. (Also available from CADO, Wright-Patterson Air Force Base, as ATI 20179.)

10. Keenan, J. H., Neumann, E. P., and Lustwerk, F.: An Investigation of Ejector Design by Analysis and Experiment. Guided Missiles Program, M.I.T. Meteor Rep. No. 18, June 1, 1948.

11. Prandtl, L., and Busemann, A.: Näherungsverfahren zur zeichnerischen Ermittlung von ebenen Strömungen mit Überschallgeschwindigkeit. Stodola Festschrift, Zürich and Leipzig, 1929, pp. 499-509.

12. Ferri, Antonio: Elements of Aerodynamics of Supersonic Flows. The Macmillan Co., 1949.

13. Tetervin, Neal: Approximate Formulas for the Computation of Turbulent Boundary-Layer Momentum Thicknesses in Compressible Flows. NACA ACR L6A22, 1946.

14. Tucker, Maurice: Approximate Turbulent Boundary-Layer Development in Plane Compressible Flow along Thermally Insulated Surfaces with Application to Supersonic-Tunnel Contour Correction. NACA TN 2045, 1950.

15. Kantrowitz, Arthur, and Donaldson, Coleman duP.: Preliminary Investigation of Supersonic Diffusers. NACA ACR L5D20, 1945.

16. Wood, Robert W.: Physical Optics. The Macmillan Co., 1919, pp. 94-98.

17. Schardin, Hubert: Toepler's Striation Method. Principles for Its Application and Quantitative Evaluation. British Air Ministry Translation No. 249, May 30, 1935.

18. Keagy, W. R., Ellis, H. H., and Reid, W. T.: Schlieren Techniques for the Quantitative Study of Gas Mixing. Battelle Memorial Inst., Rand Rep. R-164, Aug. 1949.

19. Hermann, R.: Condensation Shock Waves in Supersonic Wind Tunnel Nozzles. R.T.P. Translation No. 1581, British Ministry of Aircraft Production. (From Luftfahrtforschung, vol. 19, no. 6, June 20, 1942, pp. 201-209.)

20. Volmer, Max: Kinetik der Phasenbildung. Theodor Steinkopff (Dresden und Leipzig), 1939.

21. Oswatitsch, Kl.: Condensation Phenomena in Supersonic Nozzles. R.T.P. Translation No. 1905, British Ministry of Aircraft Production. (From Z.f.a.M.M., Bd. 22, Heft 1, Feb. 1942, pp. 1-14.)

22. Puckett, Allen E.: Performance of the 12-Inch Wind Tunnel. Memo. 4-52, Jet Propulsion Lab., C.I.T., June 1, 1949.

23. Becker, John V.: Characteristics of Wing Sections at Transonic Speeds. NACA - University Conference on Aerodynamics. Langley Aeronautical Laboratory, Langley Field, Va., June 21-23, 1948, Durand Reprinting Committee, C.I.T. (Pasadena), July 1948, pp. 127-149.

24. The Staff of the Ames 1- by 3-Foot Supersonic Wind-Tunnel Section: Notes and Tables for Use in the Analysis of Supersonic Flow. NACA TN 1428, 1947.

25. Byrne, Robert W.: Experimental Constriction Effects in High-Speed Wind Tunnels. NACA ACR L4L07a, 1944.

26. Ackeret, J.: High-Speed Wind Tunnels. NACA TM 808, 1936.

27. Moeckel, W. E.: Approximate Method for Predicting Form and Location of Detached Shock Waves ahead of Plane or Axially Symmetric Bodies. NACA TN 1921, 1949.

TABLE I.- INDUCTION-TUNNEL NOZZLE-BLOCK ORDINATES

[Refer to fig. 12]

M = 1.0		M = 1.2		M = 1.4		Straight divergent	
x	h/2	x	h/2	x	h/2	x	h/2
0	12.000	0	12.000	0	12.000	0	12.00
.200	11.864	1.000	11.316	.978	11.370	2.00	10.75
.400	11.734	2.000	10.762	2.000	10.750	4.00	9.73
.600	11.610	4.000	9.867	3.232	10.092	6.00	8.93
.800	11.502	6.000	9.248	4.000	9.730	8.00	8.31
1.000	11.389	8.000	8.779	6.000	8.926	10.00	7.83
2.000	10.893	10.000	8.456	8.000	8.310	12.00	7.47
4.000	10.153	12.000	8.200	10.000	7.830	14.00	7.22
6.000	9.661	14.000	8.042	12.000	7.466	16.00	7.07
8.000	9.315	16.000	7.930	14.000	7.220	18.00	7.04
10.000	9.037	18.000	7.868	14.947	7.136	19.50	7.04
12.000	8.818	20.000	7.819	15.947	7.074	20.50	7.062
14.000	8.637	22.000	7.793	16.947	7.053	43.00	7.552
16.000	8.487	22.650	7.788	17.850	7.044	70.00	8.14
18.000	8.364	23.750	7.784	18.000	7.043		
20.000	8.263	24.150	7.783	18.240	7.042		
22.000	8.187	27.000	7.782	19.500	7.041		
24.000	8.122	27.753	7.782	20.947	7.041		
26.000	8.080	28.199	7.784	21.285	7.044		
28.000	8.042	28.644	7.787	21.637	7.050		
30.000	8.017	29.090	7.792	22.003	7.059		
32.000	8.006	29.535	7.798	22.369	7.072		
33.000	8.003	29.981	7.807	22.721	7.088		
33.600	8.002	30.426	7.818	23.073	7.106		
34.100	8.001	30.872	7.831	23.425	7.127		
36.000	8.000	31.317	7.844	23.791	7.152		
38.000	8.000	31.763	7.857	24.157	7.180		
39.000	8.016	32.208	7.870	26.988	7.428		
40.000	8.032	32.654	7.883	29.044	7.590		
42.000	8.064	33.099	7.895	30.677	7.704		
44.000	8.096	33.545	7.907	32.057	7.789		
46.000	8.129	33.991	7.918	33.283	7.854		
47.000	8.145	34.436	7.929	34.606	7.911		
48.000	8.161	34.882	7.940	35.733	7.951		
49.000	8.192	35.327	7.951	36.831	7.979		
50.000	8.247	35.773	7.960	38.000	8.000		
51.000	8.327	36.218	7.970	39.000	8.014		
52.000	8.434	36.664	7.979	40.000	8.027		
53.000	8.555	37.109	7.987	41.000	8.041		
54.000	8.677	37.555	7.994	42.000	8.054		
56.000	8.924	38.000	8.000	43.000	8.068		
58.000	9.175	39.000	8.014	45.000	8.095		
60.000	9.429	40.000	8.027	47.000	8.122		
62.000	9.686	43.000	8.068	49.000	8.164		
64.000	9.947	46.000	8.109	52.000	8.406		
66.000	10.211	49.000	8.164	56.000	8.902		
68.000	10.479	52.000	8.406	60.000	9.412		
69.000	10.614	56.000	8.902	64.000	9.937		
70.000	10.750	60.000	9.412	70.000	10.750		
		66.000	10.204				
		70.000	10.750				

NACA

TABLE II.- BLOWDOWN-TUNNEL NOZZLE-BLOCK ORDINATES

[Refer to fig. 16]

M = 2.0		M = 2.8		M = 4.1	
x	h/2	x	h/2	x	h/2
0	5.000	0	5.000	0	5.000
.500	4.997	.500	4.998	.733	4.950
1.000	4.952	1.000	4.960	1.350	4.800
2.000	4.773	2.000	4.739	2.000	4.500
3.000	4.450	3.000	4.335	2.300	4.300
4.000	4.007	5.000	3.274	2.945	3.750
5.000	3.460	7.000	2.230	3.675	2.975
6.000	2.830	9.000	1.284	4.575	1.925
7.000	2.290	10.000	.977	5.525	.874
8.000	1.625	11.000	.635	6.200	.420
9.000	1.284	11.560	.580	7.390	.200
9.500	1.232	12.160	.556	8.077	.173
9.900	1.215	12.250	.554	8.910	.164
10.210	1.210	12.370	.552	9.775	.163
10.370	1.209	13.100	.550	10.222	.163
11.000	1.208	13.500	.550	10.444	.178
11.500	1.208	13.638	.558	10.556	.202
11.920	1.213	13.775	.578	10.778	.298
12.341	1.227	14.050	.642	10.889	.359
12.761	1.251	14.325	.728	11.111	.472
13.181	1.280	14.600	.828	11.556	.672
13.602	1.339	14.875	.934	12.000	.843
14.022	1.396	15.150	1.035	12.889	1.121
14.443	1.454	15.700	1.215	13.778	1.338
14.863	1.513	16.250	1.363	14.222	1.429
15.704	1.631	16.800	1.491	14.667	1.511
16.544	1.739	17.350	1.612	15.111	1.584
16.965	1.783	17.900	1.697	15.556	1.649
17.805	1.853	18.450	1.778	16.000	1.707
18.646	1.906	19.000	1.845	16.889	1.803
19.487	1.948	19.550	1.900	17.778	1.876
20.327	1.978	20.100	1.943	18.667	1.931
21.115	1.996	20.650	1.974	19.111	1.953
21.500	2.000	21.245	1.992	20.000	1.981
27.500	2.026	21.625	1.998	20.444	1.991
28.250	2.026	21.875	2.000	21.185	1.999
30.125	2.004	27.500	2.025	27.500	2.027
31.000	1.980	27.750	2.022	28.000	2.028
32.500	1.910	28.000	2.008	28.500	2.006
33.875	1.828	28.500	2.055	29.000	1.959
34.268	1.814	29.000	1.982	29.750	1.858
34.650	1.813	29.750	1.763	30.500	1.760
34.750	1.815	30.375	1.682	31.000	1.710
34.910	1.820	30.750	1.655	31.500	1.686
39.000	2.000	31.186	1.654	32.000	1.693
		39.000	2.000	39.000	2.000

NACA
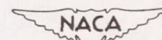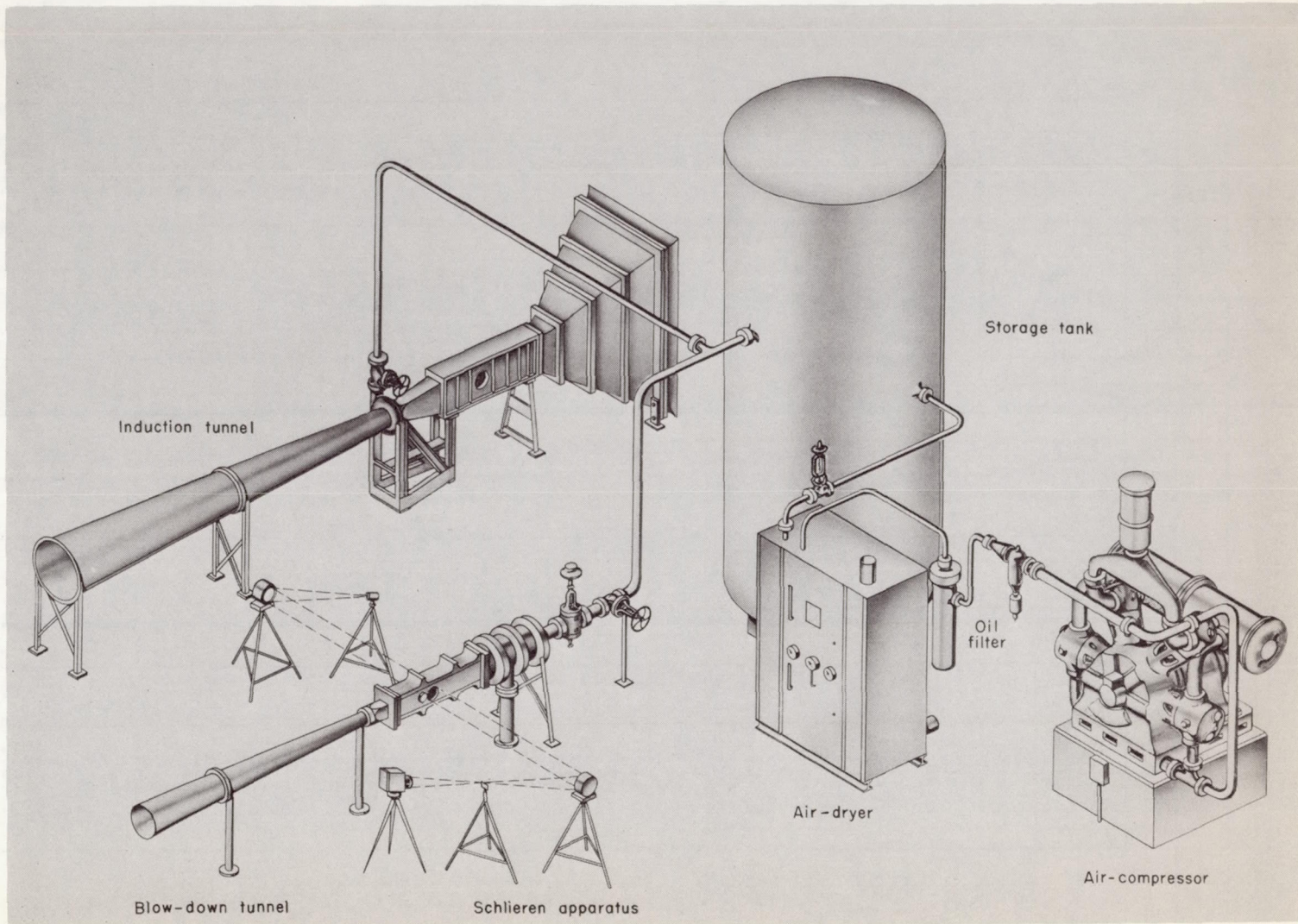
Figure 1.- Pictorial layout of the unit.

L-64349
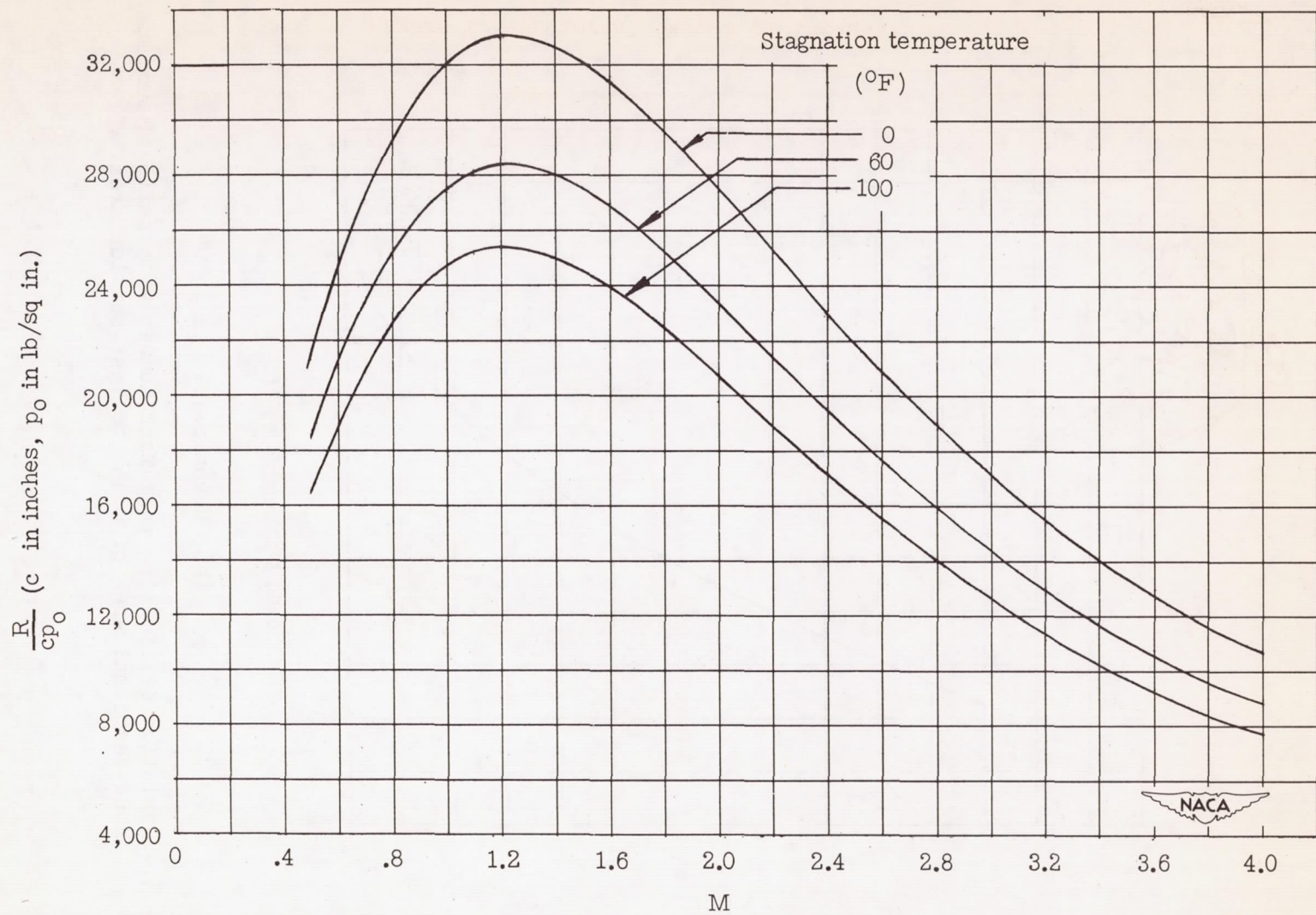
Figure 2.- Variation of Reynolds number with Mach number.
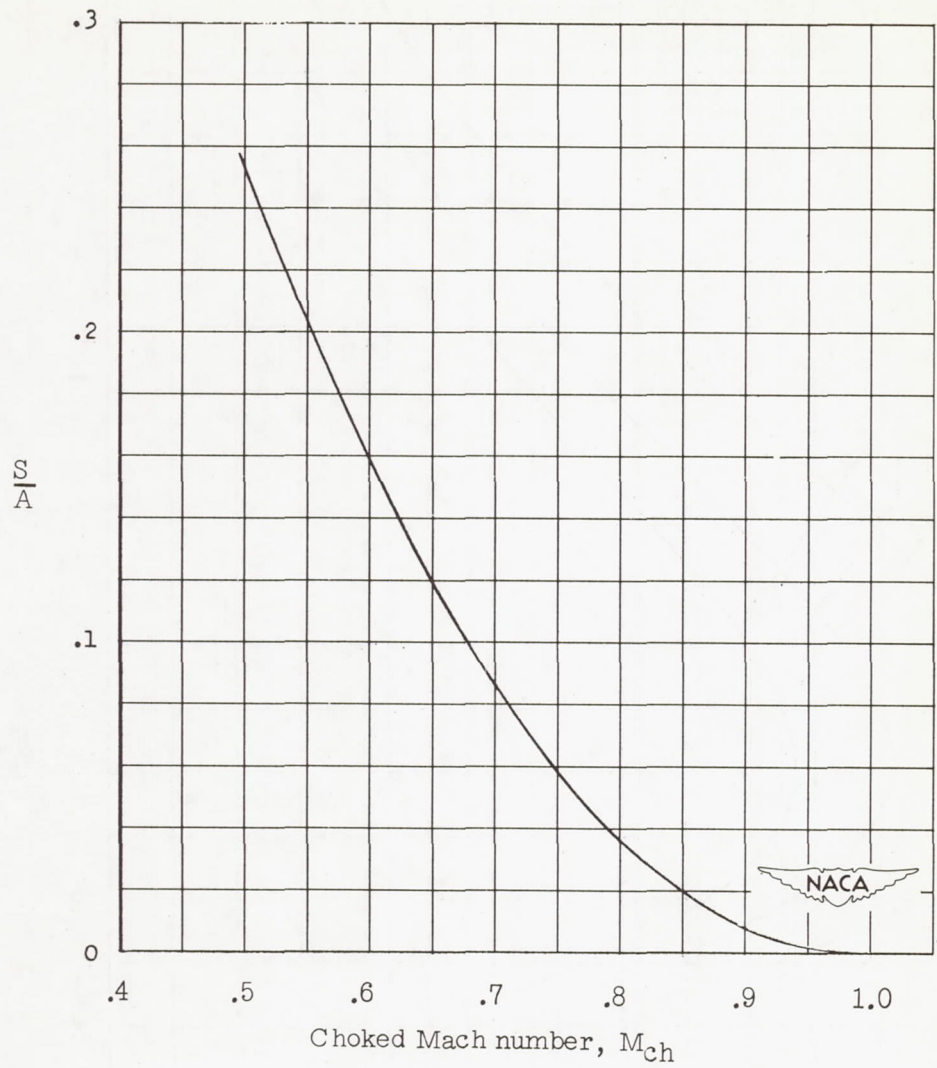
(a) Subsonic.

Figure 3.- Variation of limiting test Mach number with ratio of maximum cross-sectional area of model to test-section area.
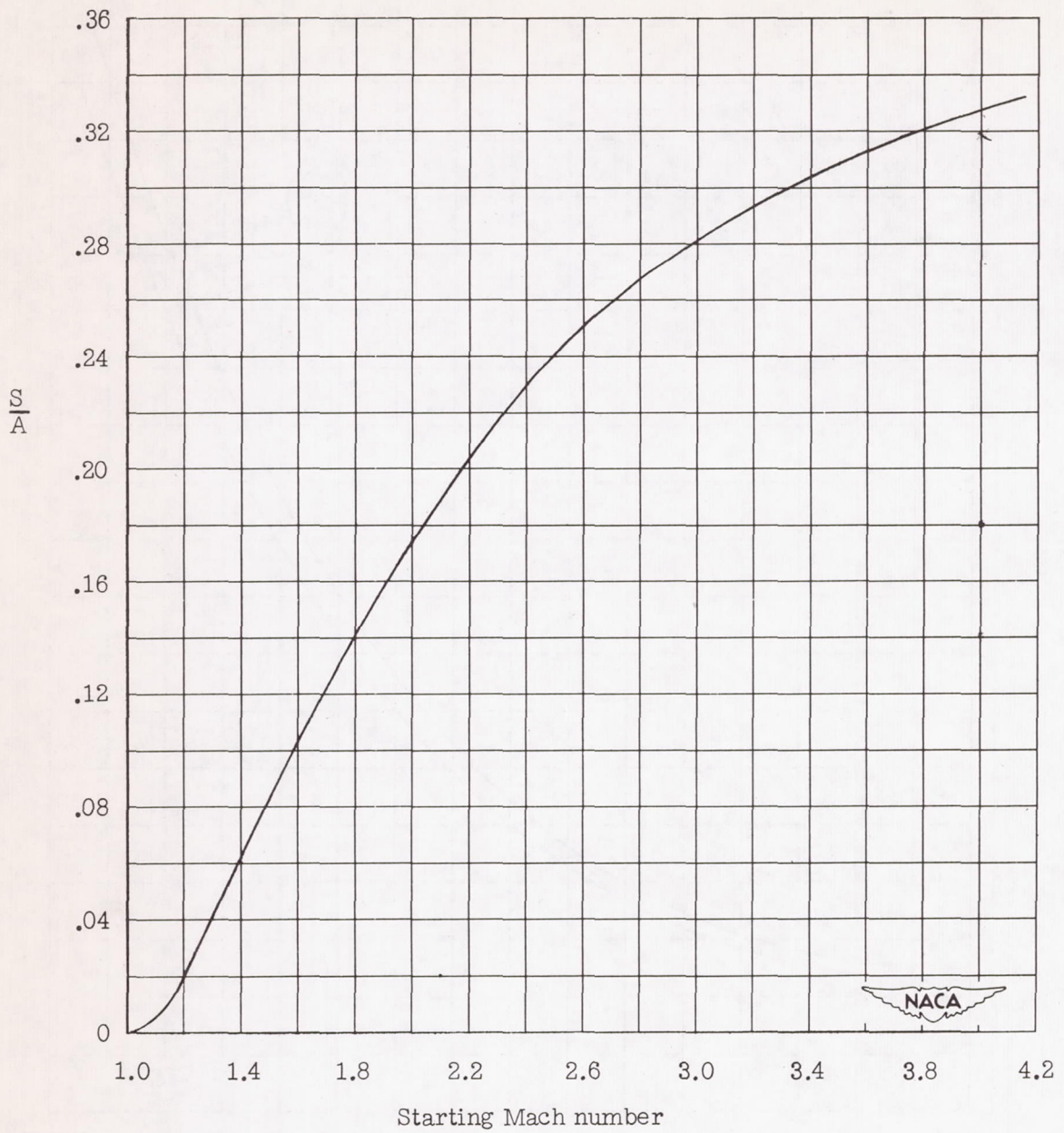
(b) Supersonic.

Figure 3.- Concluded.
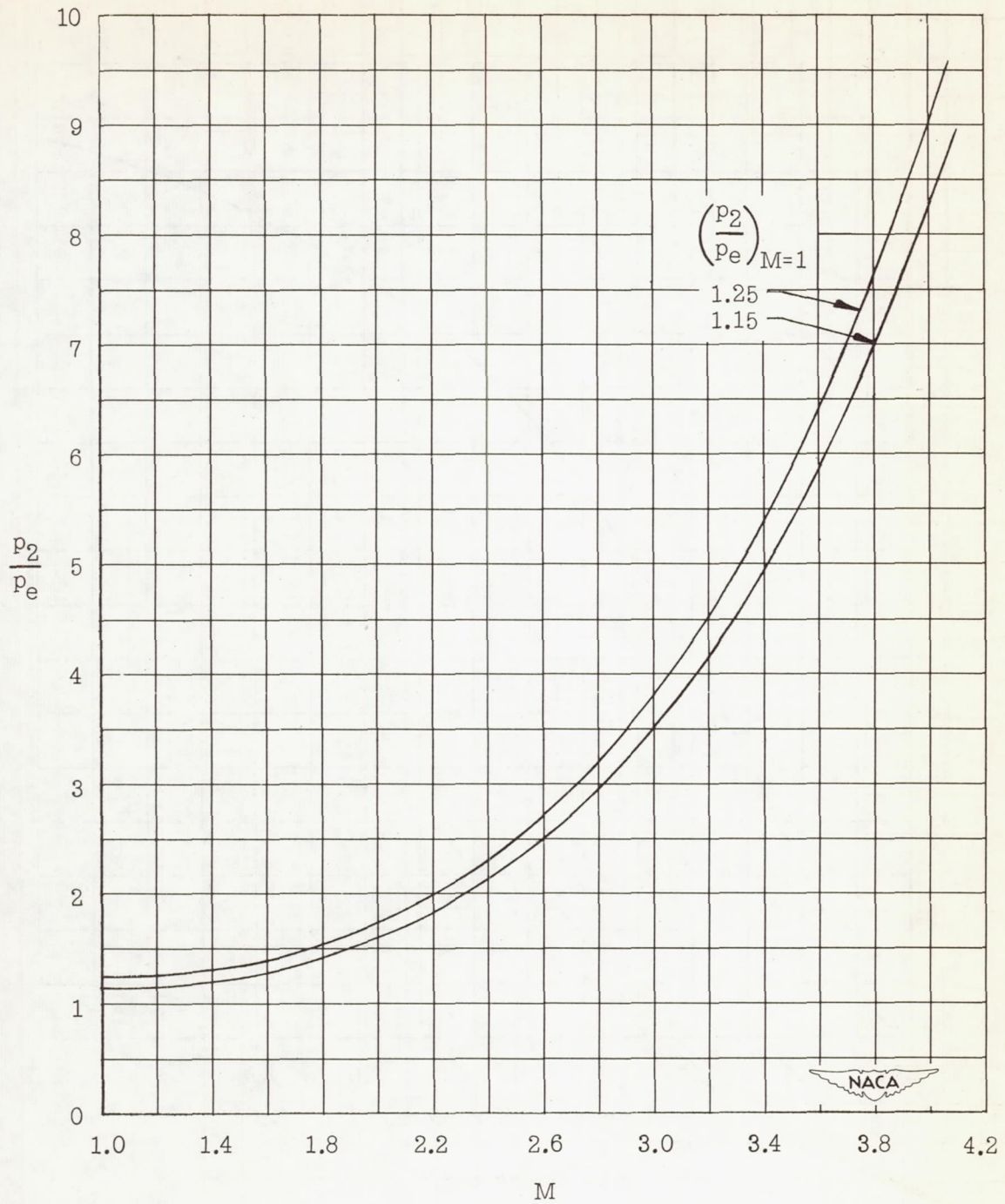
Figure 4.- Variation with test Mach number of pressure ratio required to start supersonic tunnels.
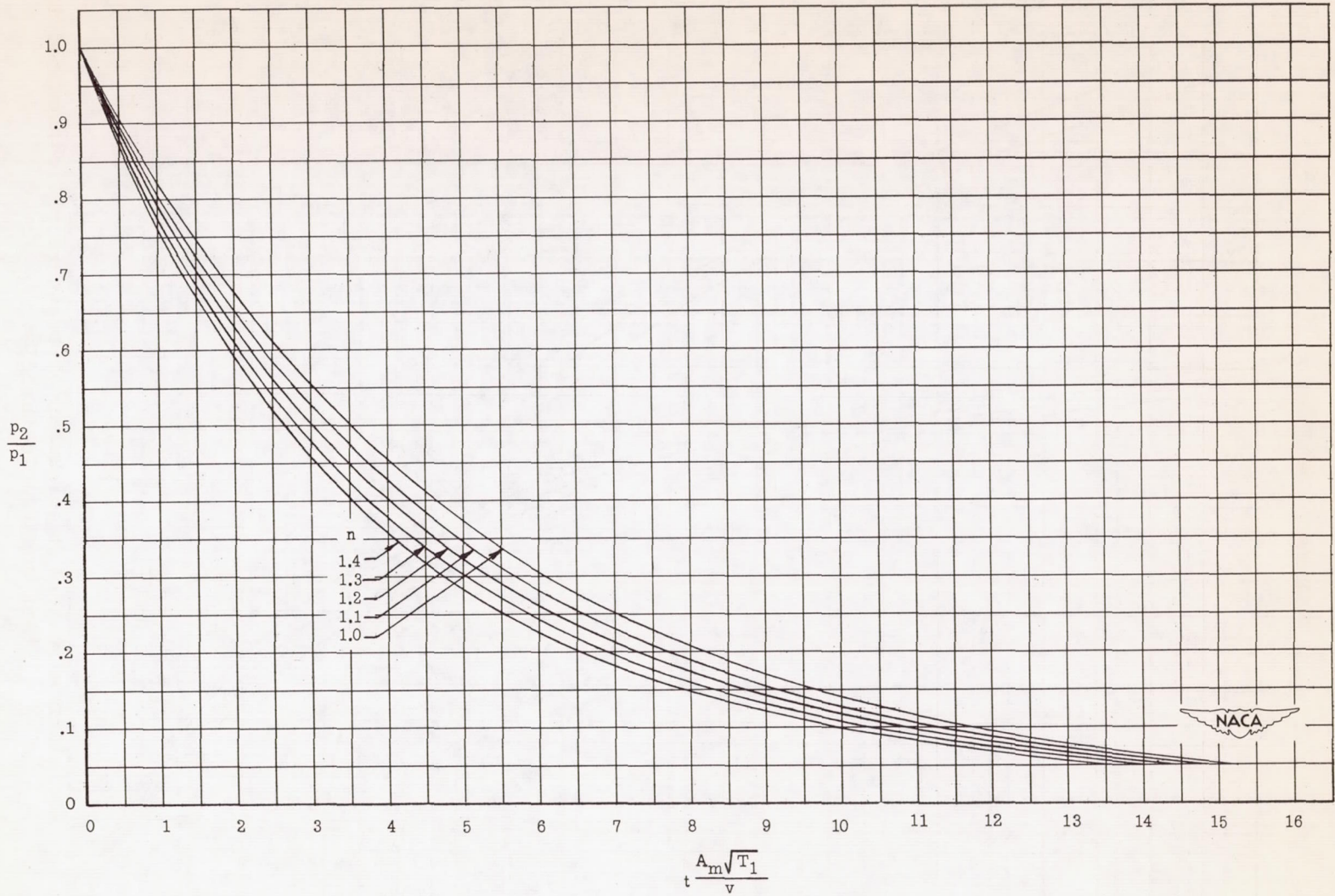
Figure 5.- Variation of pressure with time in compressed-air-storage tank (without throttling).
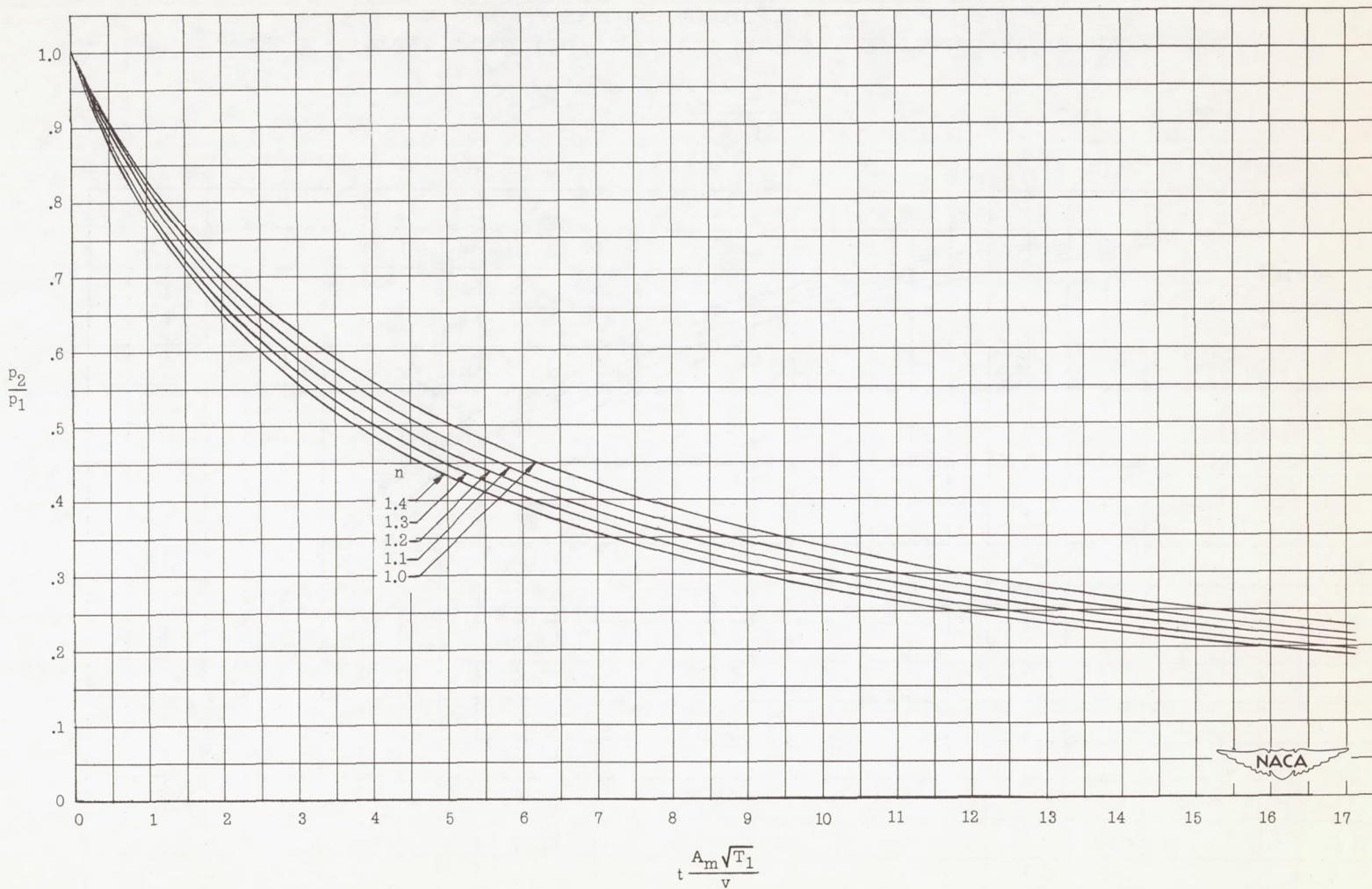
(a) High-pressure range.

Figure 6.- Variation of pressure with time in compressed-air-storage tank with throttling to a constant pressure p_2 ahead of minimum duct area.
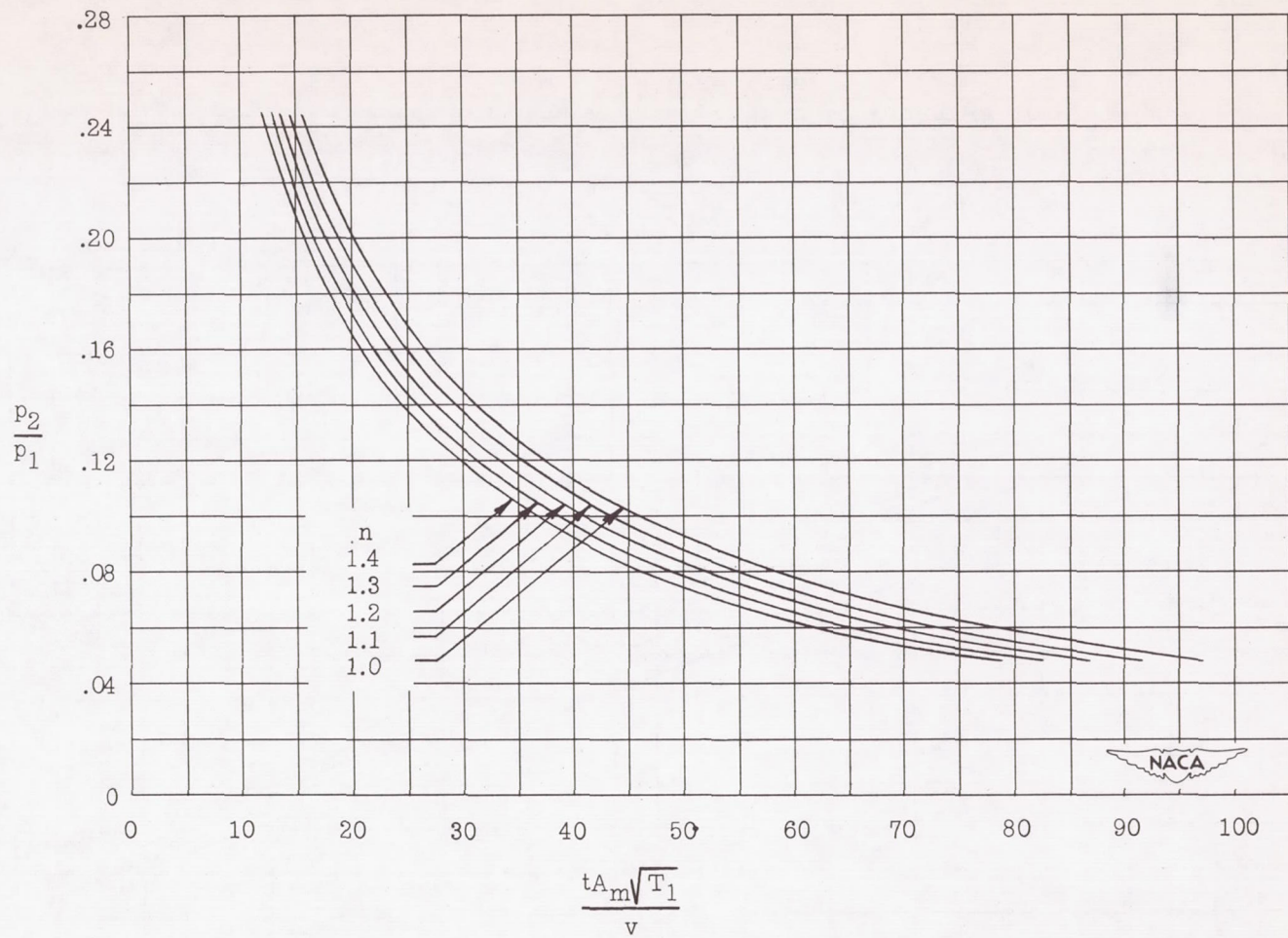
(b) Low-pressure range.

Figure 6.- Concluded.
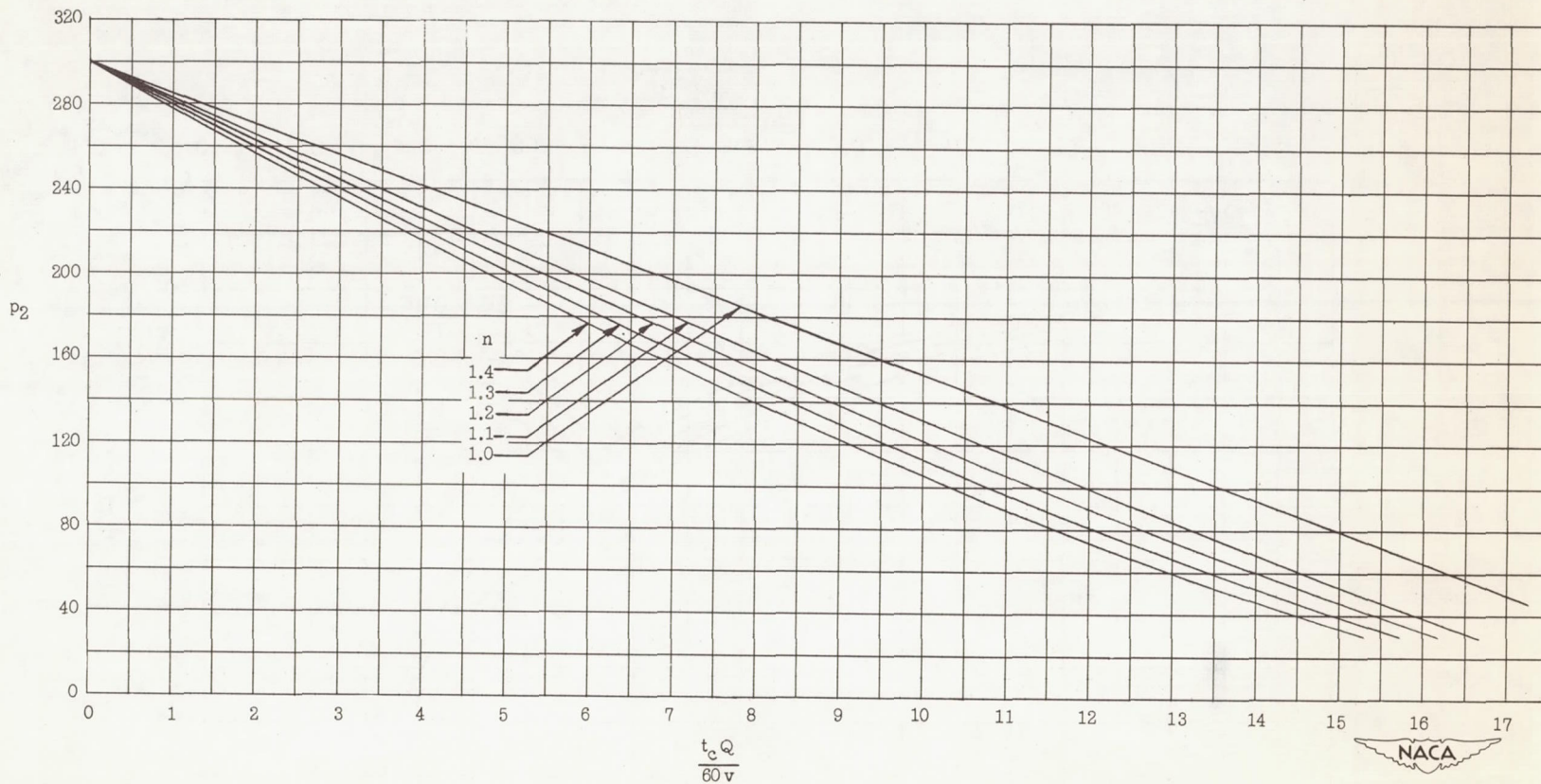
Figure 7.- Time required for compressor to recharge compressed-air-
storage tank.
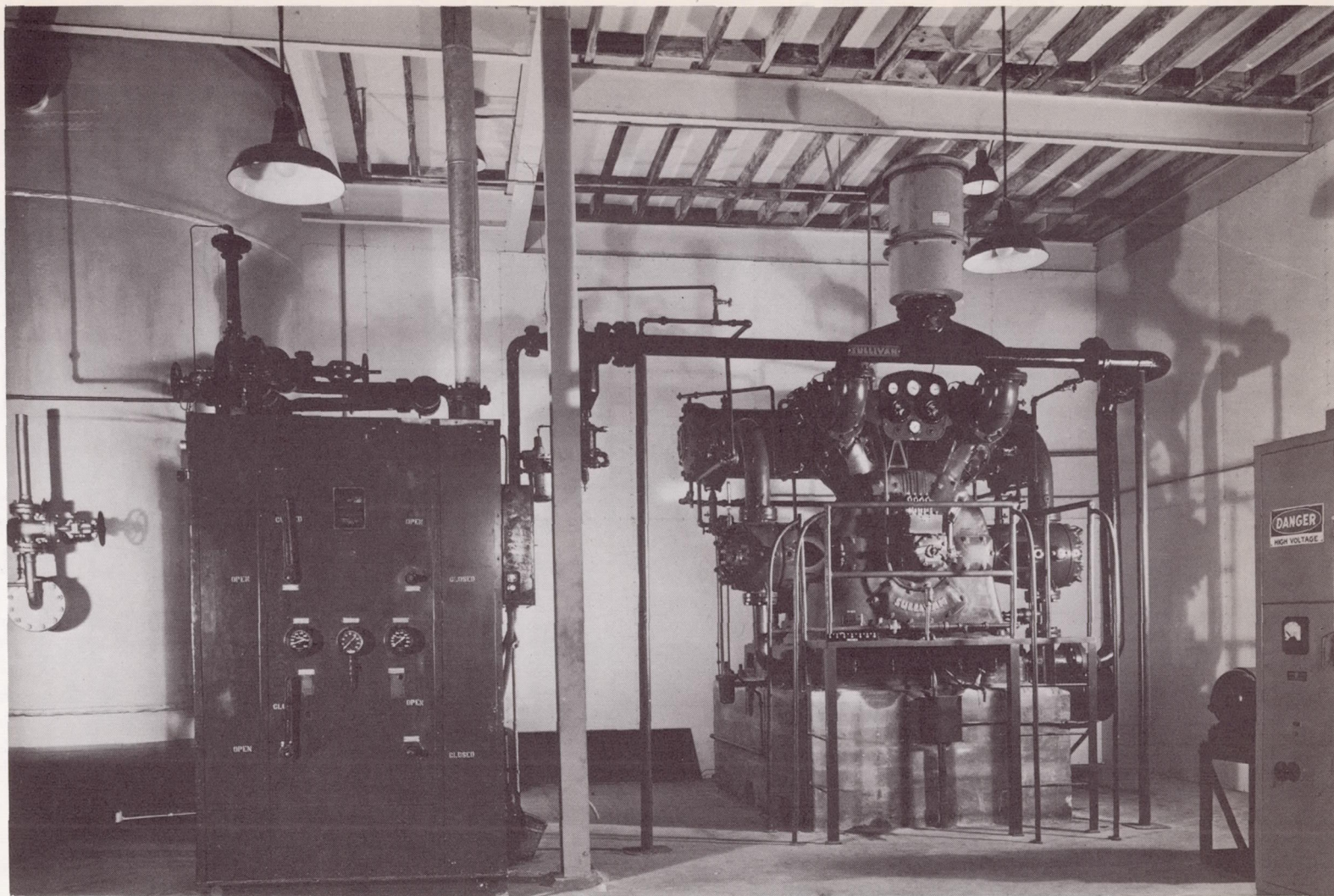
Figure 8.- Power-supply installation.

Compressed air
to dryer

Compressed air
to filter

Dessicant vessel

Dessicant

Screens

Drain

NACA
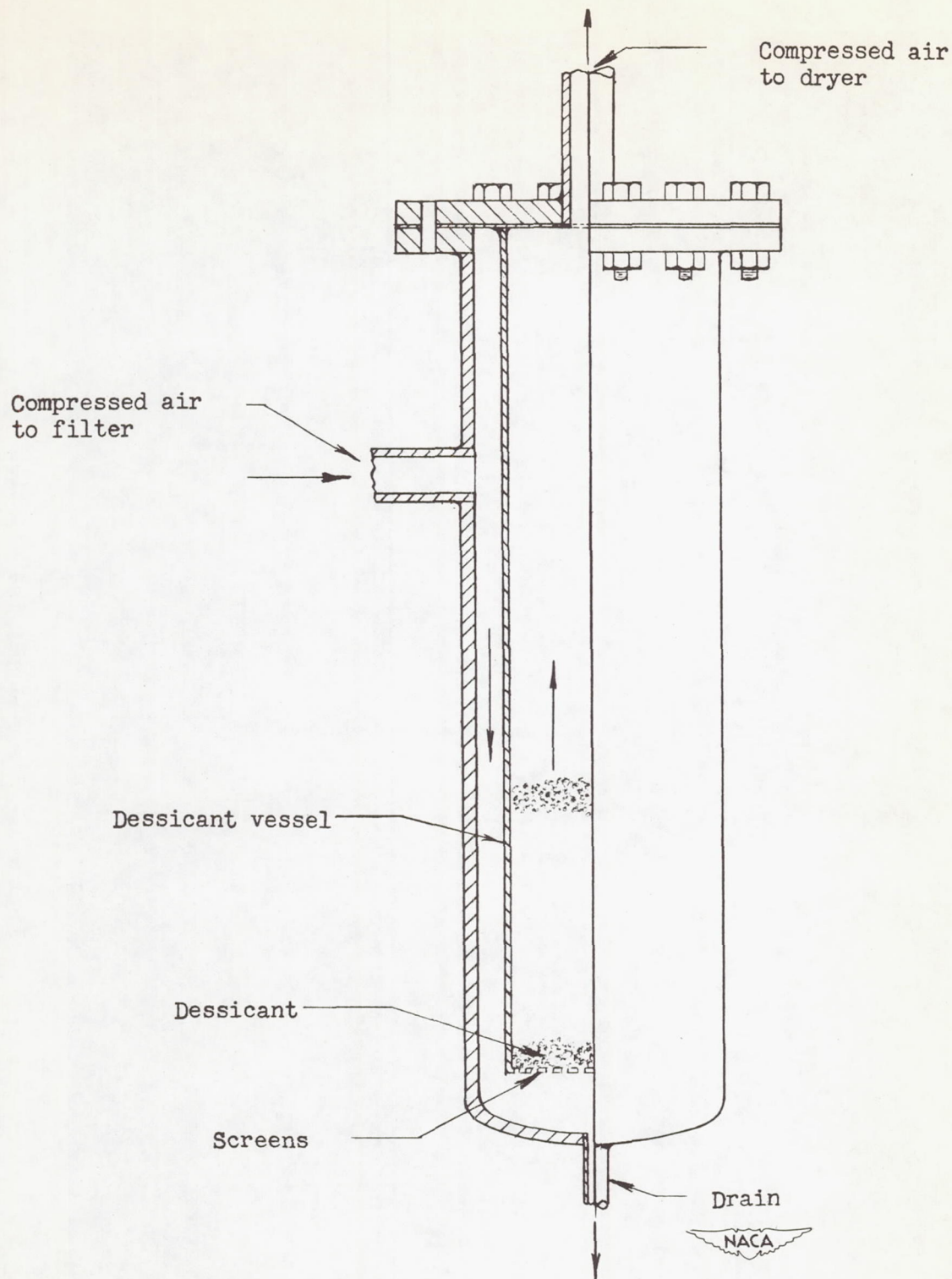
Figure 9.- Schematic illustration of oil filter.

36' 5"

21' 5"

Transition cone

Entrance cone

Diffuser

Supply line

Nozzle region

Screens

Induction jet

NACA
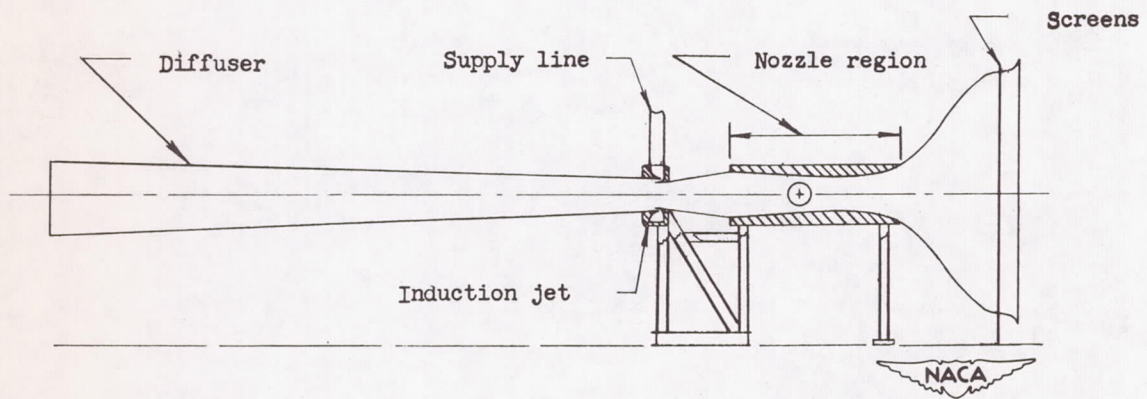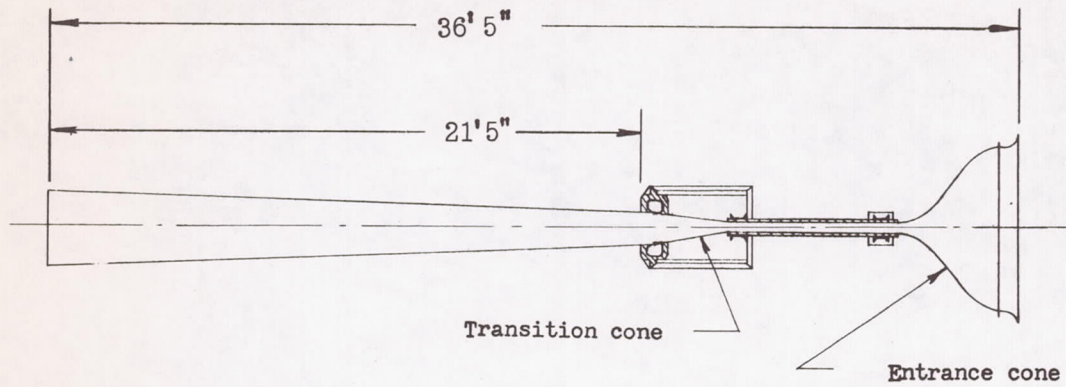
(a) Line drawing.

Figure 10.- Induction tunnel.

59
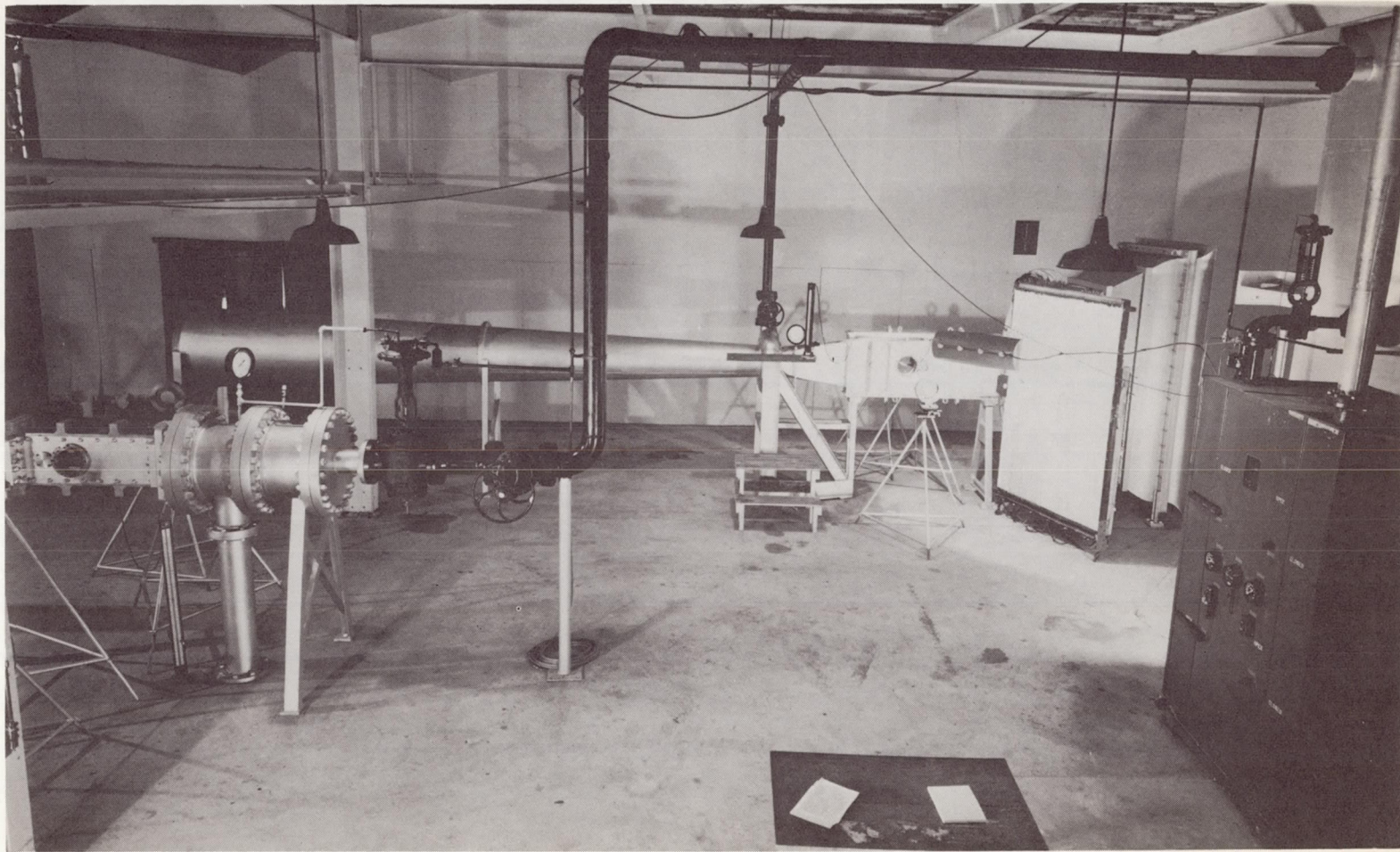
(b) General view.

Figure 10.- Continued.
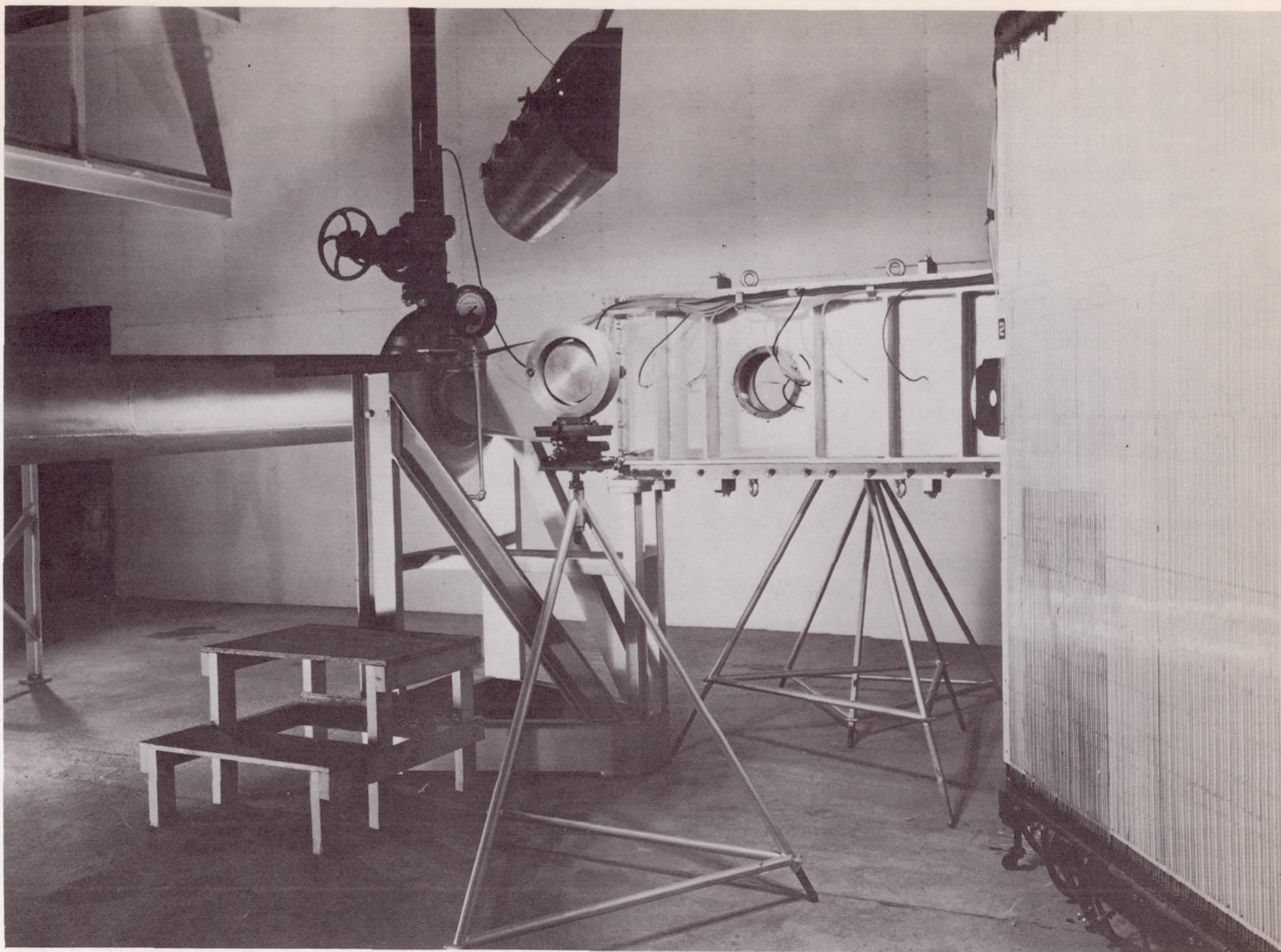
(c) Test section to diffuser portion.

Figure 10.- Concluded.
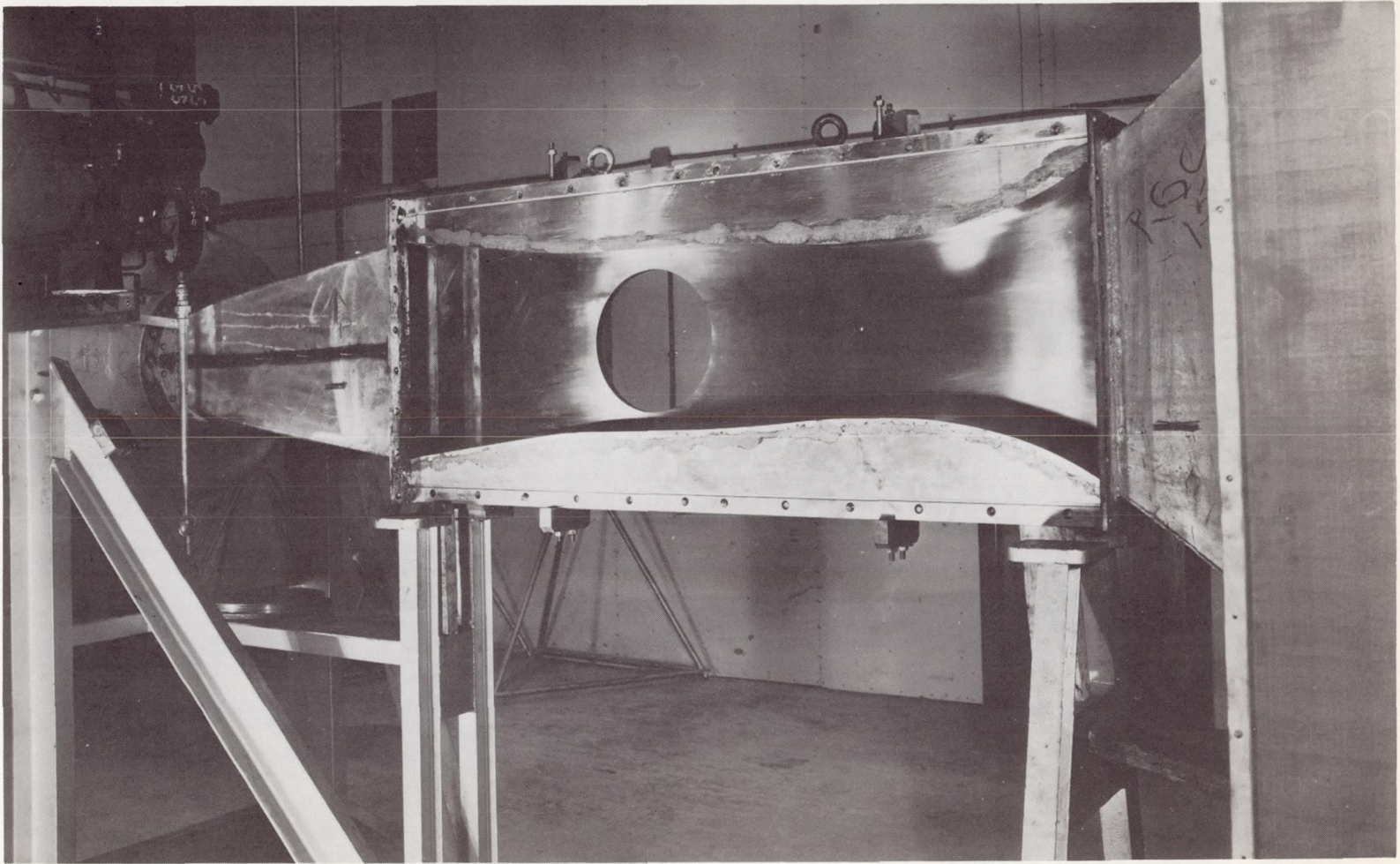
Figure 11.- Air passage formed in induction tunnel by nozzle blocks for M = 1.4.
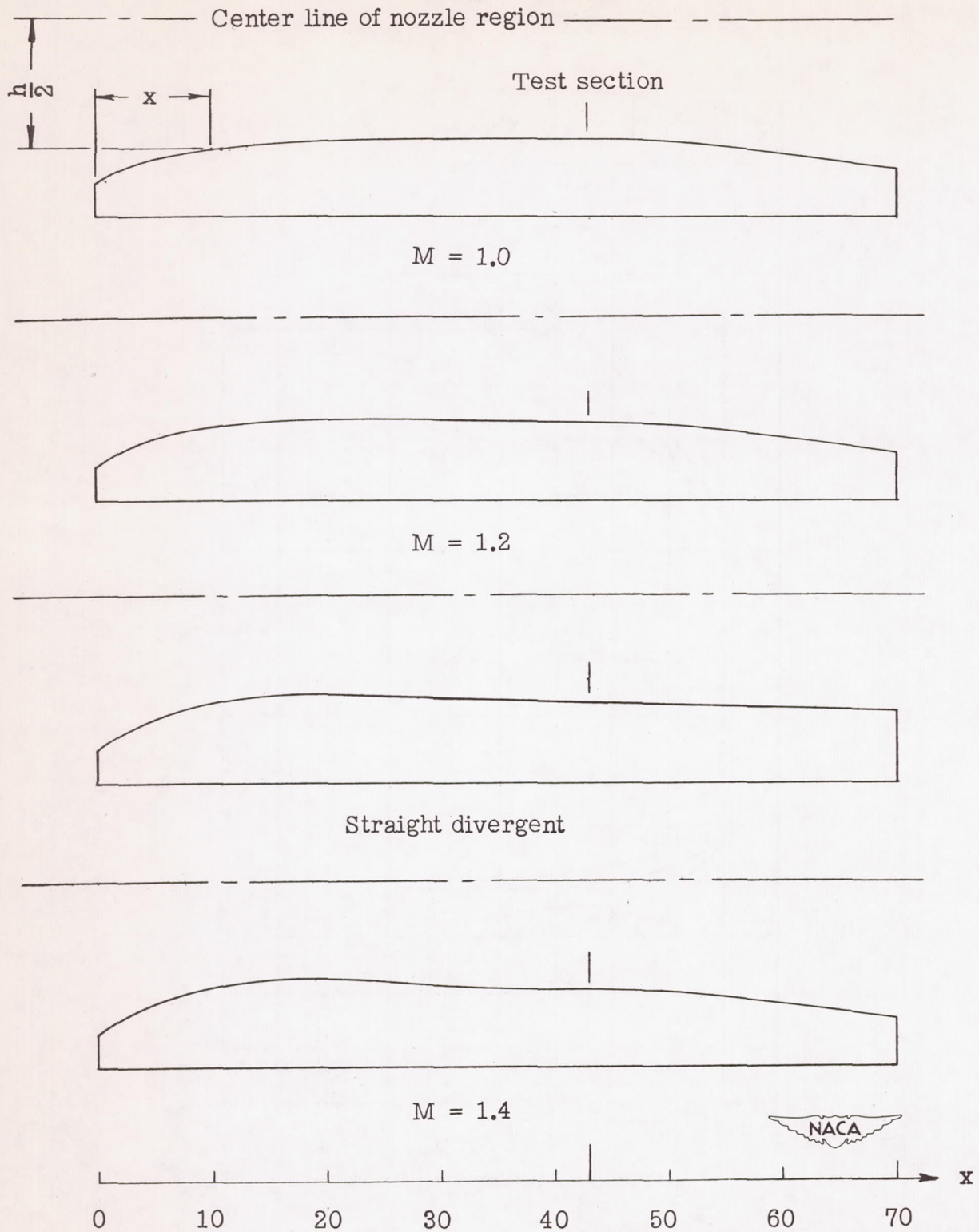
Figure 12.- Nozzle-block shapes used in induction tunnel.
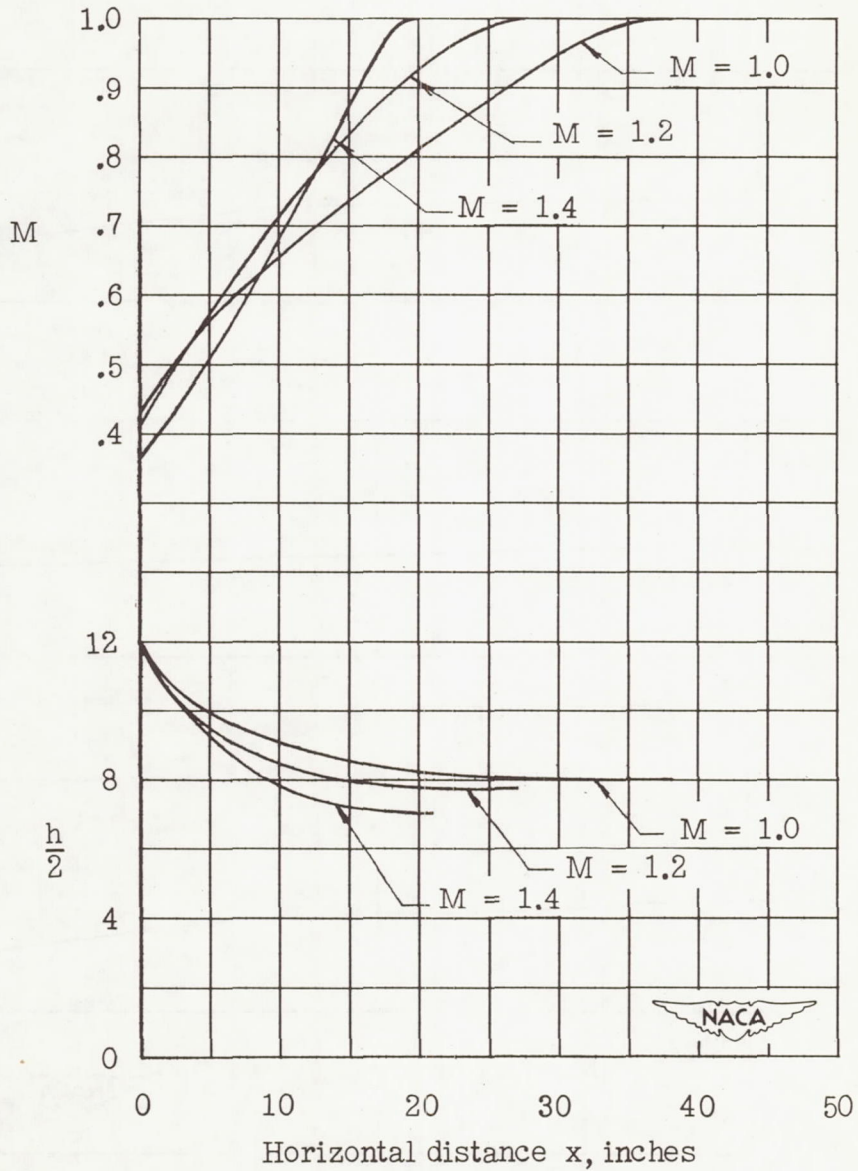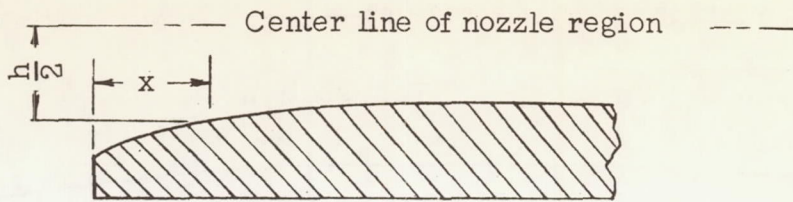
Figure 13.- Velocity distribution and shape of subsonic region of nozzle
blocks in induction tunnel as affected by test Mach number.

22' 9"

Screens   Supply line

Nozzle region

Circular diffuser   Settling chamber

Transition cone

Pressure-regulator
valve

NACA
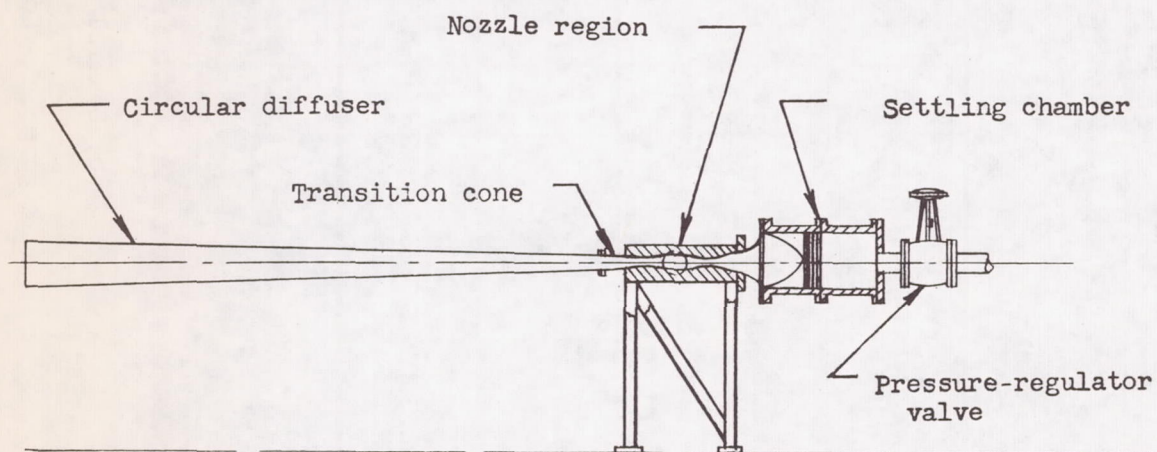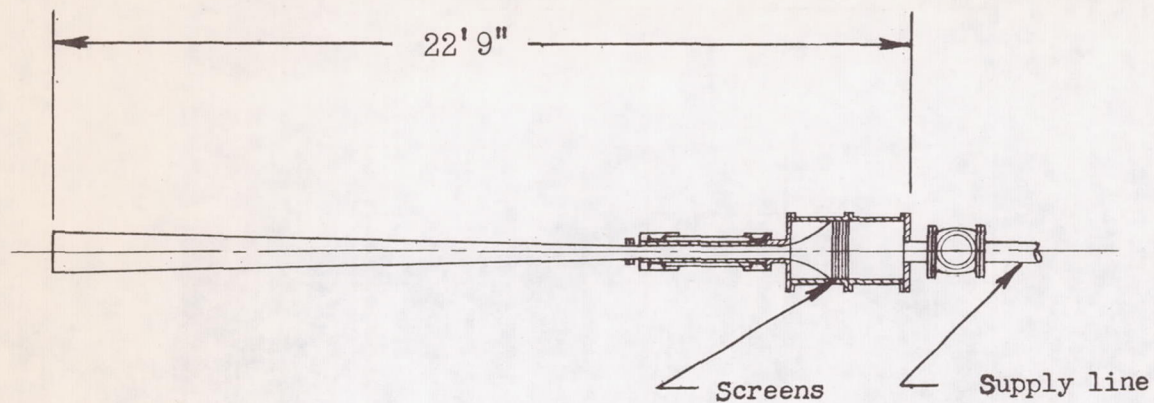
(a) Line drawings.

Figure 14.- Blowdown tunnel.
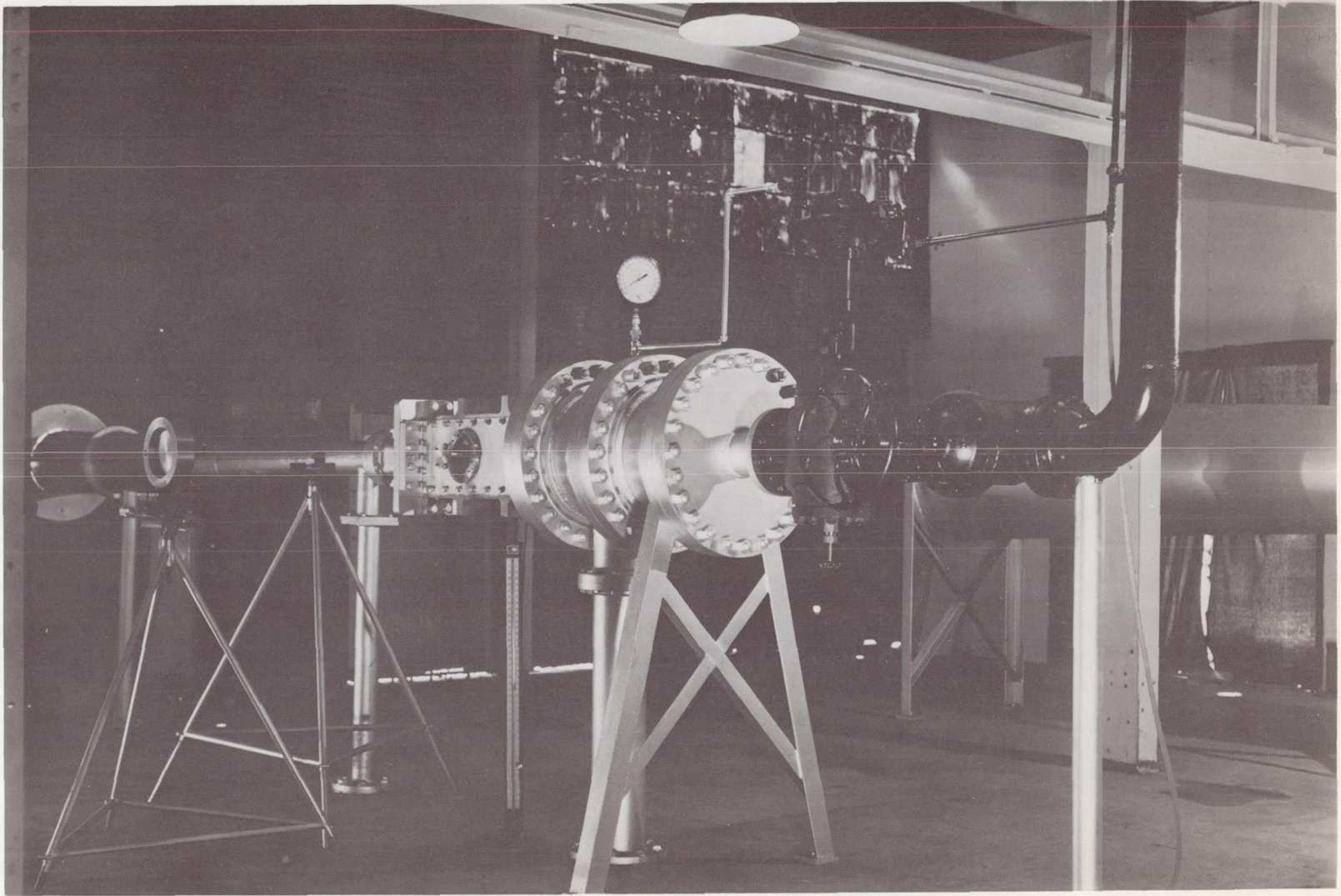
(b) General view.

Figure 14.- Concluded.
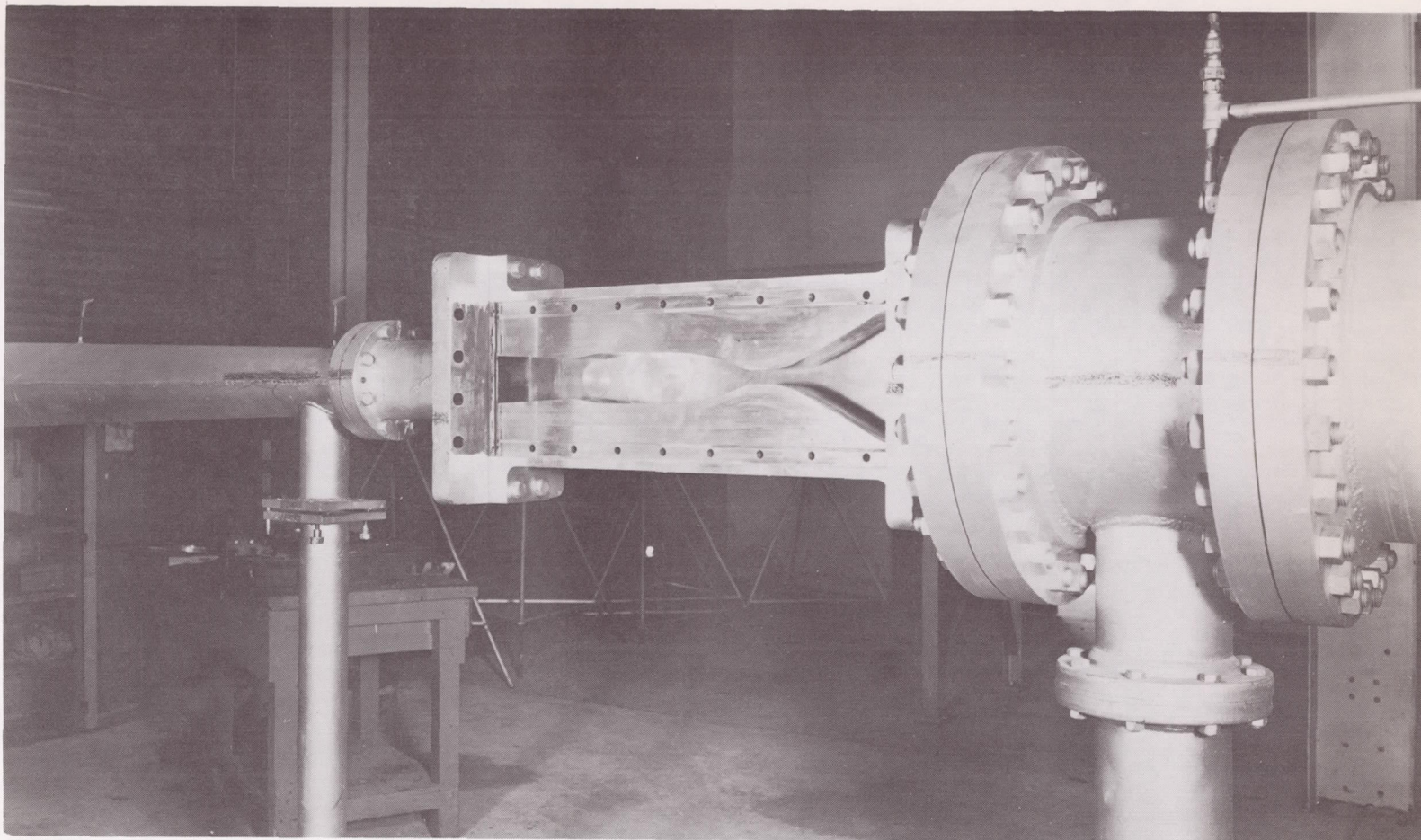
Figure 15.- Blowdown tunnel with nozzle blocks for M = 2.8.

Test section

Center line of nozzle region

$\frac{h}{2}$ x

M = 2.0

M = 2.8

M = 4.1

NACA

x

0   10   20   30   40
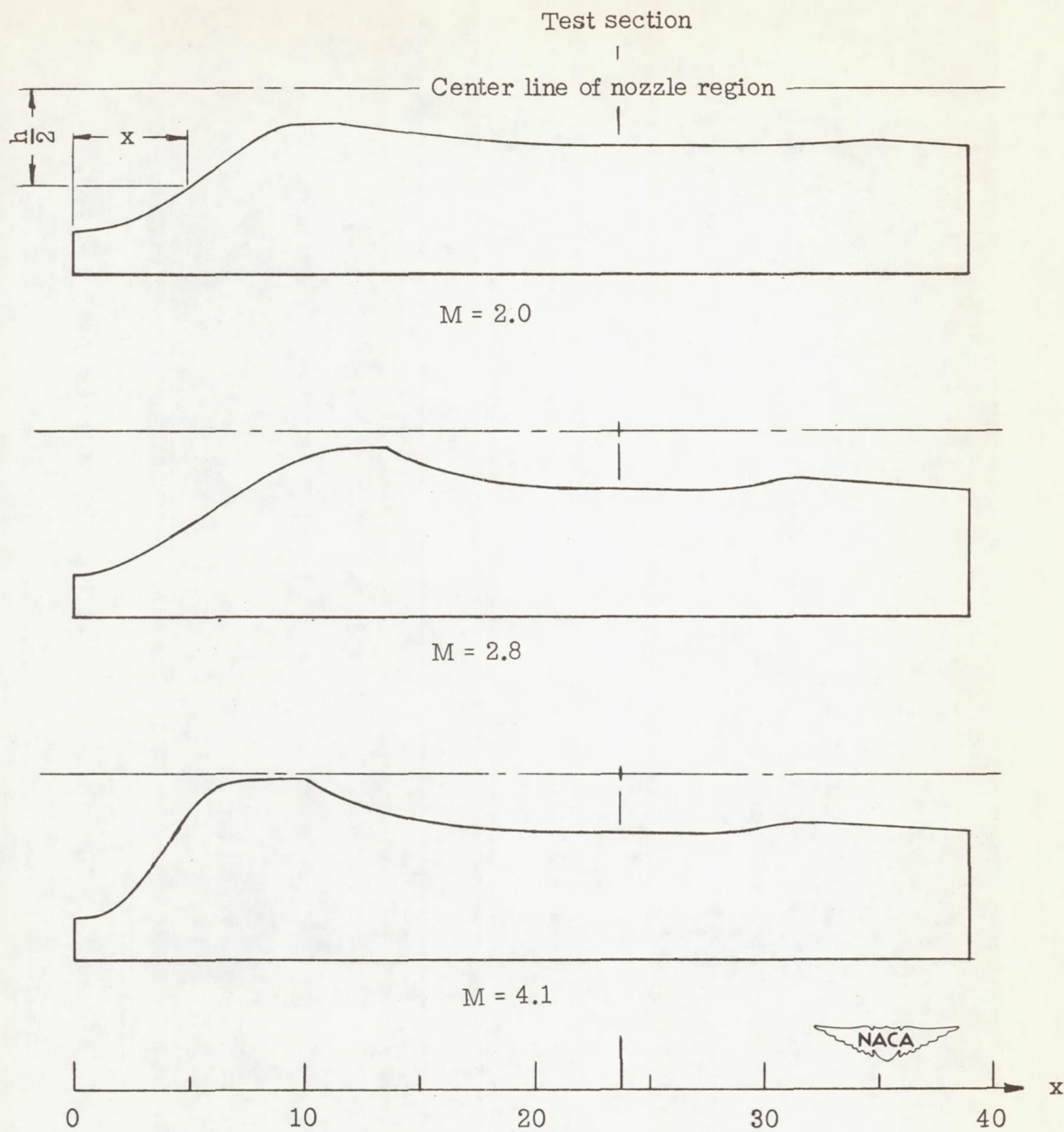
Figure 16.- Nozzle-block shapes used in blowdown tunnel.
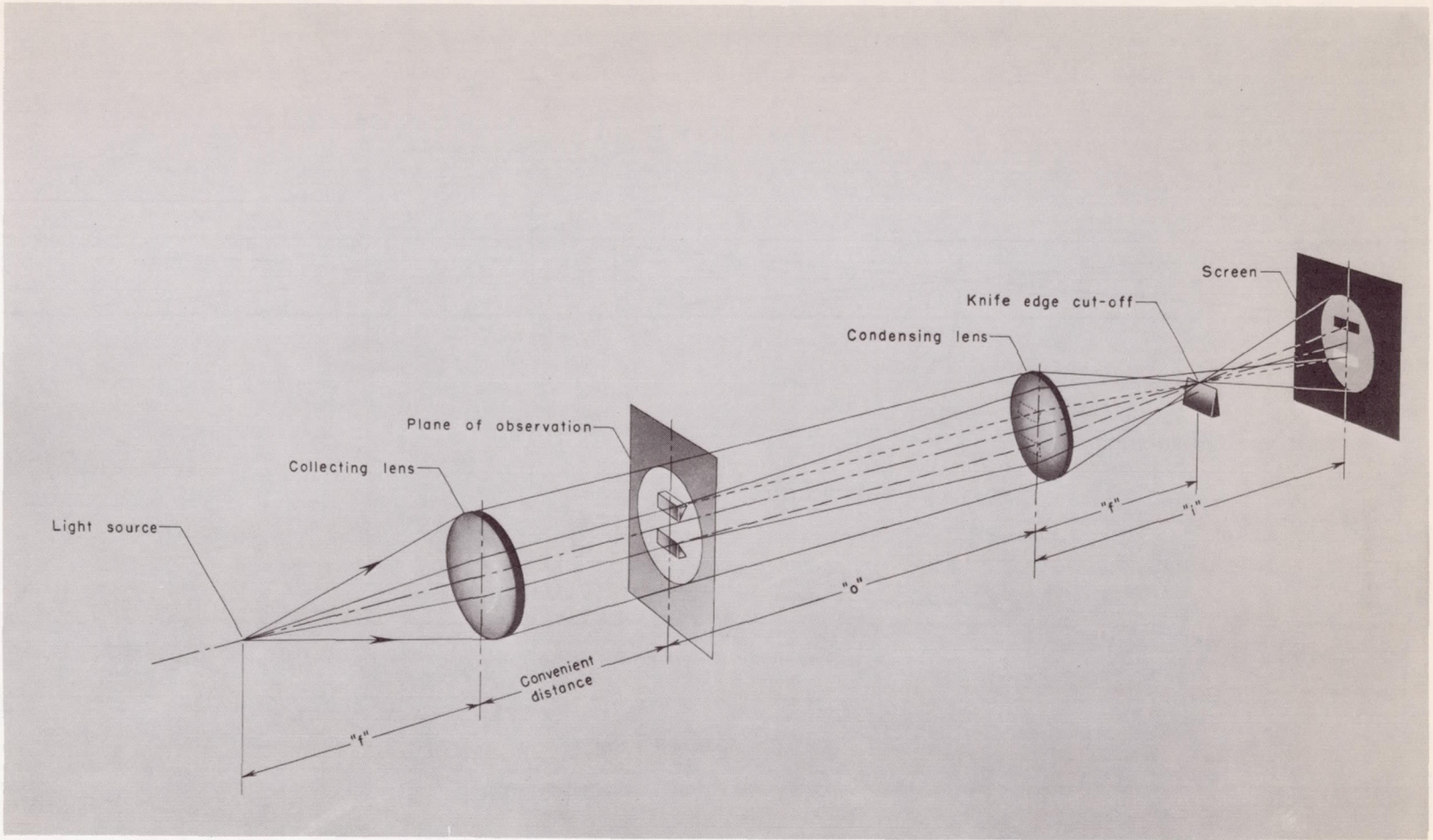
Figure 17.- Illustration of the functioning of a schlieren system.

f_1

ϕ_1

Light source

Test region

$\phi_2 = \phi_1$

d

Collimator

P

Knife edge

$f_2 = f_1$

Condenser

(a) Plan view.

(b) Elevation view.
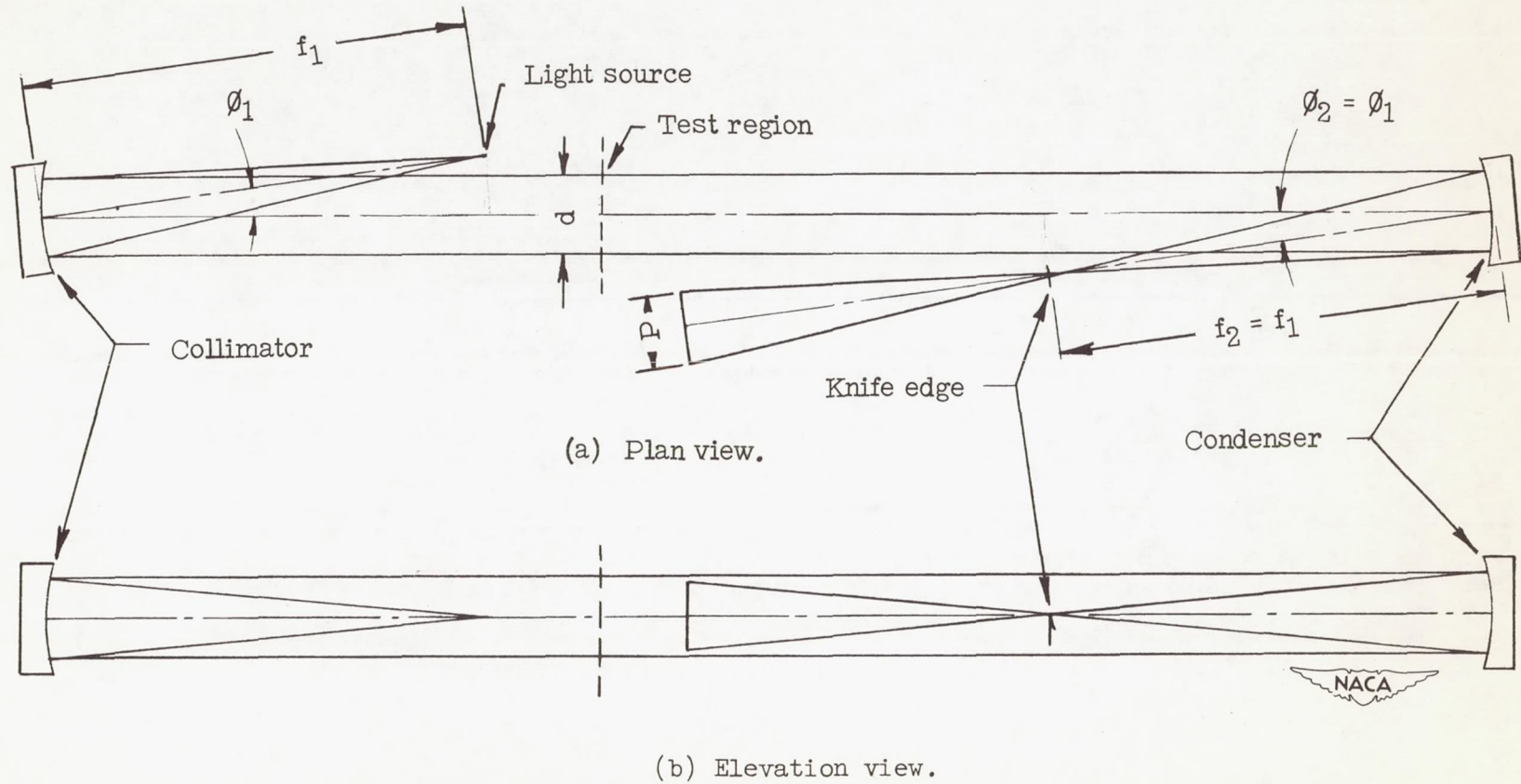
Figure 18.- Schematic of schlieren using mirrors in an off-axis system.
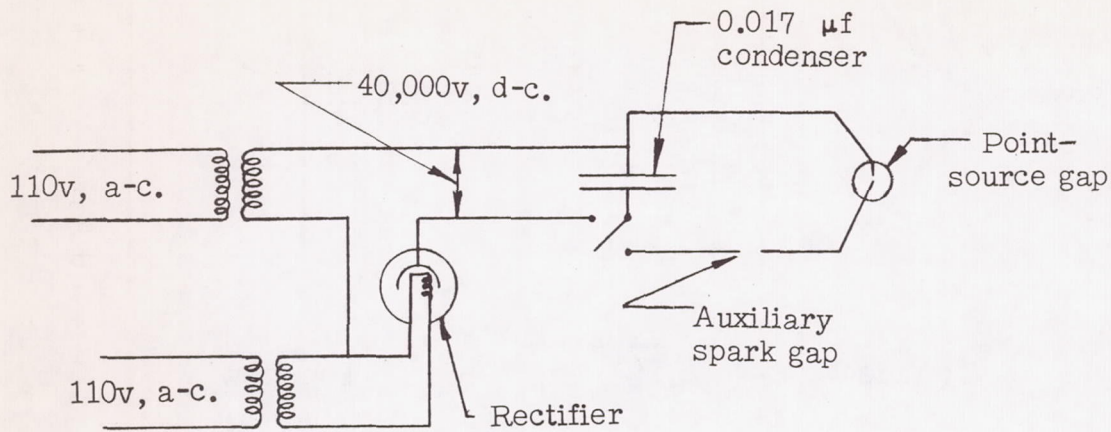
(a) Schematic of spark generator.
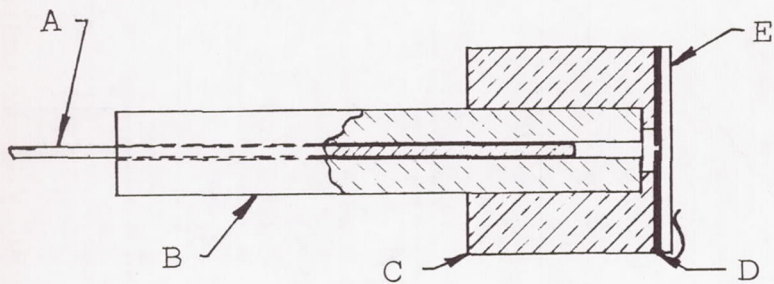
A   Wire electrode (0.030-inch diameter)

B   3-inch length; $\frac{1}{2}$-inch outside diameter - 0.040 inside diameter;
    ceramic tubing

C   Brass or copper electrode

D   Mask for light (0.025-inch-diameter hole in center)

E   Glass spark retaining shield
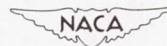
(b) Point-source spark gap.

Figure 19.- Schematic of spark apparatus.

Top view   Top view

Screen
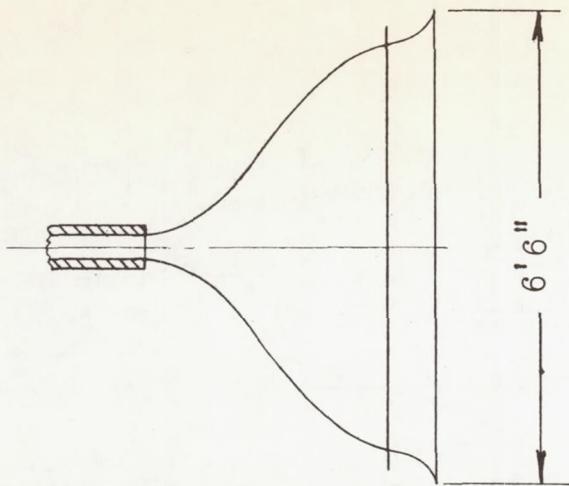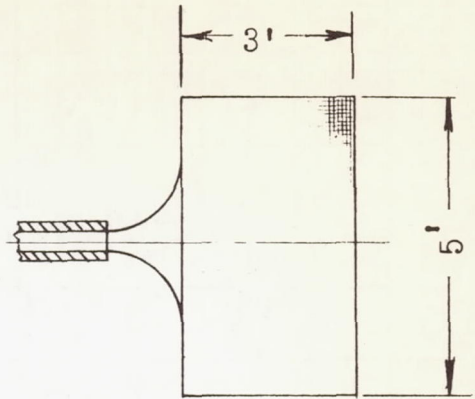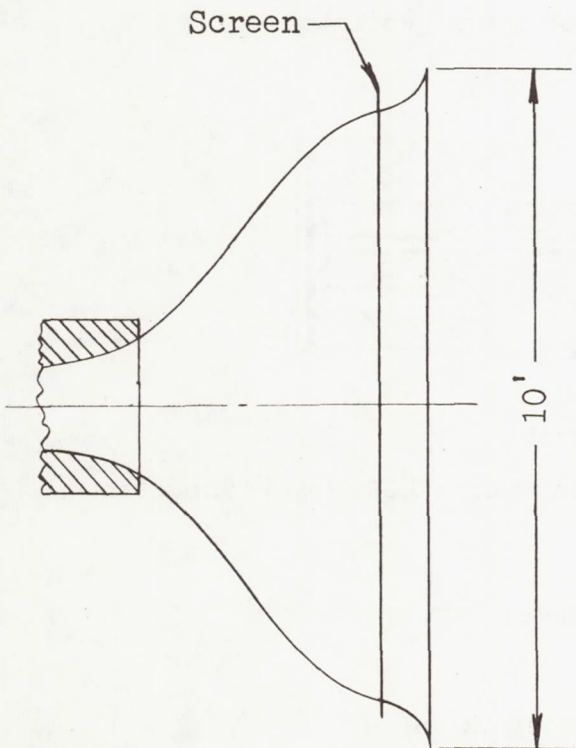
Side view   Side view
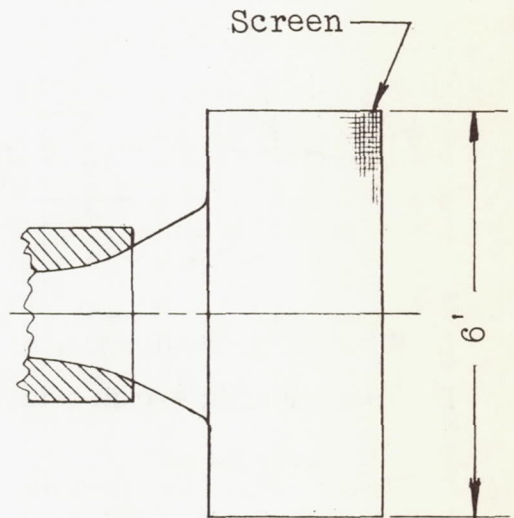
(a) Original.   (b) Revised.

Figure 20.- Change in entrance-cone shape for induction tunnel.
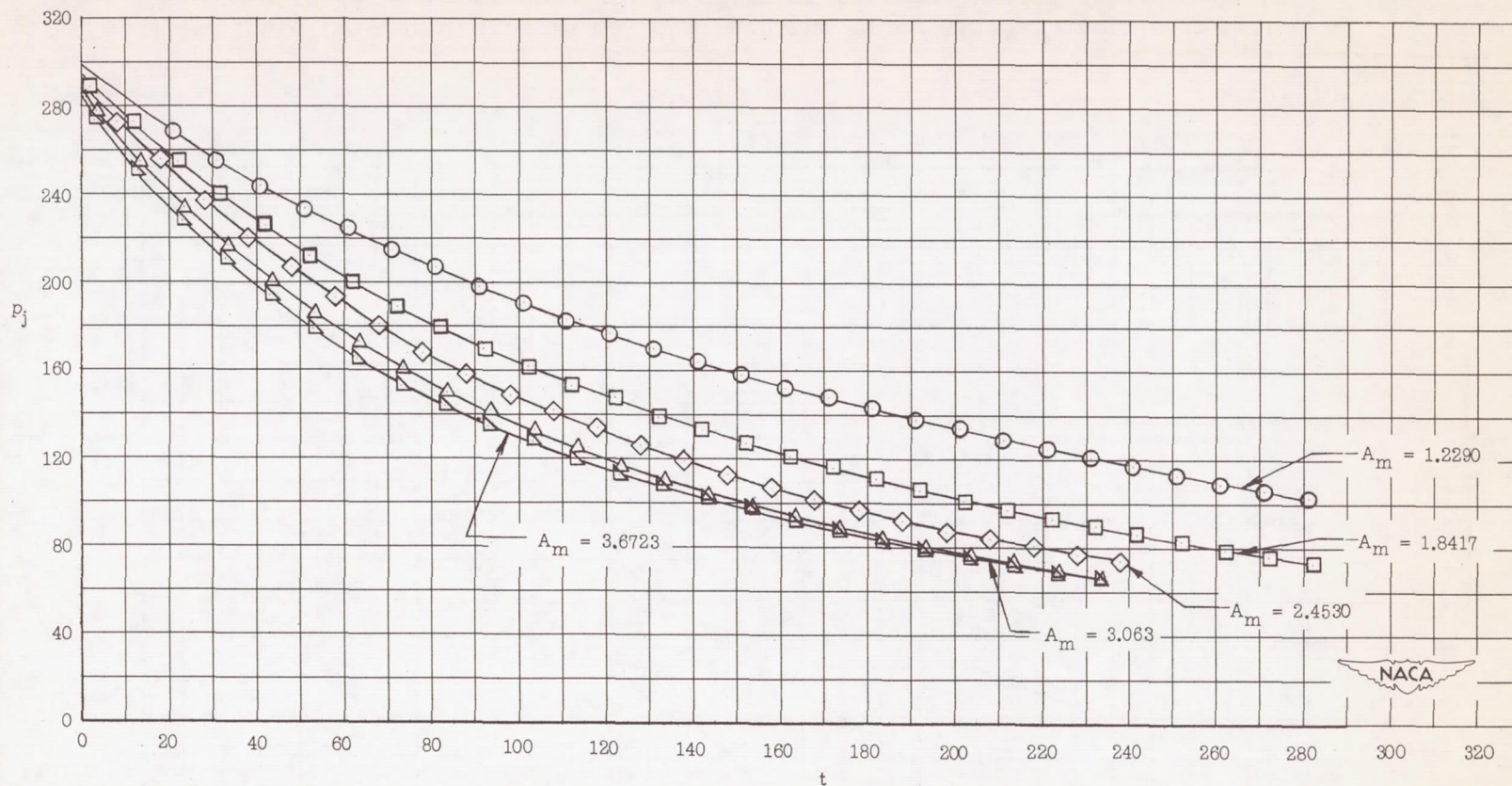
Figure 21.- Variation in jet-chamber pressure with time for induction
tunnel with various minimum jet areas.
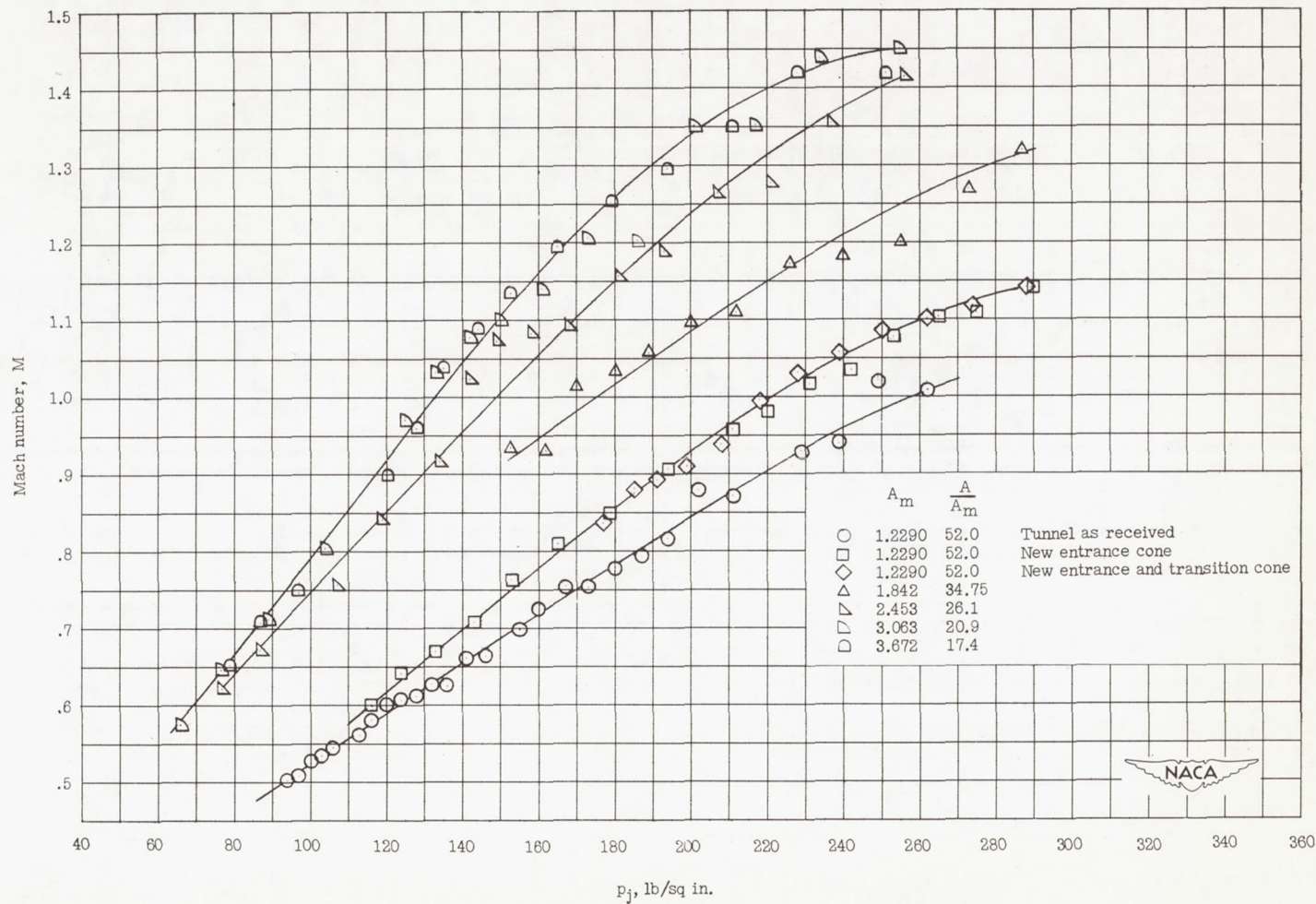
Figure 22.- Variation in maximum Mach number obtained in nozzle region
with jet-chamber pressure as affected by tunnel modifications (sonic
nozzle blocks).
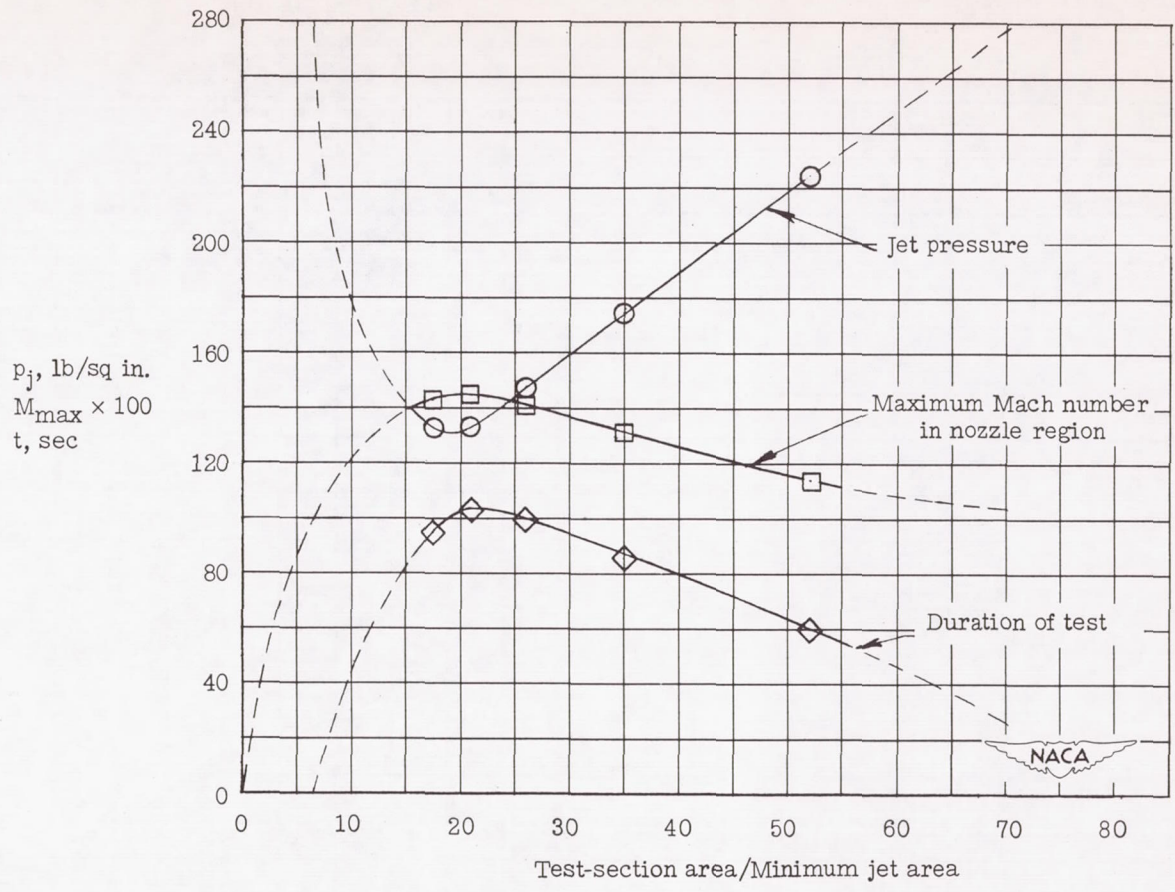
Figure 23.- Effect of varying minimum jet area on performance of induction tunnel at M = 1.0.
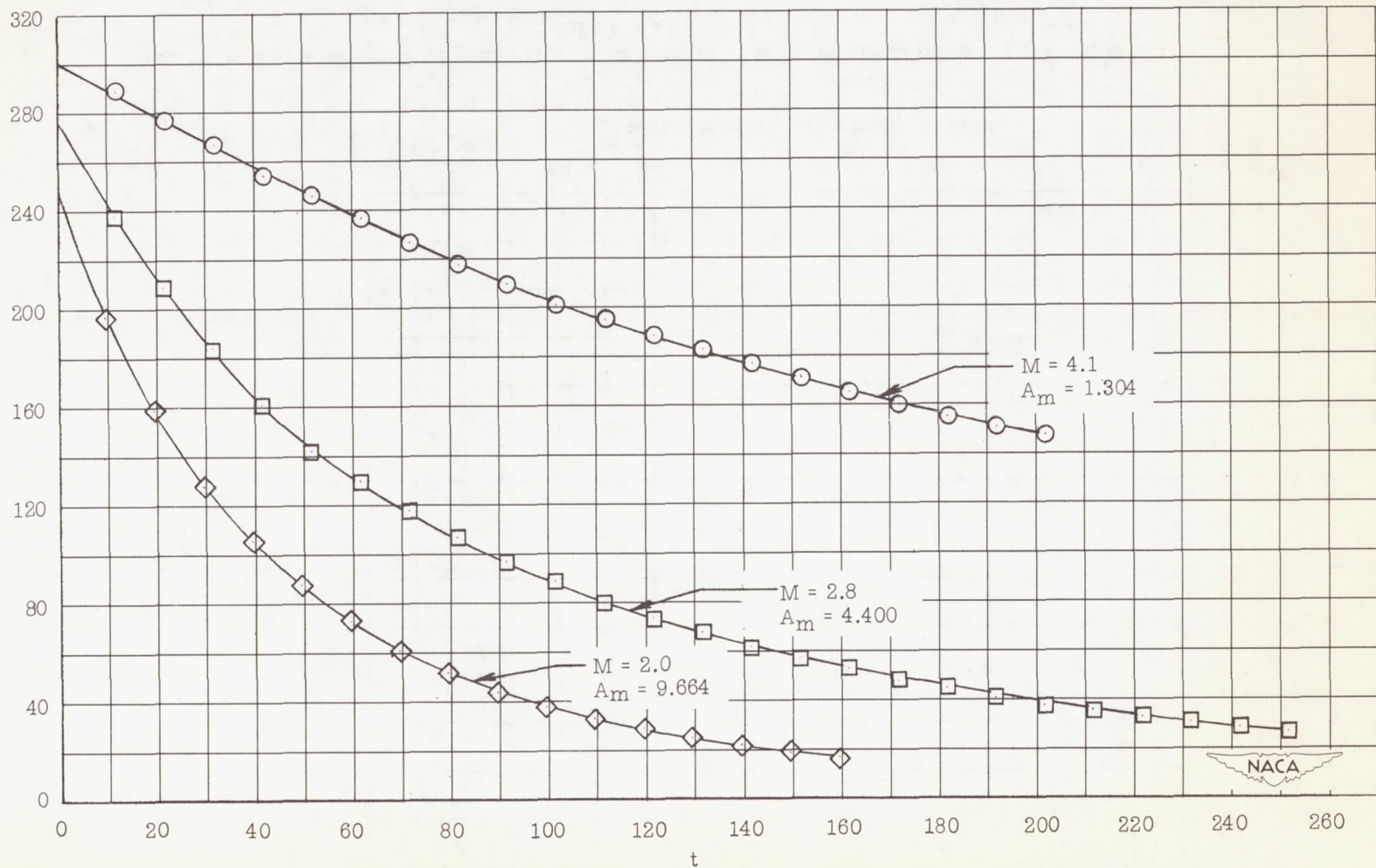
Figure 24.- Variation in settling-chamber pressure with time in blowdown tunnel (no throttling).
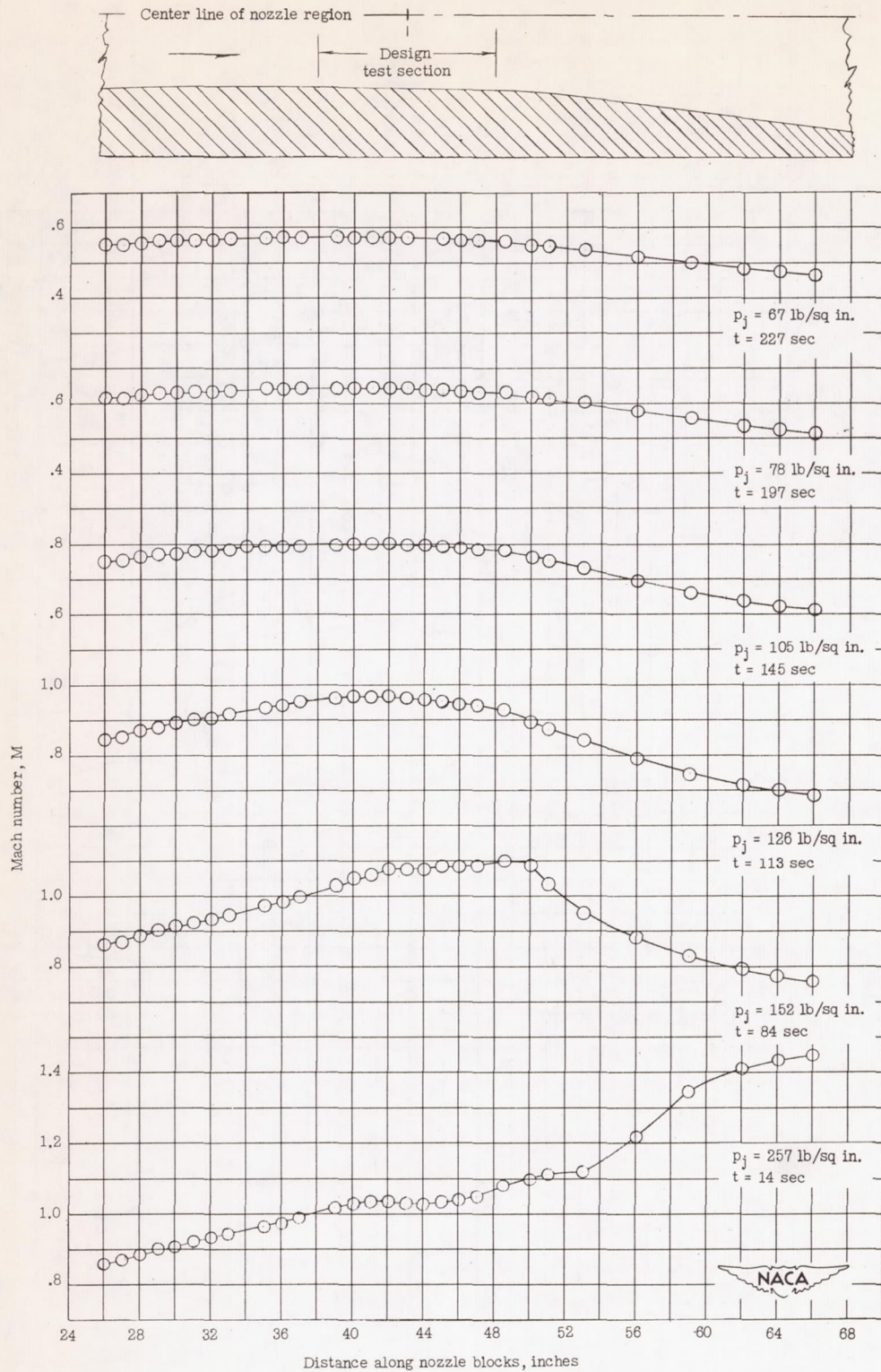
Figure 25.- Mach number distribution along side-wall center line of induction tunnel with sonic nozzle blocks (initial humidity, 60 percent).
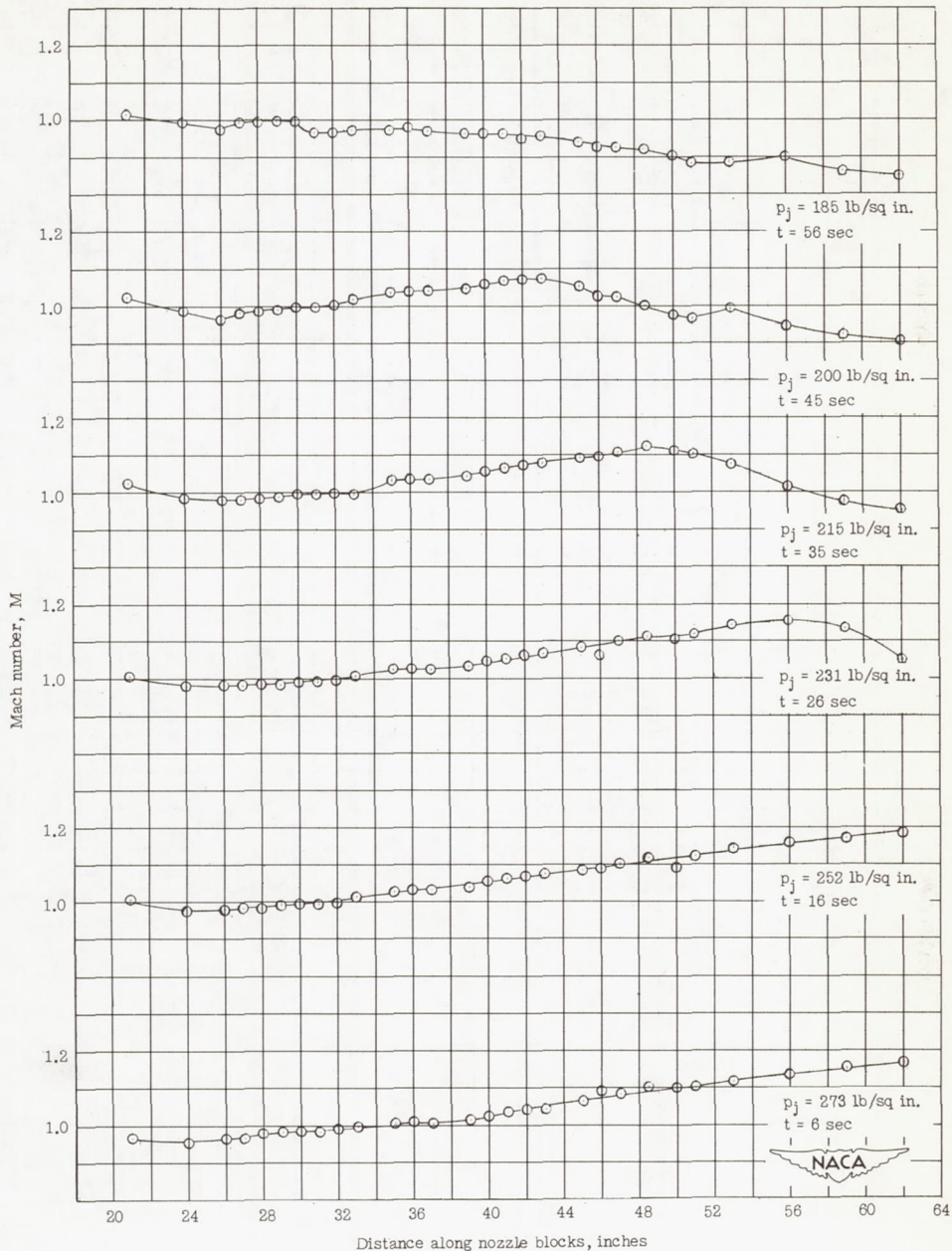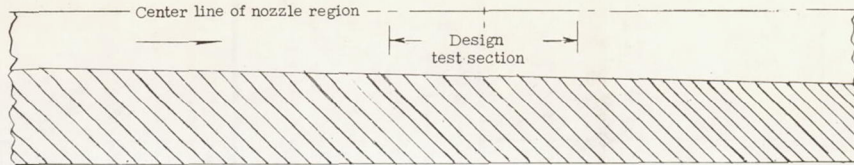
(a) Straight divergent nozzle (initial humidity, 66 percent).

Figure 26.- Mach number distribution along side-wall center line of
induction tunnel with supersonic nozzle blocks.

Center line of nozzle region

Design test section

Mach number, M

p_j = 184 lb/sq in.
t = 56 sec

p_j = 201 lb/sq in.
t = 44 sec

p_j = 215 lb/sq in.
t = 35 sec

p_j = 229 lb/sq in.
t = 27 sec

p_j = 254 lb/sq in.
t = 15 sec

p_j = 274 lb/sq in.
t = 6 sec

NACA

Distance along nozzle blocks, inches
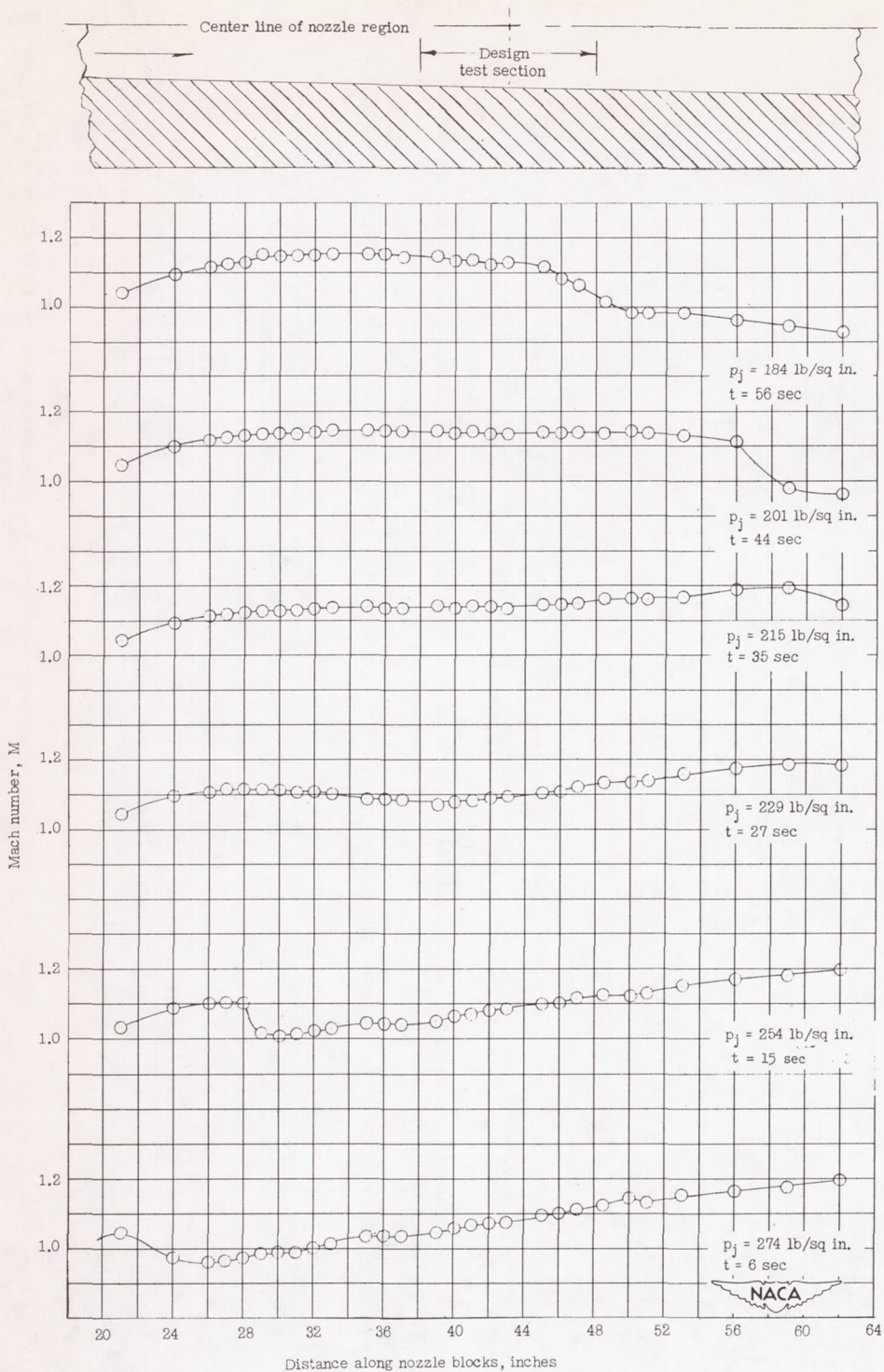
(b) Straight divergent nozzle (initial humidity, 52 percent).

Figure 26.- Continued.
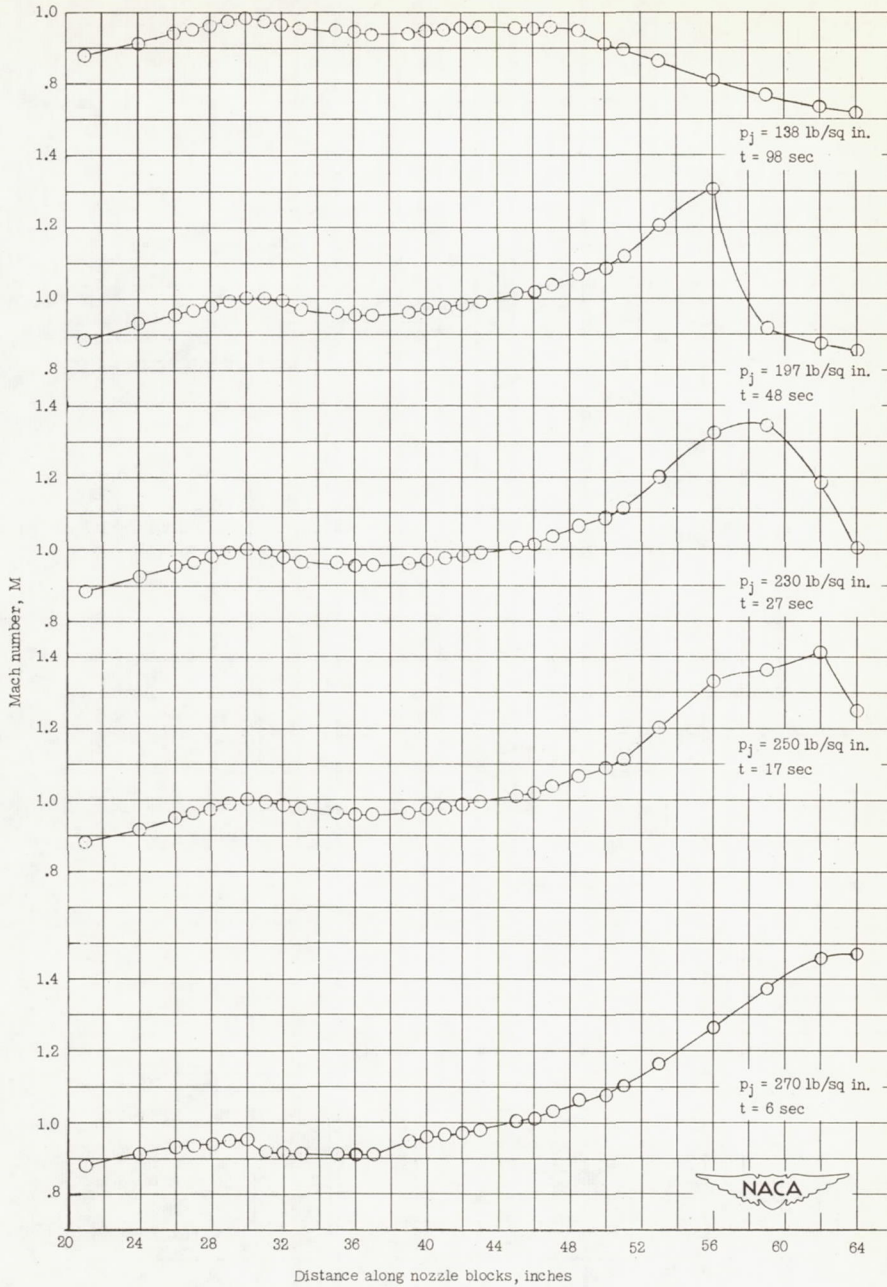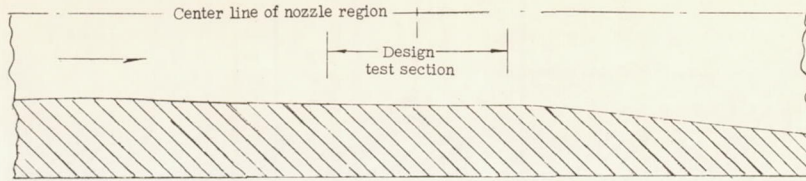
(c) Nozzle designed for M = 1.2 (initial humidity, 68 percent).

Figure 26.- Continued.
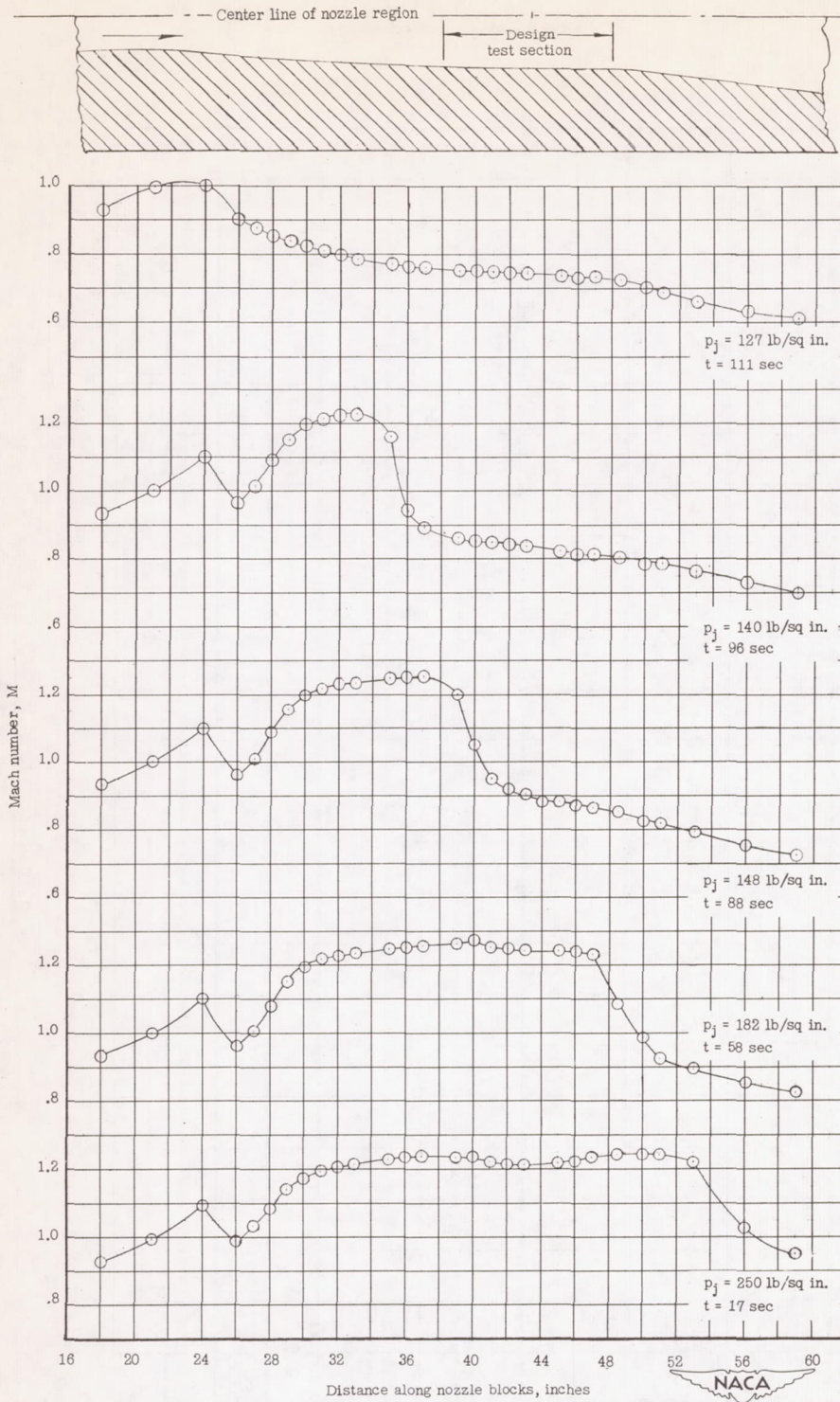
(d) Nozzle designed for M = 1.4 (initial humidity, approx. 55 percent).

Figure 26.- Concluded.
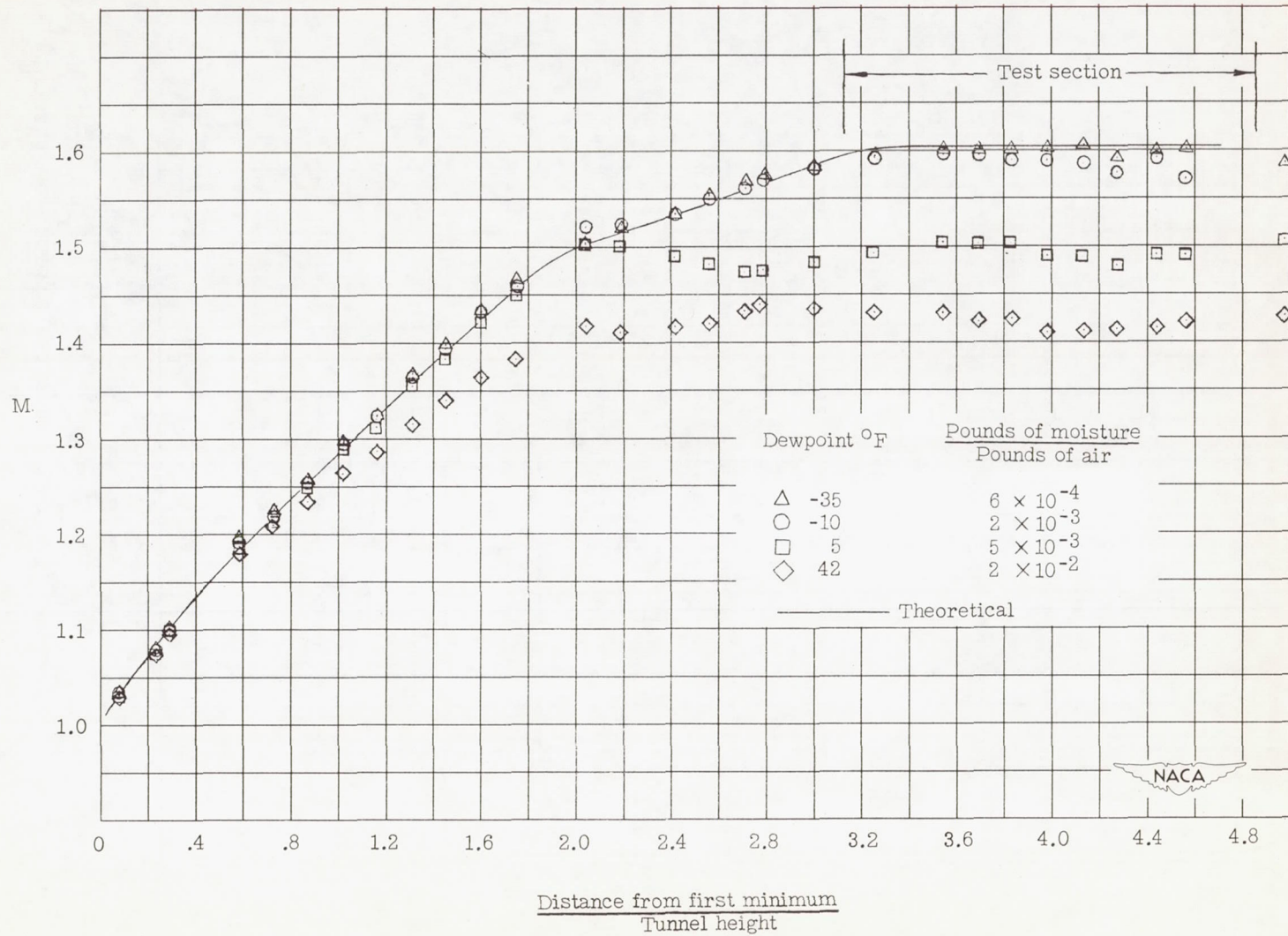
Figure 27.- Effects of moisture content on Mach number distribution through a supersonic tunnel.
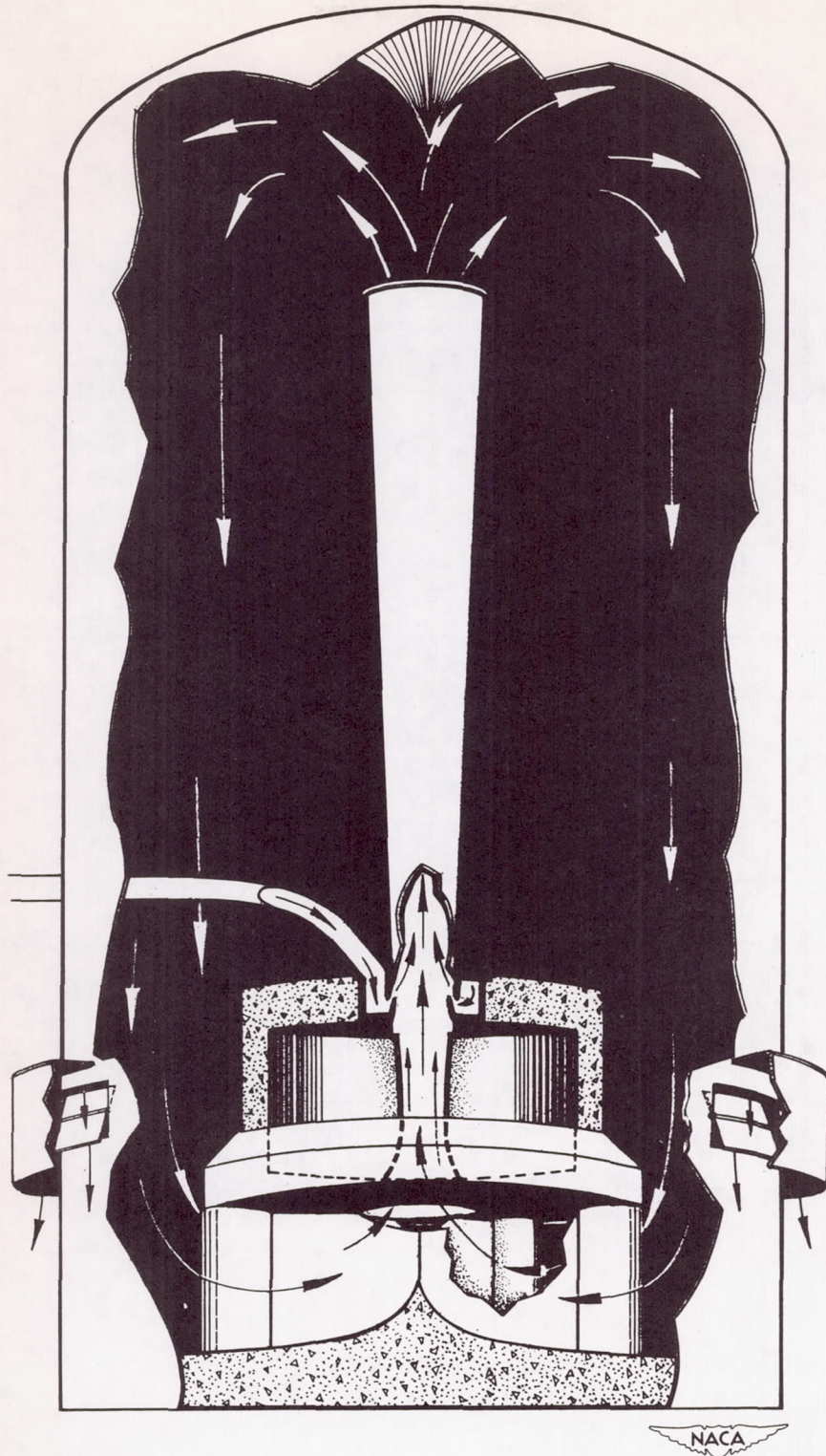
Figure 28.- Enclosure around Langley 24-inch high-speed tunnel.
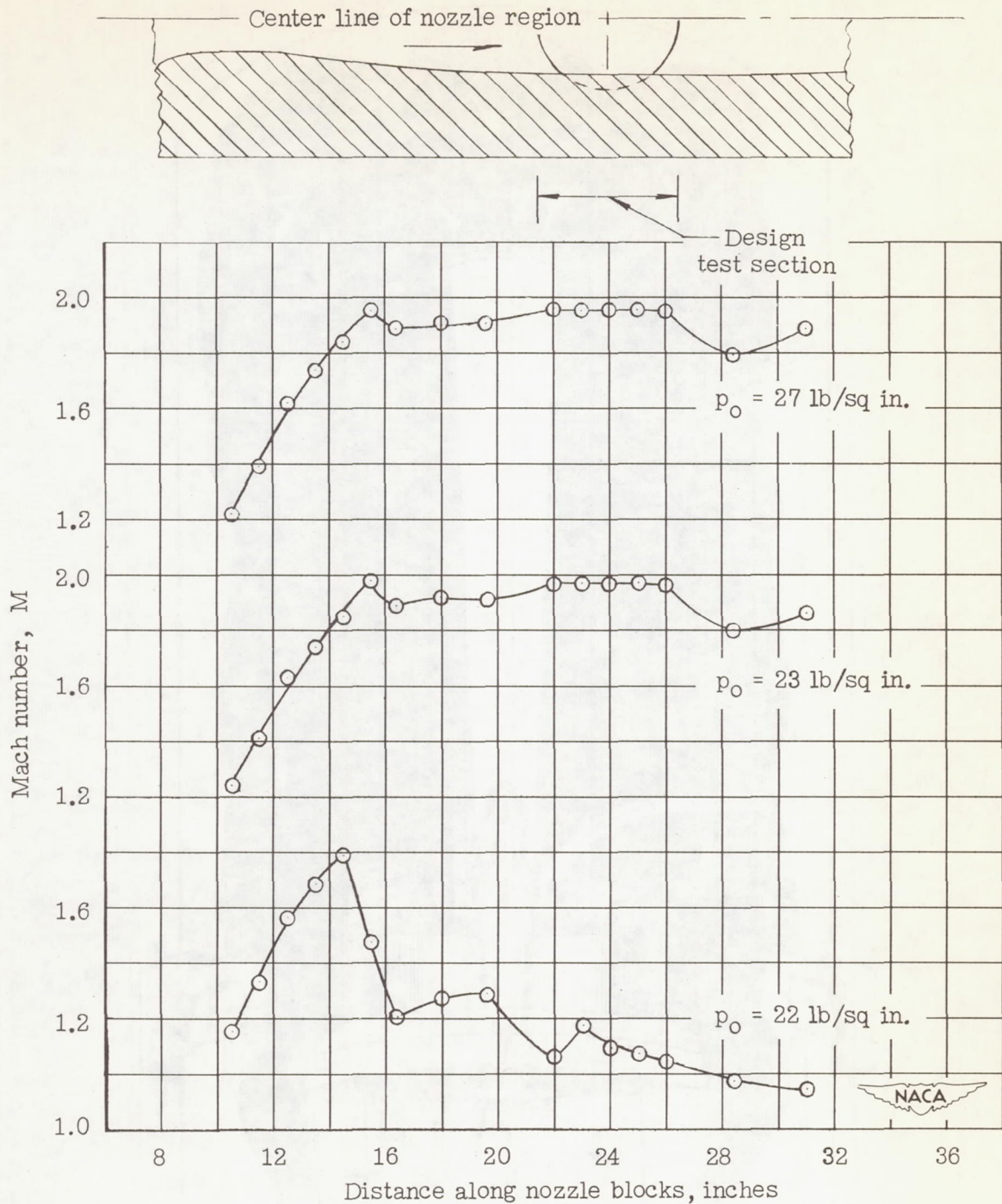
(a) Nozzle blocks designed for M = 2.0.

Figure 29.- Mach number distribution along side-wall center line of supersonic tunnel.
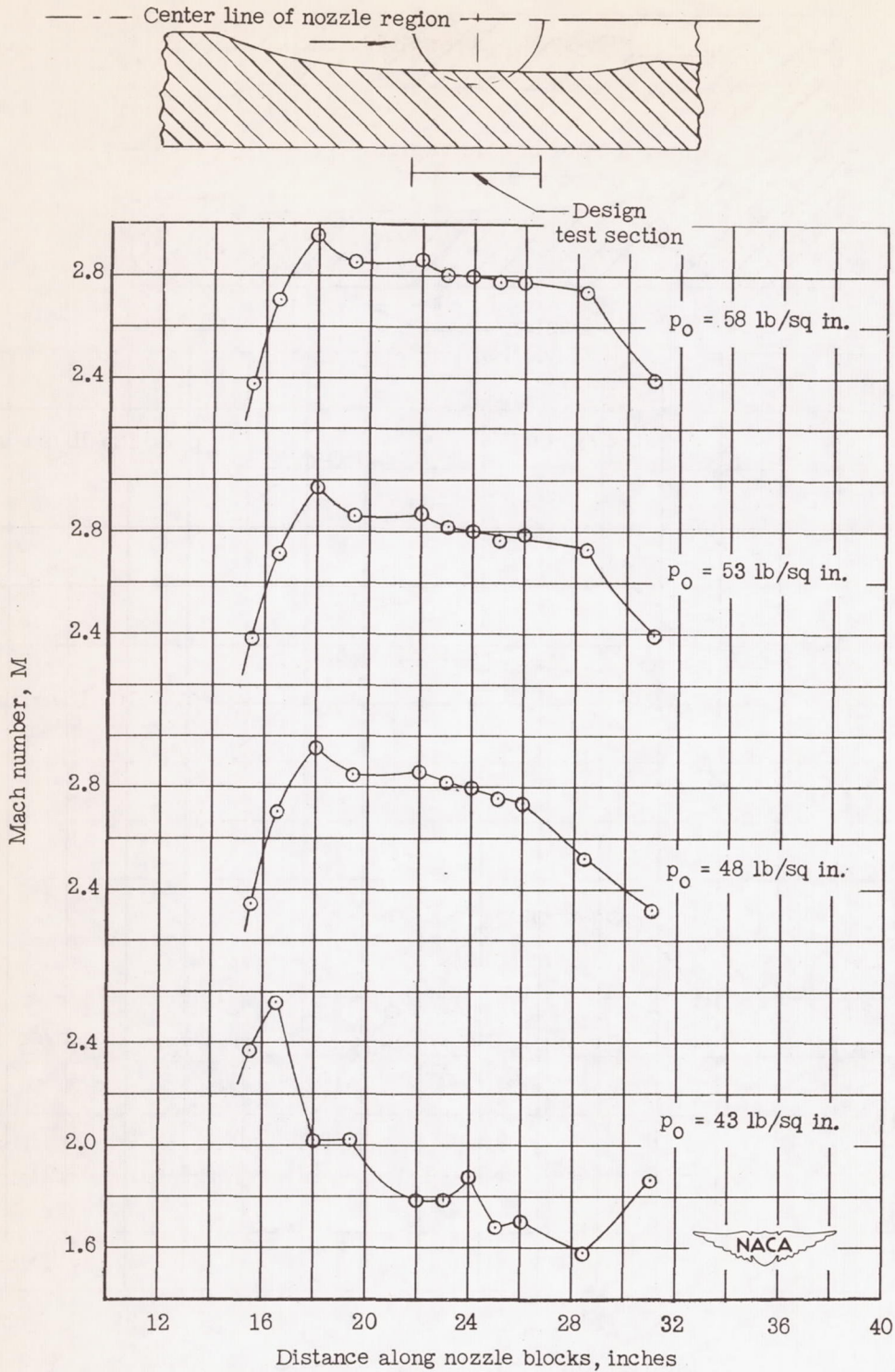
(b) Nozzle blocks designed for M = 2.8.

Figure 29.- Continued.
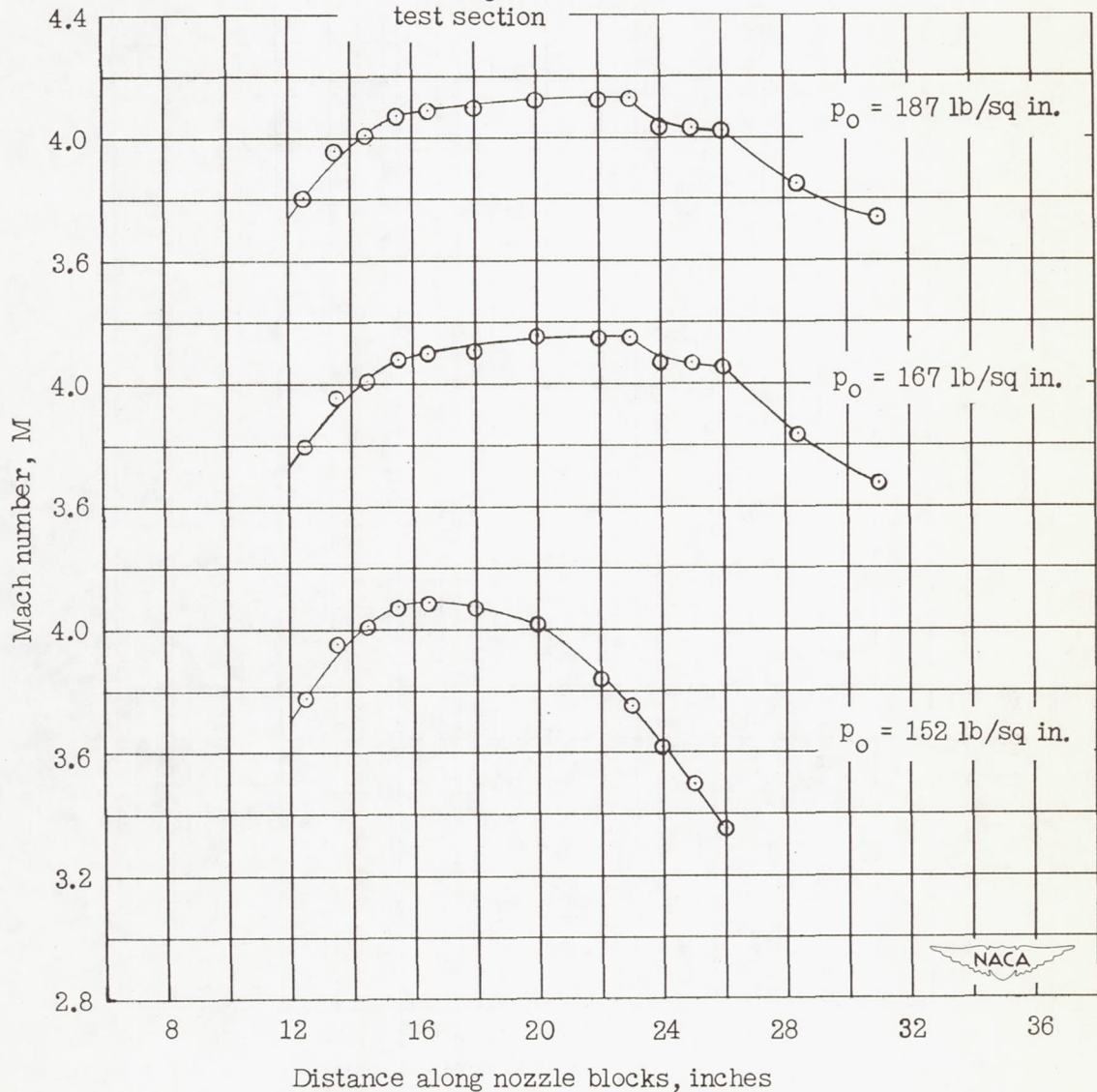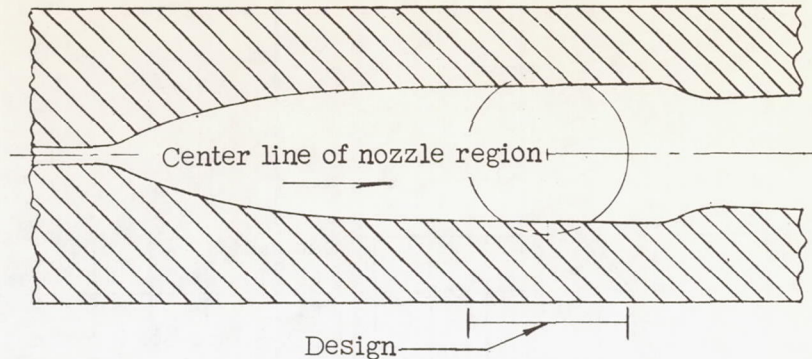
(c) Nozzle blocks designed for M = 4.1.

Figure 29.- Concluded.
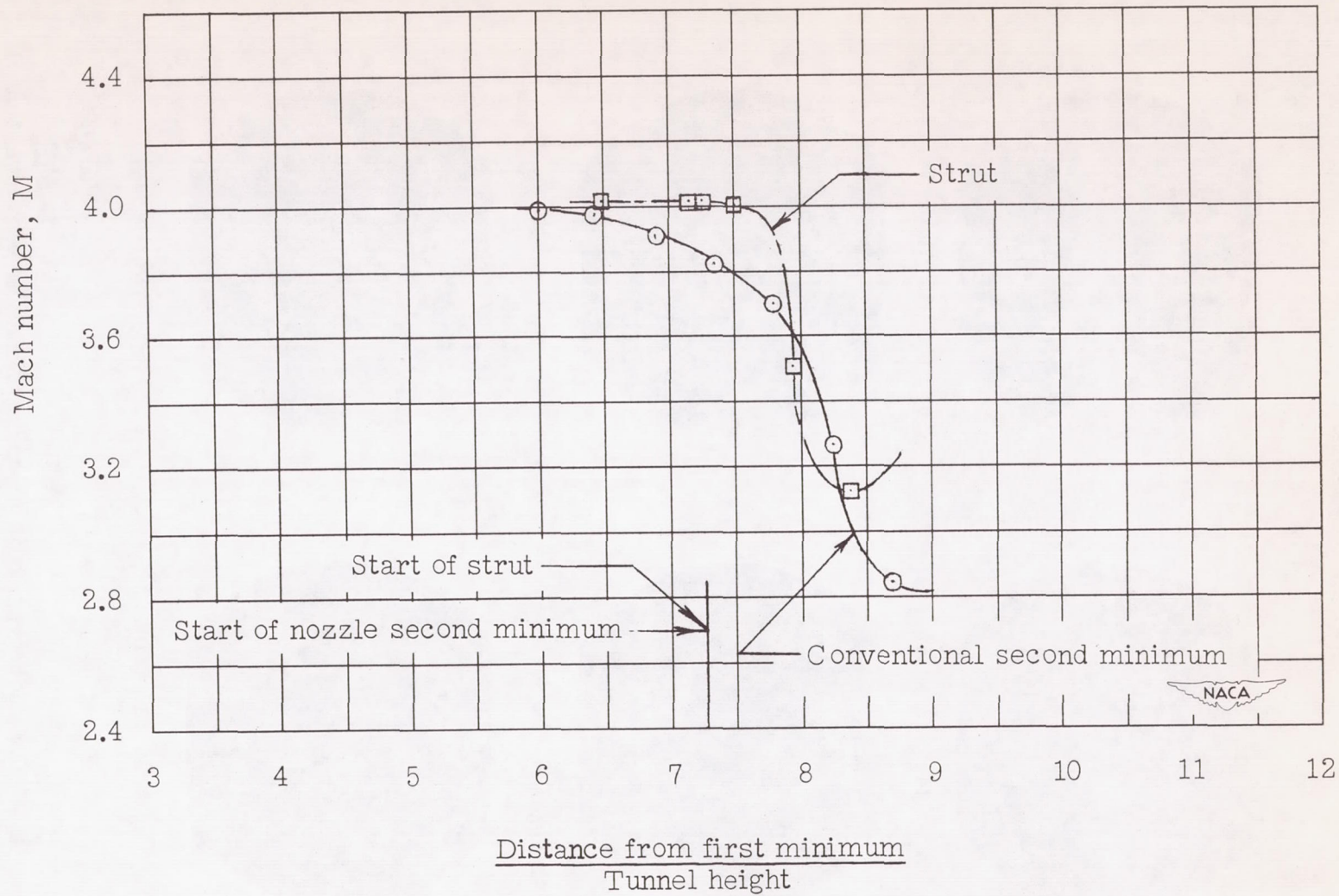
Figure 30.- Comparative effects of a strut and a conventional second minimum on variation in Mach number along side wall.
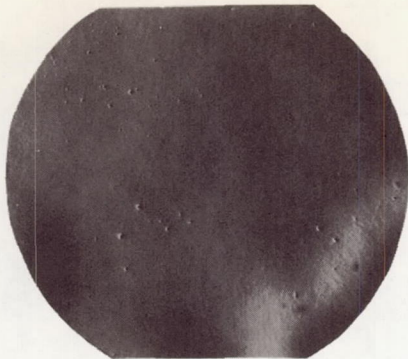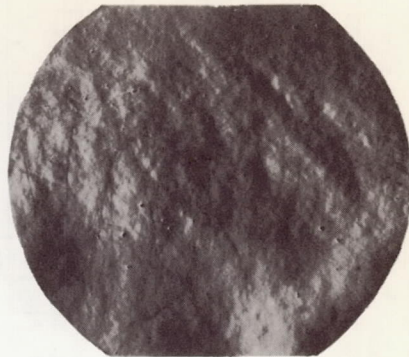
(a) $p_0 = 14.7$ lb/sq in. (M = 0).   (b) $p_0 = 21$ lb/sq in.
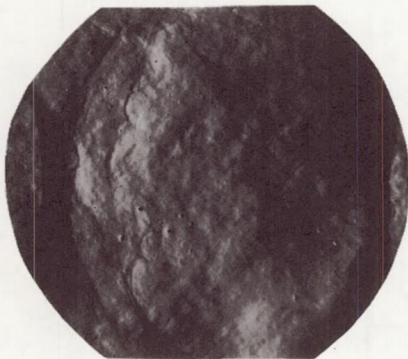
(c) $p_0 = 22$ lb/sq in.   (d) $p_0 = 23$ lb/sq in.
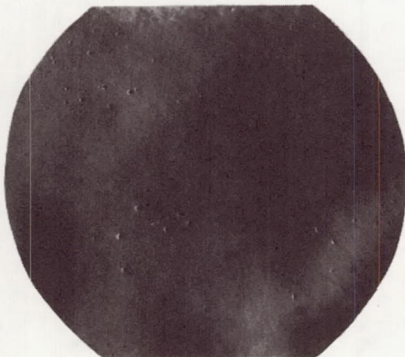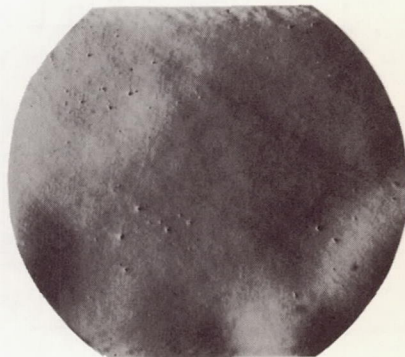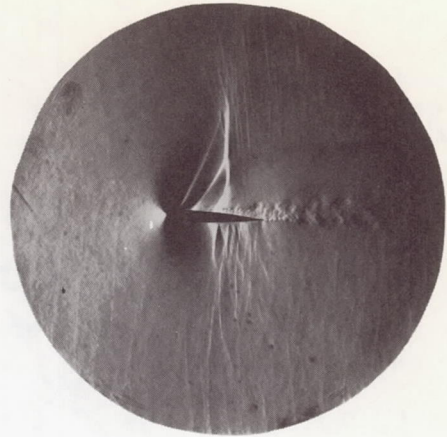
(e) $p_0 = 24$ lb/sq in.   (f) $p_0 = 27$ lb/sq in.

NACA

L-64891

Figure 31.- Flow photographs of starting cycle in blowdown tunnel
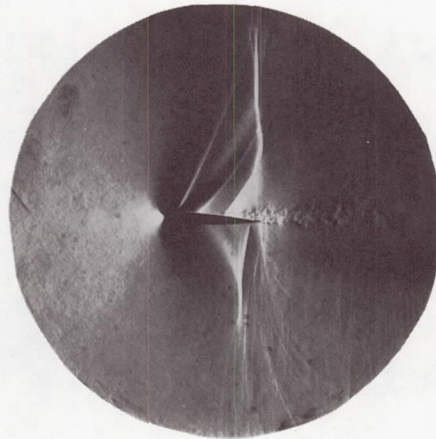with M = 2.0 nozzle blocks.
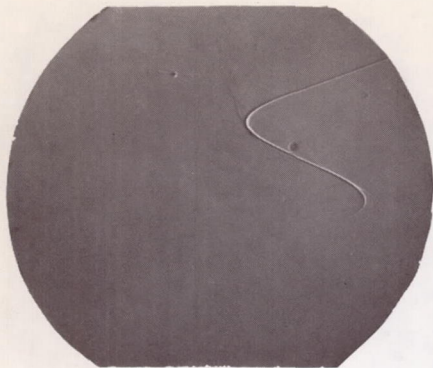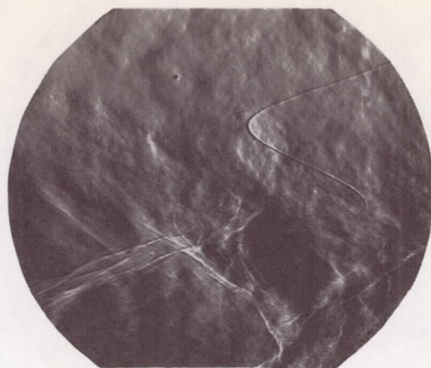
(a) p_0 = 14.7 lb/sq in. (M = 0). (b) p_0 = 128 lb/sq in.
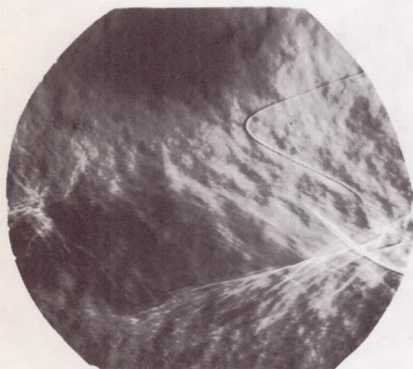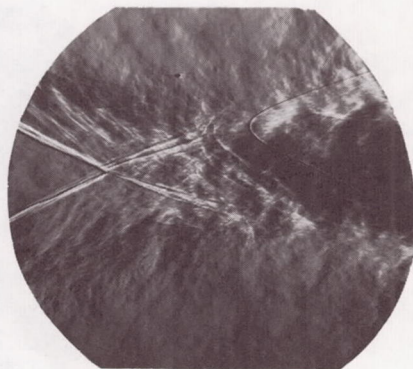
(c) p_0 = 138 lb/sq in. (d) p_0 = 140 lb/sq in.
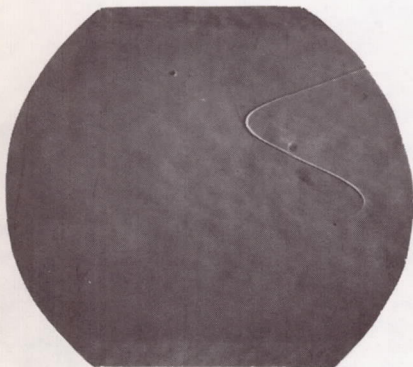
(e) p_0 = 142 lb/sq in. (f) p_0 = 147 lb/sq in.
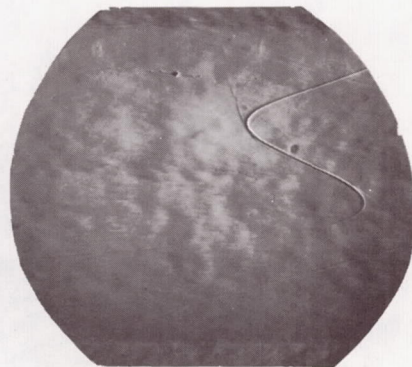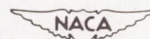
NACA
L-64892

Figure 32.- Flow photographs of starting cycle in blowdown tunnel
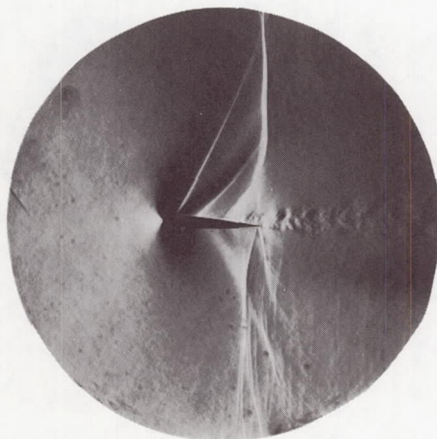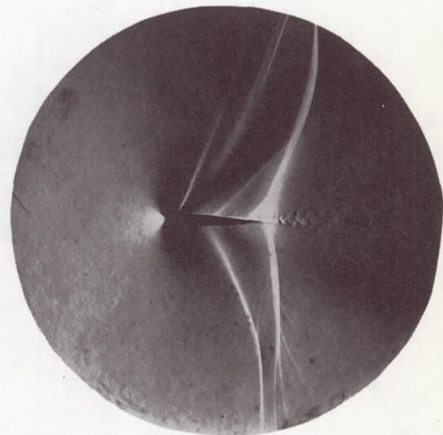with M = 4.1 nozzle blocks.
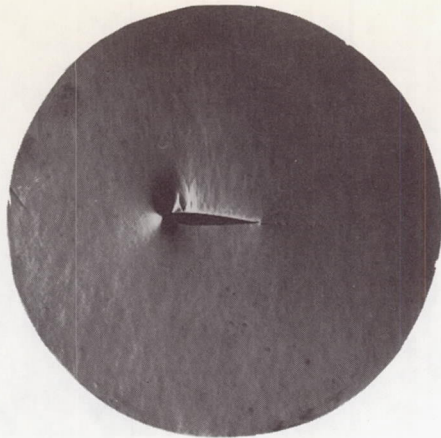
(a) M = 0.68.

(b) M = 0.85.

(c) M = 0.86.

(d) M = 0.87.

(e) M = 0.88.

L-64893

Figure 33.- Flow photographs of flow past a 2.5-inch-chord airfoil in
induction tunnel at subsonic speeds. α = 4°.